

**IMPROVEMENT OF CIRCUIT BREAKER CONTACTS AND
TERMINALS FOR POWER LOSS REDUCTION IN MEDIUM
AND HIGH VOLTAGE SYSTEMS**

BY

AKPEH VINCENT ANTHONY

REG. NO.:2012237001P

**SUBMITTED TO THE SCHOOL OF POST GRADUATE
STUDIES NNAMDI AZIKIWE UNIVERSITY, AWKA, IN
PARTIAL FULFILLMENT OF THE REQUIREMENTS FOR
THE AWARD OF DOCTOR OF PHILOSOPHY (Ph.D) IN
ELECTRICAL ENGINEERING (POWER SYSTEMS
OPTION)**

DEPARTMENT OF ELECTRICAL ENGINEERING

NNAMDI AZIKIWE UNIVERSITY, AWKA

JULY, 2019.

CERTIFICATION

This is to certify that this Dissertation was carried out by **AKPEH VINCENT ANTHONY**, with **Reg. No. 2012237001P**, Department of Electrical Engineering, Nnamdi Azikiwe University, Awka. This work has not been previously published by anyone for diploma or degree certificate. All sources of information are duly acknowledged.

Sign

.....

Akpeh Vincent Anthony

Date

APPROVAL PAGE

This dissertation has been read and approved by the undersigned as having met the requirements of the Department of Electrical Engineering, Nnamdi Azikiwe University, Awka, in partial fulfillment for the award of Doctor of Philosophy (PhD) in Power Systems Engineering

Sign
Ven. Engr. Prof. Madueme T.C (FNSE, FNIEEE)
(Supervisor 1) **Date**

Sign
Engr. Dr. Ezechukwu O.A (FNSE, FNIEEE)
(Supervisor 2) **Date**

Sign
Engr. Prof. S.A. Ike
(External Examiner) **Date**

Sign
Engr. Dr. J.C. Onuegbu
(Head of Department) **Date**

Sign
Engr. Prof. H.C. Godwin
(Dean Faculty of Engineering) **Date**

Sign
Engr. Prof. P.K. Igbokwe
(Dean School of Postgraduate Studies) **Date**

DEDICATION

This dissertation is dedicated to Almighty God who is my strength and greatest source of inspiration.

ACKNOWLEDGEMENTS

My greatest gratitude first goes to God Almighty who is the owner of wisdom. Honestly, I lack words that could really express my immense gratitude to Him who by His infinite mercies, gave me strength and provided me with everything I needed throughout the period of this research work – sound health, finances, journey mercies, quality and dedicated resource persons and favour. To Him alone be all praise and adoration in Jesus' Name.

My deep gratitude as well goes to my wonderful and dedicated Supervisors, Ven. Engr. Prof. Madueme T.C. and Engr. Dr. Ezechukwu O.A (FNSE, FNIEEE), who had always been available for me to encourage and to guide me. I must confess here that the efforts of this duo, made this research work successful. I also owe deep gratitude to the Head, Department of Electrical Engineering, Engr. Dr. J.C. Onuegbu for the fatherly advice and guide to me toward the success of this research work. I must not forget at this point to also express my deep gratitude to Engr. Prof. F.O. Enemuoh, for the sincere advice he gave to me the very first day I visited this University to apply for this program and who, coincidentally, was the Head, Department of Electrical Engineering, at the time I was offered admission by the School of Postgraduate Studies. I must also acknowledge Engr. Tomfrank Uketiu, Engr. Dr. E.A. Anazia, Engr. Dr. V.N. Agu, Engr. M.N. Eleanya, Engr. Sam Ezennaya, Engr. Sam Onyedikachi and Jachi Aghara who are lecturers/technologists of the Department of Electrical Engineering for their encouragements/contributions towards the success of this research work.

My deep gratitude also goes to the School of Postgraduate Studies that considered me worthy for a Doctorate Degree Program in Power Systems Engineering in this highly revered University.

I also wish to express my gratitude to the Department of Electrical and Electronic Engineering, Enugu State University of Science and Technology (ESUT), and my lecturers in this Department – Engr. Prof. G.N. Onoh, Engr. Prof. I.I. Eneh, Engr. Prof. Sam Ndubisi, Engr. Dr. Eke and Engr. Uchenyi, who prepared me for this higher degree. I as well acknowledge Transmission Company of Nigeria (TCN), for offering me the opportunity for practical knowledge. I must not forget to acknowledge the following retired and serving

staff of this company (TCN), for their moral support and encouragements – Engr. Collins Ugorji, Principal Manager System Operations, Enugu Region (retired), and Engr. Bakare Kazeem, Assistant General Manager (Transmission), Enugu Sub – Region.

I owe immense gratitude to my parents, late chief Matthew O. Akpeh and Mrs. Christiana O. Akpeh, who despite their meager resources, made sure that I acquired Western education. My gratitude also goes to my beloved wife, Juliana, for her care and prayers, and to my wonderful children – Rex, Anita, Joyce, Sinclair, Fergus, and Abundance, for their understanding and assistance in their own little way. Finally, my sisters and brother – Mrs. Patricia N. Emeka Nwankwo, Late Mrs. Justina Oka, Mr. John N. Akpeh, Mrs. Angela C. Thomas Elufu, Mrs. Virginia O. Fabian Nwambeke, Mrs. Stella N. Osondu Achi and Mrs. Theresa U. Okoro Ibeto, are all highly acknowledged for their contributions and sacrifices to the success of my education to this level.

ABSTRACT

This dissertation proffered ways to mitigate the enormous constant power losses encountered during implementation of Current Limiting Reactors (CLRs) on feeders. It improved on the efficiency and reduces the cost of circuit breakers required under Current Limiting Reactor implementation in medium and high voltage systems. Two methods were used. One method involved circuit breaker contacts design modification - modifying the straight moving contact to a forked moving contact and the other method - the design of adapters for coupling CLRs and circuit breakers. The results were compared with the result from the existing circuit breaker on Nkalagu-Abakaliki 132kV line, a network in Transmission Company of Nigeria (TCN), and the modified circuit breaker resulted in minimal (negligible) constant power losses in the system, among other benefits. The adapter usage is highly applicable in the Nigerian power system where increasing demand for energy and network expansions lead to short circuit levels of more than the installed capacity of the circuit breakers. The power losses as well as the behavior of the key parameters that determine the operating mechanism energy requirements of circuit breakers during the implementation of the CLRs via the use of adapters or forked moving contacts in circuit breakers were analyzed using MATLAB. The power flow on Nkalagu-Abakaliki 132kV line with the existing circuit breaker and CLR and with the improved circuit breaker and CLR were simulated on POWERWORLD environment. The results obtained showed negligible power loss across the CLR (from 128.11kW to 1.75W and 1.38W for the forked contact and the adapter application respectively) during healthy system condition, nineteen percent reduction in the CB moving contact cross-sectional area (from $9.61 \times 10^{-4} \text{m}^2$ to $7.8 \times 10^{-4} \text{m}^2$), for a 40kA short-circuit current on a 132kV CB, fifty percent reduction in interrupted fault current (from 40kA to 20kA), sixty-nine percent reduction in the CB cost (from ₦15,000,000.00 to ₦4,650,000.00) and seventy-five percent reduction in the heat generated (from 15.52kJ to 3.88kJ), when operating the CB.

TABLE OF CONTENTS

	Page
Cover page	i
Certification	ii
Approval	iii
Dedication	iv
Acknowledgement	v
Abstract	vii
Table of Contents	viii
List of Tables	xi
List of Figures	xiii
List of Abbreviations	xvii
List of Symbols	xx
CHAPTER ONE: INTRODUCTION	
1.1 Background of the Study	1
1.2 Statement of the Problem	3
1.3 Aim of the Study	3
1.4 Objectives of the Study	3
1.5 Significance of the Study	4
1.6 The Scope and Limitations of Study	4
1.7 Organization of the Dissertation	4

CHAPTER TWO: LITERATURE REVIEW	
2.1 Circuit Breaker Architecture	5
2.2 Arc Control in Circuit Breakers	10
2.3 Current Limiting Techniques	16
2.4 Adapter	26
2.5 Review of Related Literatures	27
2.6 Summary of the Reviewed Works	39
2.7 Research Gaps	39
CHAPTER THREE: METHODOLOGY	
3.1 Methodology	41
3.2 System Modeling	43
3.3 System Simulations	94
3.4 Result Validation Models	100
CHAPTER FOUR: RESULTS AND DISCUSSIONS	
4.1. Power Loss Reduction	102
4.2 Reduction in the heat generated when operating a CB	110
4.3 Technique for connecting CB and CLR in parallel	112
4.4 Circuit Breaker Cost Reduction	112
4.5 Simulation Result Validation	130
CHAPTER FIVE: CONCLUSSION AND RECOMMENDATION	
5.1 Conclusion	134
5.2 Recommendation	134
5.3 Contributions to Knowledge	135
REFERENCES	136

LIST OF APPENDICES

Appendix A: MATLAB codes for Figure 3.2 and Table 3.4	146
Appendix B: Terminals of the Existing CB for fitting the Adapter shown in Figures 3.13 and 14	149
Appendix C: Time Multiplier Setting (TMS), for an Electromechanical Relay	150
Appendix D: Plug Setting Multiples (PSM), for an Electromechanical Relay	151
Appendix E: Time - Current Characteristic Curves for a Standard 3.0 seconds Inverse Time Relay CDG11 for 50HZ and 60HZ (BS 142)	152
Appendix F: Relay Discrimination Curves	153
Appendix G: Input Data for the Simulated Network	154
Appendix H: Line Records (branch state) for Figures 3.23 and 3.24	155
Appendix I: Bus Records for Figures 3.23 and 3.24	156
Appendix J: Line Records (branch state) for Figures 3.25 and 3.26	157
Appendix K: Bus Records for Figures 3.25 and 3.26	158
Appendix L: Line Records (branch state) for Figures 3.27 and 3.28	159
Appendix L1: Bus Records for Figures 3.27 and 3.28	160
Appendix M: Line Records (branch state) for Figures 3.29 and 3.30	161
Appendix M1: Bus Records for Figures 3.29 and 3.30	162
Appendix N: MATLAB codes for Figure 4.3	163
Appendix O: MATLAB codes for Figure 4.4	166
Appendix P: MATLAB codes for Table 4.7	168
Appendix Q: MATLAB codes for Figure 4.5	169
Appendix R: MATLAB codes for Figure 4.6	171
Appendix S: MATLAB codes for Figure 4.7	173

Appendix T: MATLAB codes for Tables 4.9 and 4.10	176
Appendix U: MATLAB codes for Table 4.11	178
Appendix V: MATLAB codes for Table 4.12	180
Appendix W: MATLAB codes for Table 4.13	182
Appendix X: MATLAB codes for Table 4.14	184

LIST OF TABLES

Table 2.1: Components of the Protective System and their Functions	27
Table 3.1: Measured Dimension for 132kV CB Moving Contact at TCN Nkalagu Transmission Station	47
Table 3.2: Nkalagu-Abakaliki 132kV Line Data	48
Table 3.3: Transformer Data at Abakaliki Transmission Station	48
Table 3.4: Effect of CLR Reactance on Fault Current Level	54
Table 3.5: Calculated Dimension for Modified CB Moving Contact	62
Table 3.6: Dimension for Straight Part of Forked Moving Contact	62
Table 3.7: Dimension for the Longer Prong of Forked Moving Contact	64
Table 3.8: Dimension for the Shorter Prong of Forked Moving Contact	65
Table 3.9: Summary of the Calculated Dimension for the Forked Moving Contact	67
Table 3.10: Summary of the Existing CB and the Modified CB Compared	68
Table 3.11: Calculated Dimensions for the Adapter Parts	75
Table 3.12: Relay Characteristics	81
Table 3.13: North American IDMT Relay Characteristics	81
Table 3.14: Data for the Protective System for Nkalagu – Abakaliki 132kV line	82
Table 3.15: Summary of CB/CLR Relay Coordination	85
Table 4.1: Tariff and Load Data	102
Table 4.2: Summary of the Calculated/Measured Result from the Use of Forked Moving Contact CB and the Existing CB	107
Table 4.3: Summary of the Result from the Adapter Implementation on	

CB Terminal and the Existing CB	109
Table 4.4: Total Break Time and the Corresponding Breaker Ready Time for a 50Hz System	114
Table 4.5: Breaker Ready Time and the Corresponding Kinetic Energy Requirement for a 50Hz System	115
Table 4.6: Total Break Time and the Corresponding Kinetic Energy Requirement for a 50Hz System	115
Table 4.7 Fault Current and the Corresponding Blast Pressure	119
Table 4.8: Fault Current and the Corresponding CB's Compression Work Requirement	122
Table 4.9: Fault Current and the Corresponding Mass of Moving Contact Rod (straight rod of 1.20m length)	125
Table 4.10: Fault Current and the Corresponding Mass of Moving Contact Rod (forked rod of 1.24m overall length)	126
Table 4.11: The Effect of the Use of CLR on the Overall Mass of the Forked CB Moving Contact Rod	127
Table 4.12: The Effect of the Use of CLR on the Overall Mass of the Forked CB Moving Contact Rod	128
Table 4.13: The Effect of the Use of CLR on the Overall Mass of the Forked CB Moving Contact Rod	129
Table 4.14: The Effect of the Use of CLR on the Overall Mass of the Forked CB Moving Contact Rod	129
Table 4.15: Simulation Result Data Extracted from Appendices L and L1	130
Table 4.16: Simulation Result Data Extracted from Appendices M and M1	131
Table 4.17: Simulation Result Data Extracted from Appendices J and K	133

LIST OF FIGURES

Figure 2.1: Post Insulator/Interrupter Unit of a CB	6
Figure 2.2: Constricted Flow Paths of Current in a Set of Contacts	7
Figure 2.3: Conducting Contacts under Pressure	11
Figure 2.4: Parts of the Electric Arc	12
Figure 2.5: Short Circuit Fault on a Feeder	15
Figure 2.6: Equivalent Circuit of Figure 2.5	16
Figure 2.7: Current Limiting Reactor	18
Figure 2.8: CLR in Circuit	19
Figure 2.9: Effect of Inductance on Fault Current Level	19
Figure 2.10: Superconducting Fault Current Limiter	22
Figure 2.11: Current Limitation and Peak Let-Thru Current	23
Figure 2.12: Tulip Contacts in Dell Alsthom Air-Blast Circuit Breaker	28
Figure 2.13: Waveforms of Short-Circuit Current and System Voltage when Operating a CB	30
Figure 2.14: I_s -Limiter and Reactors Connected in Parallel	38
Figure 3.1: Nkalagu-Abakaliki 132kV Line with the Existing CB without CLR	49
Figure 3.2: Effect of CLR Reactance on Fault Current Level	54
Figure 3.3: Nkalagu-Abakaliki 132kV Line with the Existing CB and 2.0 ohms CLR	56
Figure 3.4: Straight Part of the Forked Moving Contact	63
Figure 3.5: Diameter of the Circumscribing Circle on the Straight Part of the	

Moving Contact	63
Figure 3.6: Longer Prong of the Forked Moving Contact	64
Figure 3.7: Shorter Prong of the Forked Moving Contact	65
Figure 3.8: The Forked Moving Contact	66
Figure 3.9: Diameter of the Circumscribing Circle on the Forked	
Moving Contact prongs	67
Figure 3.10: Post Insulator/Interrupter Unit of an Existing CB Showing its	
Terminals	69
Figure 3.11: Post Insulator/Interrupter Unit of a CB showing the Modification	
On the Fixed Contact Terminal	70
Figure 3.12: CLR/CB Prototype Connection for Forked Moving Contact	71
Figure 3.13: The Adapter	72
Figure 3.14: Dimensions for the Adapter	76
Figure 3.15: CLR/Adapter/CB Prototype Connection	77
Figure 3.16: CLR/Adapter/CB Prototype Connection	78
Figure 3.17: Block Diagram showing the Locations of CB, Adapter, CLR,	
CT and Relays	79
Figure 3.18: Single Line Diagram of Current Limiting Reactor Implementation	
On the Existing CB	86
Figure 3.19: Single Line Diagram of Current Limiting Reactor Implementation on a	
Modified Feeder Circuit Breaker	86

Figure 3.20: CB/CLR in Parallel when the Modified CB is in Closed Position	87
Figure 3.21: CB/CLR in Series Before the Modified CB Contacts Separate during Opening Operation	88
Figure 3.22: The Modified CB in Open Position	88
Figure 3.23: Network Model for Nkalagu – Abakaliki 132kV Line with the Existing CB without CLR	96
Figure 3.24: The Power Flow on Nkalagu – Abakaliki 132kV Line with the Existing CB without CLR	96
Figure 3.25: Network Model for Nkalagu – Abakaliki 132kV Line with the Modified CB and a CLR of 2 ohms Impedance in Closed Position	97
Figure 3.26: The Power Flow on Nkalagu – Abakaliki 132kV Line with the Modified CB in Closed Position and a CLR of 2 ohms Impedance	98
Figure 3.27: Network Model for Nkalagu – Abakaliki 132kV Line with the Modified CB and a CLR of 2 ohms Impedance during Opening Operation	99
Figure 3.28: The Power Flow on Nkalagu – Abakaliki 132kV Line with the Modified CB and a CLR of 2 ohms Impedance during Opening Operation	99
Figure 3.29: Network Model for Nkalagu – Abakaliki 132kV Line with The Existing CB in Series with 2.0 ohms CLR	100
Figure 3.30: The Power Flow on Nkalagu – Abakaliki 132kV Line with The Existing CB in Series with 2.0 ohms CLR	100
Figure 4.1: Nkalagu-Abakaliki 132kV Line with the Modified CB and CLR	105
Figure 4.2: Nkalagu-Abakaliki 132kV Line with the Existing CB and CLR	106

Figure 4.3: Response Curve of CB Total Break Time (t_0) Against the Kinetic Energy Requirement (W_{KIN})	114
Figure 4.4: Response Curve of Blast Pressure against Fault Current	117
Figure 4.5: Response Curve of the Moving Contact Area against the Fault Current	120
Figure 4.6: Response Curve of Compression Work against Fault Current	122
Figure 4.7 Response Curve of the overall Mass of the Forked Moving Contact against the Fault Current	125

LIST OF ABBREVIATIONS

A_A	Cross Sectional Area of an Arc
CB	Circuit Breaker
CLR	Current Limiting Reactor
Cos	Cosine
CT	Current Transformer
f	Nominal Frequency
f_n	Natural Frequency
FCL	Fault Current Limiter
HV	High Voltage
Hz	Hertz
I	Current
IDMT	Inverse Definite Minimum Time
I_{SC}	Short Circuit Current
KV	Kilo Volts
L	Inductance
M	Mass
Max	Maximum
MgB_2	Magnesium diboride
Min	Minimum

N Total Number of Breaks of a Circuit Breaker

NbTi Niobium-Titanium

P Pressure

P_0 Filling Pressure of a Circuit Breaker

PSM Plug Setting Multiplier

rms Root Mean Square

RRRV Rate of Rise of Re-Striking Voltage

SCCR Short Circuit Current Rating

SCR Silicon Controlled Rectifier

SFCL Superconducting Fault Current Limiter

SSFCL Solid State Fault Current Limiter

t_{BR} Circuit Breaker Ready Time

TCN Transmission Company of Nigeria

TMS Time Multiplier Setting

t_0 Total Break Time of a Circuit Breaker

TRV Transient Restriking Voltage

VA Volt-Ampere

VT Voltage Transformer






W_{COMP} Compression Work Requirement of a Circuit Breaker

W_{KIN} Kinetic Energy Requirement of a Circuit Breaker

X'_d Transient Reactance

YBCO Yttrium Barium Copper Oxide

LIST OF SYMBOLS

\int	Integral
Ω	Ohm
//	Parallel
\approx	Approximately Equal To
ω	Omega
\gg	Much Greater Than
ΔP	Blast Pressure necessary to warrant reliable Arc Quenching in a Circuit Breaker
\propto	Proportional To
	AC Generator
	Circuit Breaker
	Power/Distribution Transformer
	Current Transformer
	Fuse.

CHAPTER ONE

INTRODUCTION

1.1 Background of the Study

When reasonable voltage is applied across an air gap, the air mass becomes ionized. The ionized gas conducts in form of continuous spark or arc since it consists of molecules that have lost one or more electrons. The electrons which are negatively charged are attracted towards the anode with a high velocity. The positive ions on the other hand are attracted towards the cathode but they move towards it relatively slowly due to their weight. The electrons so emitted from the cathode make many collisions with the atoms and molecules of gases and vapours existing between the two contacts during their journey towards the anode. Such collisions cause ionization of atoms and molecules, thus dislodging more electrons. The ionization is further facilitated by:

- (i) High temperature of the medium around the contacts caused by high current densities. With high temperature, the kinetic energy gained by the moving electrons is increased.
- (ii) The field strength or voltage gradient which increases the kinetic energy of moving electrons and increases the chances of detaching electrons from neutral molecules.
- (iii) An increase of mean free path – the distance through which the electrons move freely. As the contacts move apart, the mean path increases and the number of neutral molecules increases. Also the increase in mean path decreases the density of gas which further increases the free path movement of the electrons.

All the above three processes (thermal emission, field emission and ionization) may start either one after the other or almost simultaneously and enable the arc to be initiated and maintained and if the arc current is high, the arc may attain a temperature high enough for thermal ionization to become the main source of electrical conductivity.

The above scenario plays out as soon as the contacts of a circuit breaker begin to separate in medium and high voltage systems. This happens both under faults and during opening

at normal conditions but is more pronounced and more worrisome under fault conditions due to the level of currents involved (Gupta, 2012).

Field emission and thermionic emission are the two processes that produce the initiating electrons. The contact area and pressure between the separating contacts decrease as the moving contact is withdrawn. The reduced contact area causes an increase in the resistance. Contact resistance is quite small but due to large magnitude of fault current, a sufficiently high potential drop of the order 10^6V/cm is caused between the separating contacts so as to dislodge electrons from the cathode surface (field emission). On the other hand, as the contacts move apart, the decrease in contact area causes increase in current density to very high values of the order 10^6A/cm^2 . These very high current densities raise the temperature of the contact (cathode) surface, resulting into thermionic emission (Gupta, 2012).

Circuit breakers are rated both by the normal current that they are expected to carry and the maximum short circuit current that they can safely interrupt. Under short circuit conditions, a current many times greater than normal can exist. When electrical contacts open to interrupt a large current, there is a tendency for an arc to form between the opened contacts, which would allow the current to continue. This condition can create conductive ionized gases and molten or vapourized metals, which can cause further continuation of the arc, or creation of additional short circuits, potentially resulting in the explosion of the circuit breaker (Gupta, 2012).

It is very important to emphasize here that arc does not just form on its own accord. It is caused by current. As already explained, the initiating processes namely: field emission and thermionic emission; are current driven. The magnitude of the arc developed across a gap in medium and high voltage systems depends on the interrupted current magnitude. What this means is that keeping the anticipated arc to a low value can easily be achieved by reducing the anticipated interrupted current level. The arc management principles in AC circuit breakers namely: resistance switching, current interruption at natural zero of the current wave and the type of extinguishing medium employed, all work better when the anticipated current level is kept as low as possible. Therefore, it is necessary to develop a system that will reduce the anticipated current level to the barest minimum.

The use of series Current Limiting Reactors (CLRs) to lower interrupted short circuit level is known to be the best way to lower anticipated arc when Circuit Breakers (CBs) are opened. However, this has not been properly harnessed due to the enormous constant power losses that arise from their use since they carry the full load current as they are permanently serially connected in the circuit.

This work therefore focused on improving circuit breaker contacts and terminals and the design of adapters for existing CBs to ensure that current limiting reactors can still be permanently connected on feeder circuit breaker circuits without carrying the full load current except when the circuit breaker is breaking. That is to say that the CB contacts and terminals or the use of adapters on existing CBs should be capable of keeping the CLR and the CB in a parallel arrangement when the CB is in closed position but must ensure that the CLR and CB are in series just before the CB contacts separate.

1.2 Statement of problem

The magnitude of the interrupted current determines the arc magnitude when contacts of a circuit breaker separate. However, the constant power losses encountered during the use of series short circuit Current Limiting Reactors (CLRs) – the most practical and effective short circuit current limitation technique, to manage arc is quite enormous. This problem has limited the use of CLRs to only the critical feeders, while circuit breakers of higher operating mechanism energy (meaning higher costs than necessary) are deployed to the rest of the feeders.

1.3 Aim of Study

The aim of the work is to improve CB contacts and terminals for power loss reduction in medium and high voltage systems.

1.4 Objectives of Study

The specific objectives to actualize the aim are:

1. to develop a model for power loss reduction in the use of CLRs and CBs.
2. to develop a model for reduced heat generation during CB operation.
3. to develop a technique that connects CB and CLR in parallel when CB is in closed position and in series during CB opening operation.

4. to reduce the cost of CBs for specific loads via reduction in operating mechanism energy requirements of CBs.

1.5 Significance of the Study

Arc control in medium and high voltage systems is a global problem. So this study will go a long way in alleviating this problem and will be beneficial to Transmission Company of Nigeria (TCN). The study will also earn huge financial savings to power utilities globally, especially to countries like Nigeria that import circuit breakers. The study will also be of benefit to power system researchers.

1.6 The Scope and Limitations of Study

This work covers existing conventional medium and high voltage circuit breaker designs of less or equal to 132kV rating with improvements on the contacts and terminals. This will allow Current Limiting Reactor (CLR) connection such that they (the CLR) could be permanently connected in the circuit, yet without carrying the full load current but, limiting fault currents to desired levels. It does not seek to introduce a completely new circuit breaker design with different operating principles.

1.7 Organization of the dissertation

This dissertation is organized in five chapters. A general introduction and background information about arc in medium and high voltage systems is given in chapter one. A detailed review of related literature is presented in chapter two. The design methodology is presented in chapter three. The Results and Discussions are presented in chapter four, while the Conclusion and Recommendation are presented in chapter five.

CHAPTER TWO

LITERATURE REVIEW

2.1 Circuit Breaker Architecture

A circuit breaker (CB) is a device which can make or break a circuit either manually or automatically under normal or fault conditions. It breaks a circuit under short circuit, overload condition or at normal load condition (Heinemann et al, 2014), (Energysiemens, 2014). Unlike a fuse, which operates once and then has to be replaced, a circuit breaker can be reset (either manually or automatically) to resume normal operation. Circuit breakers are made in varying sizes, from small devices, which protect an individual household appliance, up to large switchgear designed to protect high voltage circuits feeding an entire city (Zensol, 2007).

The high voltage circuit breaker has three major components:

(1) **Interrupting Chamber**

This is where the current conduction and interruption in the power circuit occurs. It is usually a closed volume containing the make/break contacts and an interrupting medium (compressed air, oil, SF₆, vacuum, etc.) used for insulation and arc quenching.

(2) **Operating Mechanism**

This is where the needed energy to close or to open the contacts and to quench the arc is initiated.

(3) **Control**

This is where the orders to operate the breaker are generated and its status is monitored.

At the top of the interrupter unit as well as the junction of the interrupter unit and the post insulator are terminals where the power lines are connected to the CB. In other words, the CB is always in series with the feeder. The terminals on the interrupter unit/post insulator are as shown in Figure 2.1.

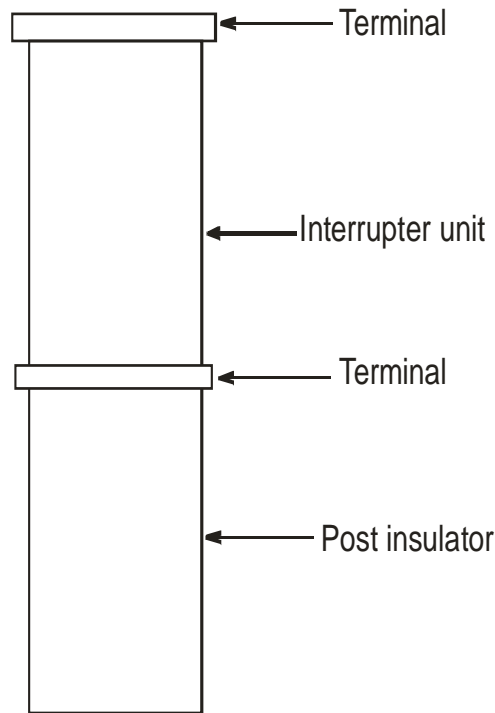


Figure 2.1: Post Insulator/Interrupter unit of a CB

2.1.1 Contact Dynamics in Circuit Breakers

The current in circuit breakers passes through both a detection mechanism and a set (or sets) of electrical contacts. The contacts are generally spring-loaded and latch restrained. When triggered by the over current detection mechanism, the latch will release a movable contact arm. The arm then withdraws from the fixed contact at a rate determined by spring loading and electromagnetic forces due to the contact current.

When the contacts are closed, or “latched”, current flows between the contacts only at very small physical contact points, or asperities, due to surface roughness on the bulk contact faces. The actual area of electrical contact is only a small fraction, less than 1%, of the apparent area of the bulk contact surface. This is as shown in Figure 2.2. The surface roughness is not an ideal feature of the contacts; hence, effort is always made during preparation of the contact surfaces to make them smooth.

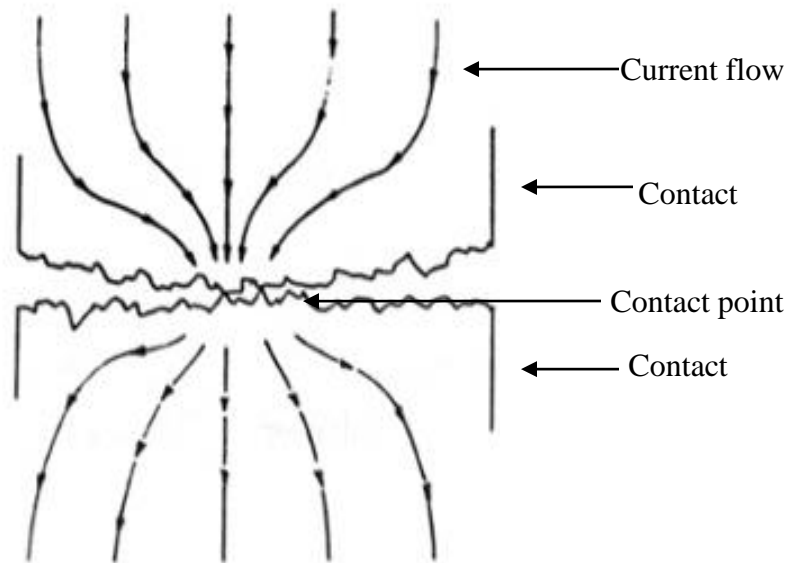


Figure 2.2: Constricted flow paths of current in a set of contacts (Mechprod, 2012).

Current flowing in the contact bulk regions is constricted at these contact points, much like fluid flowing through a pipe with an insert containing very small holes. The extra electrical resistance due to this current restriction is referred to as the spreading or constrictive resistance of the contact.

The effective radius of each contact spot a_i is dependent on the preparation of the bulk contact surface, the normal forces applied to the contacts, the “hardness” of the contact material (i.e. whether each contact asperity be under elastic or plastic deformation), and the temperature at the contact interface. In addition to constrictive resistance at contact asperities, there may be a resistance due to a thin film or layer of material oxide between contacting asperities. Electrons either tunnel quantum mechanically through this thin film, or break through the film by a process referred to as “fritting”. The film resistance is between the constriction resistances of individual asperities (Mechprod, 2012).

In practice, there is no attempt to determine the contributions to contact resistance ($R_{contact}$) due to individual contact spots. The net excess resistance of the contact system, beyond the bulk resistances of the two contacting bodies, is simply referred to as the contact resistance. The voltage drop across this resistance is commonly referred to as the

contact drop. In most cases, this contact drop does not exceed 0.1 - 0.2 volts. Contact drops tend to saturate at these levels since, as the magnitude of the current rises, the asperity interface temperature rises thereby softening the asperity material. The softer material spreads out and increases the actual asperity contact area, thus lowering the contact resistance (Mechprod, 2012).

When two bulk metallic contacts which are carrying an electrical current separate, the last point or points of physical and electrical contact are at one or more constriction asperity spots. The current density at these points are very large, easily enough to melt the asperity material and form molten bridges between the two contacts. These bridges are then heated and stretched to the point that they vaporize. The process initiates the arc between the two contacts. If the contacts are not metallic, such as carbon, the asperity points do not melt, but rather arc immediately upon physical separation (Mechprod 2012).

2.1.2 Circuit Breaker Operating Mechanism

According to Fuchsle and Heinemann (2009), Rees and Peters (1995) and Claessens et al, (2006), circuit breaker operating mechanisms are characterized by different technologies. In principle, they can be divided into five groups namely:

(a) Pneumatic Operating Mechanism

These mechanisms were first in the market when high energy demand for circuit breaker was required. Typical applications were high voltage puffer circuit breakers for high short circuit ratings, generator circuit breakers or air blast circuit breakers. Energy storage requires a large separate gas container. Operation control is initiated by valves. Energy transmission is achieved by pneumatic pistons and damping via internal gas dampers. Intensive maintenance requirements of the compressor made this technology more and more unpopular. The working pressure of the gas energy storage tank is around 30 bars. Hence, this technology has to meet pressure vessel regulation in certain countries. In addition, the high pressure made the available energy for switching operation very temperature sensitive (Heinemann and Glock, 2010).

(b) Hydraulic Operating Mechanism

Here, the energy is stored in a nitrogen accumulator. The hydraulic mechanism works with a much higher working pressure (around 300 bars) compared to pneumatic operating mechanism. The pressure is generated by a hydraulic pump. Energy transmission is realized by a wear-free hydraulic system. Damping during opening and closing operation is integrated in the working piston. To keep the sealing system of the nitrogen accumulator in proper condition, frequent maintenance of the hydraulic operating mechanism is required (Rees and Peters, 1995).

(c) Spring Operating Mechanism

With the introduction of the self-blast breaker technology interrupters and the reduced required switching energy, spring operating mechanisms are continuously replacing pneumatic and hydraulic operating mechanisms. A mechanical spring mechanism usually consists of two springs, one for open and one for close operation. The closing spring generates the required force to close the circuit breaker and charge the opening spring. Hence, the mechanical energy needed for the re-opening is always stored in the opening spring when the circuit breaker is in the closed position. The opening spring is either mounted in the operating mechanism and/or in the circuit breaker Heinemann et al, (2014).

(d) Hydro-Mechanical Spring Operating Mechanism

The Hydro-Mechanical Spring Operating Mechanism is basically a combination of the hydraulic Operating Mechanism and the Spring Operating Mechanism. It combines the advantages of these two technologies. The main feature is the energy storage in highly reliable disc springs. Operation is controlled by hydraulic valves widely used in industrial application and aeroplanes. The energy transmission is realized by hydraulic pistons. The damping of the circuit breaker is integrated in the hydraulic system. Due to the low number of moving parts and the operating principle, the operating mechanism is almost maintenance free (Holaus and Stucki, 2008), (Heinemann and Besold, 2009).

(e) Power Electronic Based Operating Mechanism

One of the most recently developed operating mechanisms is the electrical motor drive. The energy is stored in a capacitor bank and can be delivered instantaneously to the converter, which transforms DC voltage from the capacitors and feeds the motor with regulated AC voltage. The motor drive is essentially a digital system. The required operating motions are digitally programmed in a control unit (Heinemann et al, 2014).

Spring mechanisms have gained increasing acceptance as the most reliable form of operating mechanism (Cigre, 1996). Failure rates on spring operated CBs are extremely low. According to Michael and Richard, (2001), today's conventional spring operated mechanisms are generally characterized by:

- (1) 10,000 close-open operation life
- (2) Over 30 years field life
- (3) Operation in all environments
- (4) Very low maintenance
- (5) Modular core designs

2.2 Arc Control in Circuit Breakers

In this section, how to control arc in circuit breakers is reviewed. However, to better appreciate this, the phenomenon is first presented.

2.2.1 Arc Phenomena

The arc consists of a column of ionized gas having molecules which have lost one or more electrons. The electrons are negatively charged and so are attracted towards the positive contacts with a high velocity and on the way they detach more electrons by impact. The positive ions are attracted towards the negative contacts, but they move towards it relatively slowly due to their weight (Gupta, 2012).

2.2.2 Arc Initiation in Circuit Breakers

Under closed conditions, the electrodes of a circuit breaker are maintained in conducting contact under pressure as shown in Figure 2.3. As the contacts separate arc is formed as shown in Figure 2.4.

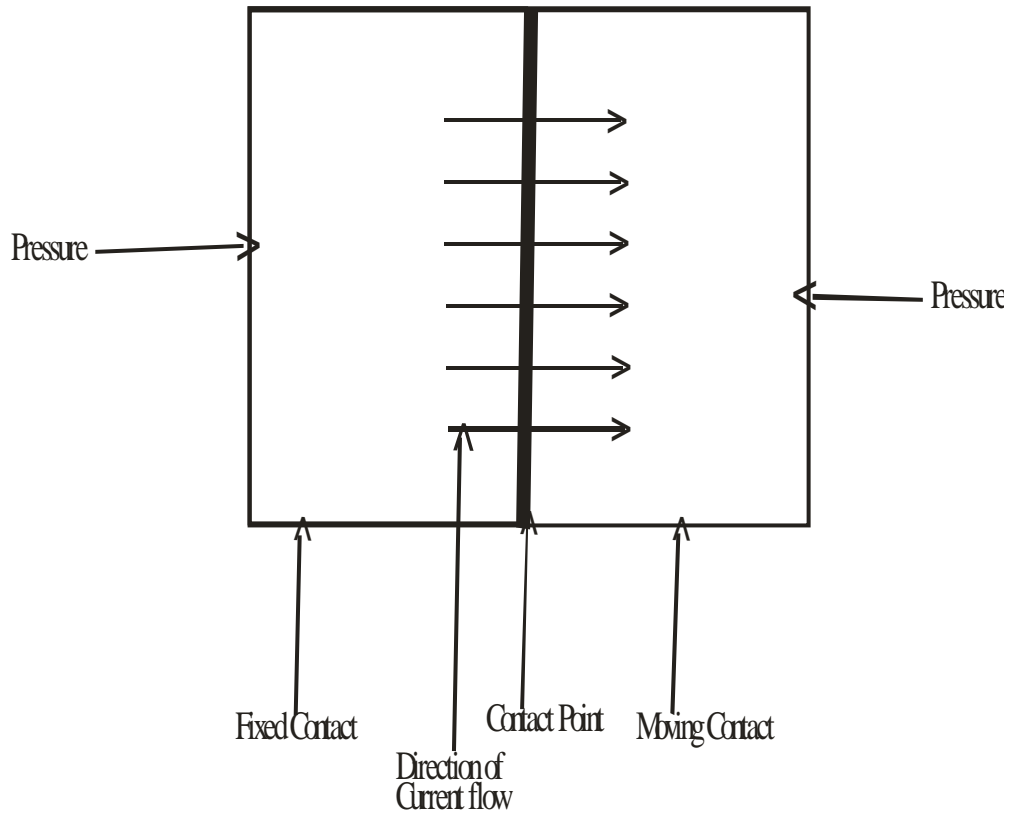


Figure 2.3: Conducting contacts under pressure (Nagrath and Kothari, 2004)

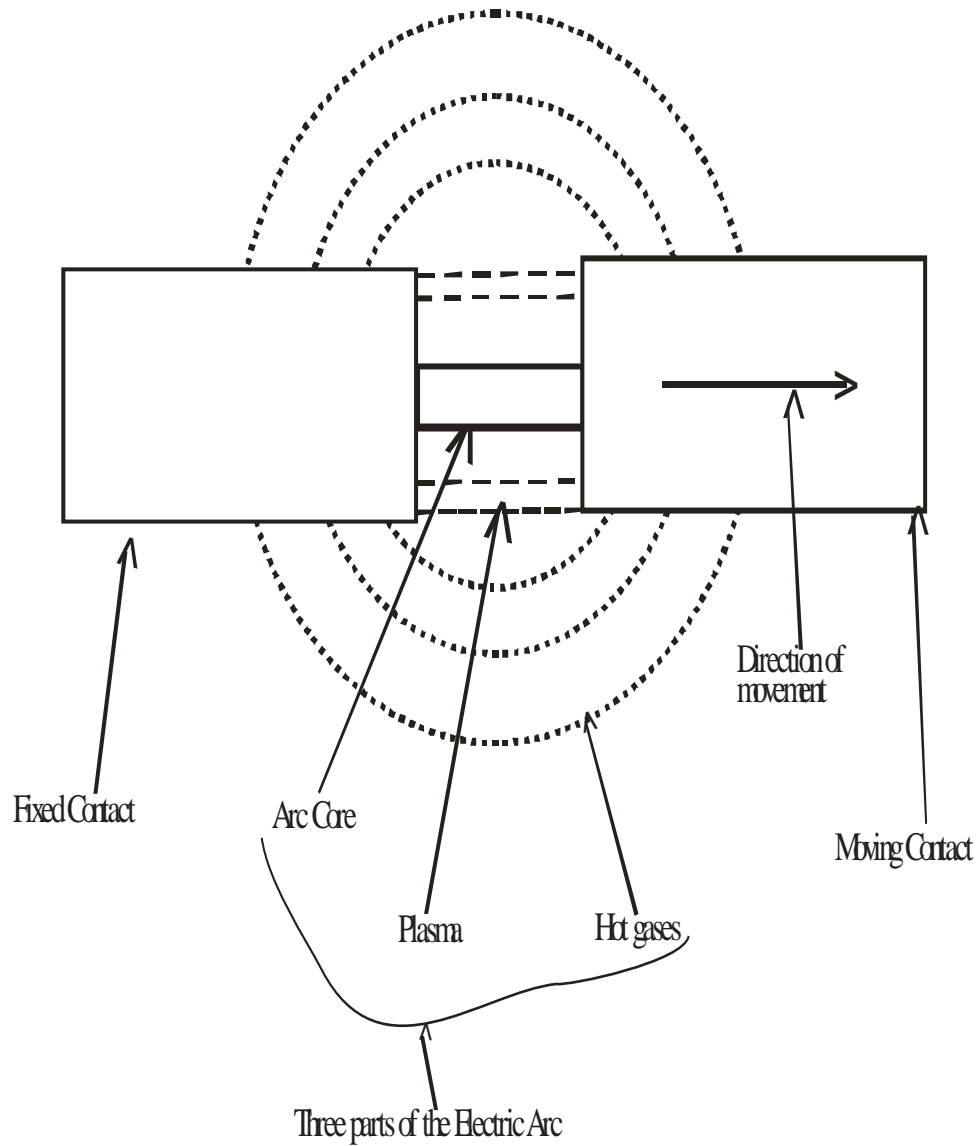


Figure 2.4: Parts of the electric arc (Nagrath and Kothari, 2004)

As the pressure is released, the electrodes remain in contact at a small number of points, causing contact resistance to increase considerably. As the same current is still to be conducted, large contact losses occur, leading to formation of hot spots and ionization of air voids. As the contacts separate, an arc is struck between the electrodes as shown in Figure 2.4. The current is now conducted by ionized gas (plasma) with electrons moving towards the anode and slow moving positive ions towards the cathode (Nagrath and Kothari, 2004).

- (a) The arc can be divided into three parts as shown in Figure 2.4, namely: The arc core, with the temperature ranging from 6000°C to 25000°C
- (b) The plasma, with boundary temperature of the order of 2000°C
- (c) The hot gases.

2.2.3 Maintenance of Arc

During contacts separation, atoms and molecules of gases and vapours exist between the contacts. As the electrons emitted from the cathode journey towards the anode, they collide with these atoms and molecules of gases and vapours. Collision between the electrons and atoms and molecules of the gases and vapours cause the ionization of the atoms and molecules, leading to emission of more electrons (Gupta, 2012). During the contacts separation process, there are:

- (i) Increased current densities at the contact points. This proportionately raises the temperature of the surrounding medium. This favours ionization as the kinetic energy gained by the moving electrons is increased.
- (ii) Increased voltage gradient between the parting contacts. This again favours ionization. The increased voltage gradient here results due to large fault current magnitude and the increased resistance resulting from the reduced contact area.
- (iii) Progressive decrease in the density of the gases. This enhances free movement of the electrons and increases the number of neutral molecules for ionization.

The above processes which start almost simultaneously combine to maintain the arc during circuit breaker contacts separation in medium and high voltage systems.

2.2.4 Arc Control

During circuit breaker opening under large currents interruption, the contact area reduces, this reduced contact area causes increased current density and hence a rise in the temperature. The heat produced in the medium in between the contacts is sufficient to cause ionization of the medium. This ionized medium acts as a conductor and arc is struck between the contacts of the circuit breaker. The arc provides a low resistance path to the current. The arc provides a gradual transition from the current-carrying to the voltage

isolating states of the contacts, but it is dangerous on account of the energy generated in it in the form of heat which may result in explosive force. The circuit breaker should be capable of extinguishing the arc without causing any damage to the equipment or any danger to the operating personnel. Ionization of medium in between the contacts and potential difference across the contacts are responsible for the production and maintenance of arc. Reduction in the level of fault current being interrupted lowers the ionization process and thus is a good measure for controlling the arc (Nagrath and Kothari, 2004).

For arc extinction, the separation between the contacts can be increased to such an extent that potential difference across the contacts is not sufficient enough to maintain the arc. But this philosophy is impractical as: in extra high voltage (EHV) systems, the separation between the contacts to extinguish the arc can be many meters which is not practically achievable (Electricalbaba, 2017). Another way for extinction of arc is to de-ionize the medium in between the contacts. If the arc path is de-ionized, the arc extinction will definitely be facilitated. This may be achieved by cooling the arc or by quickly removing the ionized particles from the space in between the contacts. This principle of arc extinction is used in all modern Circuit Breakers. In AC circuit breakers, current interruption takes place at the natural zero of the current wave.

2.2.5 Restriking Voltage

At current zero, a high frequency transient voltage appears across the breaker contacts and is caused by the rapid distribution of energy between the magnetic and electric fields associated with the plants and transmission lines of the power system. This transient voltage defined as the resultant transient voltage which appears across the breaker contacts at the instant of arc extinction is known as the restriking voltage. It has a profound influence on the arc extinction process. It tends to maintain the arc at current zero (i.e. under its influence, the arc tries to re-strike). The restriking voltage is of higher natural frequency than the power frequency system voltage, but vanishes rapidly after a short time of the order of 0.1ms, due to damping effect of system resistance (Gupta, 2012).

2.2.6 Recovery Voltage

This is the power frequency root mean square (rms) voltage which appears across the breaker contacts after the transient oscillations die out and final extinction of arc has resulted in all the poles.

2.2.7 Restriking Voltage Transient

This is the voltage that tends to re-establish the arc in a circuit breaker when the circuit breaker is opened under fault condition. According to Gert (1968) and Gert and Valasek (1982), a positive linear correlation exists between the magnitudes of the interrupted fault currents and Transient Restriking Voltage, (TRV). Considering a simple circuit shown in Figure 2.5 having a Circuit Breaker (CB) and with a short-circuit on the feeder close to the bus bar; the equivalent circuit also shown in Figure 2.6. If L is the inductance per phase of the system up to the fault point, R is the resistance per phase of the system up to the fault point and C the capacitance to earth of the circuit breaker porcelain bushing. If the circuit breaker is opened under fault condition shown in the equivalent circuit in Figure 2.6, before current interruption, the capacitance, C , is short-circuited by the fault and the short circuit current through the breaker is limited by the resistance, R , and the inductance, L , of the system.

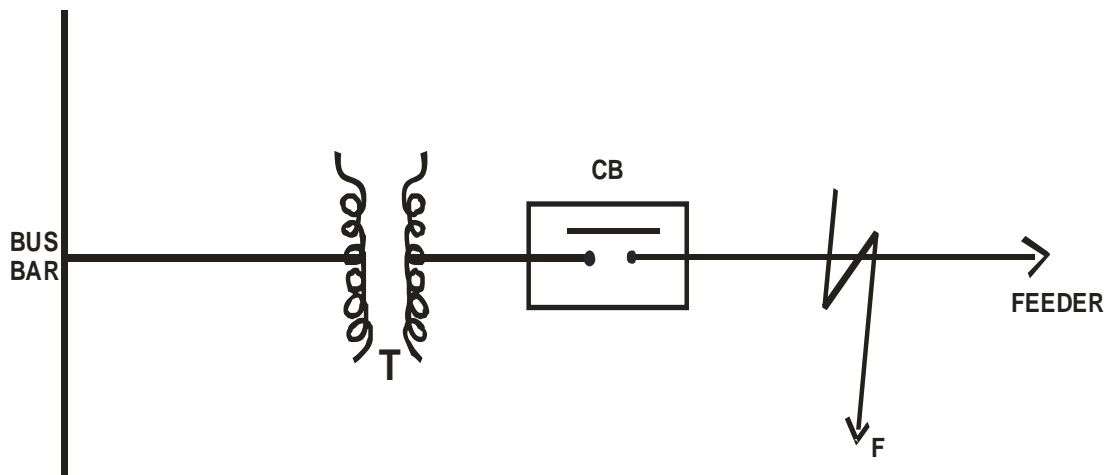


Figure 2.5: Short Circuit Fault on a feeder (Gupta, 2012)

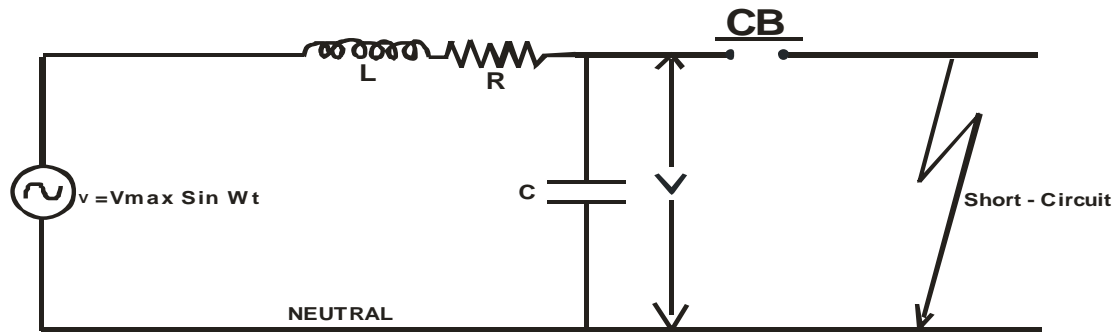


Figure 2.6: Equivalent circuit diagram of figure 2.5 (Gupta, 2012)

2.2.8 Effects of Short Circuit Current on Arc Phenomena

Circuit breakers are rated both by the normal current that they are expected to carry and the maximum short circuit current that they can safely interrupt (Wikipedia, 2014). Under short circuit conditions, a current many times greater than normal can exist. When electrical contacts open to interrupt a large current, there is a tendency for an arc to form between the opened contacts, which would allow the current to continue. This condition can create conductive ionized gases and molten or vapourized metals, which can cause further continuation of the arc, or creation of additional short circuits, potentially resulting in the explosion of the circuit breaker. According to Kopplin (1980), the use of SF₆ gas as arc quenching and insulating medium plays a role in mitigating this problem when very high short circuit currents are anticipated. However, it is not absolutely all that is needed to mitigate the problem.

2.3 Current Limiting Techniques

Some short circuit current limitation techniques are given as:

2.3.1 The Current Limiting Reactors (CLRs)

According to Trench Group, (2014) and Wikipedia (2014), of the numerous short circuit current reduction techniques available, Current Limiting Reactor (CLR) is the most practical; it can reduce short circuit current, which results from plant expansion and power source additions, to levels within the rating of the equipment on the load side of the reactor.

According to Amon et al, (2005) and Geng et al, (2008), this is a well-known current limiting technique. Compared with many other methods, it is more economical. In addition, its effect on the reliability of substation is negligible. However, according to Peelo et al, (1996) and Khorrami et al, (2010), it occupies a relatively large area in the substation.

The Current Limiting Reactor (CLR), apart from limiting short circuit current can also provide wave shape smoothing and absorb transients caused by phase fired Silicon Controlled Rectifiers (SCRs), and provide protection to the HV rectifiers and the controller SCRs by limiting the current flowing during an arc or spark (Nwl, 2014), (Neundorfer, 2014). Due to the linear inductance-characteristics over the current range, the full reactor impedance is also maintained during system fault conditions (coilinnovation, 2011).

Other special applications of current limiting reactors are:

- (1) Load balancing reactors for load sharing in parallel circuits
- (2) Bus tie reactors installed between two different bus systems
- (3) Capacitor inrush current limiting or damping reactors

The use of current limiting reactors in limiting short circuit currents is however limited to critical feeders due to the constant power losses that it imposes on the system, as it carries the full load current (Gupta, 2012) and the voltage transients caused by the added reactance which stresses system insulation levels, with motor windings as one of the biggest worries (Vincent-Saporita, 1999).

The reactors are of two types namely: Dry (Open) and Oil-immersed. In open type construction, circular coils of bars of stranded copper are embedded in a number of specially shaped concrete slabs. The whole is placed on a concrete base and mounted on porcelain footstep insulators. Reactors of this type are very simple from the construction point of view and are robust but have got the following disadvantages:

1. Large space is required because the magnetic field on account of load current is practically unrestricted.

2. Difficulty is experienced in cooling of large coils by fans.
3. These are unsuitable for indoor services.
4. Their use is limited to the voltage of 33kV

The oil-immersed type reactors employ insulation and cooling arrangement similar to those of the ordinary transformers. In an air-cored construction, there must be laminated-iron shields or copper shields around the outside of the conductors in order to prevent the magnetic flux entering the tank walls and causing excessive losses and heating. In iron-cored construction, air gaps are introduced in the core to prevent saturation and to give a magnetizing current of the desired value. Oil-immersed type reactors are used for voltages above 33kV (Coil Innovation, 2011).

A typical current limiting reactor is as shown in Figure 2.7 (Cooperindustries, 2016), while Figure 2.8 shows current limiting reactor in circuit (Mkireps, 2016).

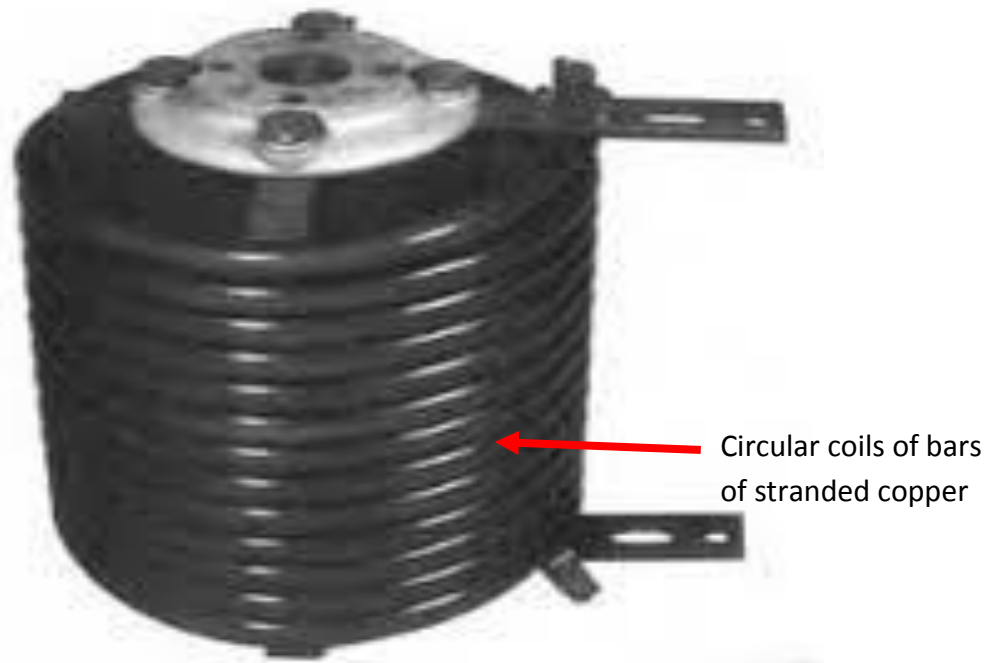


Figure 2.7: Current Limiting Reactor (Cooperindustries, 2016)



Figure 2.8: CLR in circuit (Mkireps, 2016)

2.3.1.1 Selection of CLR Inductance

Appropriate value of the CLR inductance, L , is dependent on the system under study. In Figure 2.9, maximum short circuit current of a simulated system is depicted as a function of CLR reactance, ωL (Seyedi and Barzan, 2012).

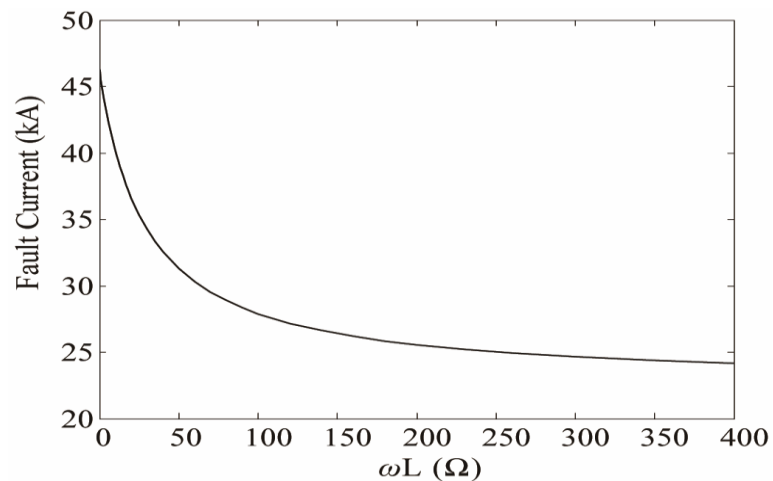


Figure 2.9: Effect of inductance on fault current level (Seyedi and Barzan, 2012).

As seen in Figure 2.9, as the inductance L increases, the slope of the $I_{SC} - L$ curve keeps decreasing until the efficiency limit (in this case, 50Ω) is reached, beyond which variation of L will not significantly change I_{SC} . From the short circuit reduction point of view, this efficiency limit is an effective value for ωL (Geng et al, 2008). However, in practice,

since transient stability, voltage stability and transient restriking voltage (TRV) restrictions should also be taken into consideration; ωL is not necessarily selected to be the effective value.

2.3.2 Fault Current Limiters (FCL)

A Fault Current Limiter (FCL) limits the amount of current flowing through the system and allows for the continual, uninterrupted operation of the electrical system, similar to the way surge protectors limit damaging currents to household devices. Currently, two broad categories of FCL technologies exist: solid-state technology and high-temperature superconducting technology (Walter et al, 2009).

(1) Solid State Fault Current Limiters (SSFCLs)

SSFCLs apply power electronic switches. Ahmed et al, (2004) and Karady, (1992) affirmed that these limiters are, practically restricted to the distribution voltage level. Moreover, they are complicated and expensive. Some types of SSFCLs apply series resonance or parallel resonance circuits.

(2) Superconducting Fault Current Limiters (SFCLs)

Lee et al, (2008), Fedasyuk et al, (2008) and Noe et al, (2008) affirmed that superconducting materials such as Yttrium Barium Copper Oxide (YBCO), Niobium-titanium (NbTi) and Magnesium diboride (MgB_2) transit from superconducting state to the normal state, if exposed to high current levels. Due to this feature of superconductors, they can be applied as fault current limiters. During normal operation of power system, SFCL resistance is negligible. However, as soon as the fault current shows up, SFCL quenches and consequently its resistance increases considerably.

FCLs offer numerous benefits to electric utilities. For instance, utilities spend millions of dollars each year to maintain and protect the grid from potentially destructive fault currents. These large currents can damage or degrade circuit breakers and other expensive Transmission and Distribution system components. Utilities can reduce or eliminate these replacement costs by installing FCLs. Other benefits include:

- (1) Enhanced system safety, stability, and efficiency of the power delivery systems
- (2) Reduced or eliminated wide-area blackouts, reduced localized disruptions, and increased recovery time when disruptions do occur
- (3) Reduced maintenance costs by protecting expensive downstream Transmission and Distribution system equipment from constant electrical surges that degrade equipment and require costly replacement.
- (4) Improved system reliability when renewable, Distribution and Generation are added to the electric grid.
- (5) Elimination of split buses and opening bus-tie breakers
- (6) Reduced voltage dips caused by high resistive system components
- (7) Single to multiple fault protection plus automatic resetting

Detlev and Herbert, (2015) affirmed that the desired characteristics of ideal Fault Current Limiters (FCLs) are:

- (i) Increase the impedance on the line well before the first fault peak (when the most damage occurs).
- (ii) In normal operation, it is virtually "transparent" (no power or voltage loss) to the network.
- (iii) Diminish the fault current by at least a factor of 2 for its duration.
- (iv) Return the source impedance to its original value when fault is cleared.

Resistive, inductive and transformer type SFCLs are important types of this device (Choi and Lim, 2007). This limiter seems to be an ideal fault current limiter; however, according to Lin et al (2007) and Janowski et al, (2003), it is still too expensive, especially due to the cost of its complicated cryogenic system. A typical Superconducting Fault Current Limiter is as shown in figure 2.10 (Electricaltechnology, 2016).



Figure 2.10: Superconducting Fault Current Limiter (Electricaltechnology, 2016)

2.3.3 Fuse

Fuse is a fast short circuit interrupting device. It is simple and cost-effective. A current limiting device is one that reduces the peak let-through current to a value substantially less than the potential peak current that would occur if the current – limiting device were not used (Cbi-electric, 2012), (Chao, 1995). When applied to current limiting fuses, a current-limiting fuse opens and clears the current in less than $\frac{1}{2}$ of an AC cycle (i.e. 0.0083 seconds, for a 60Hz system or 0.01 seconds, for a 50Hz system). Figure 2.11 shows the maximum instantaneous peak current during the first $\frac{1}{2}$ cycle after initiation of a fault.

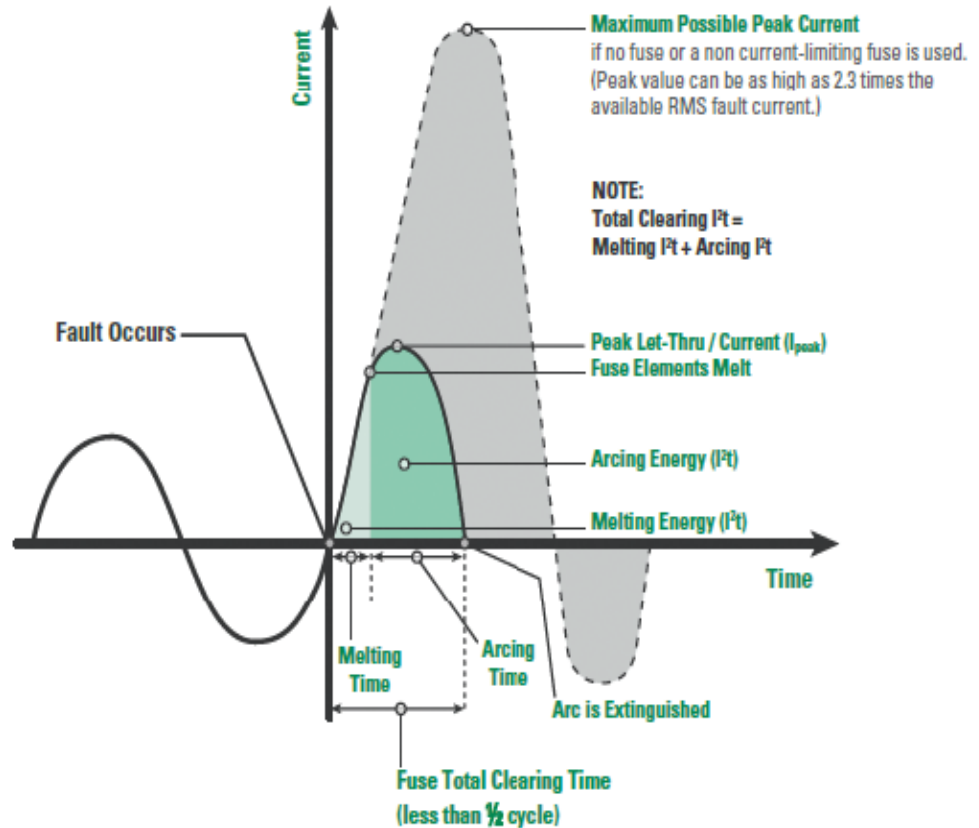


Figure 2.11: Current Limitation and peak let-thru current (Cbi-electric, 2012)

Depending on the power factor and when the fault occurs, the maximum possible instantaneous peak current (I_{peak}) without current limitation can be 2.3 times the available rms fault current when the fault occurs. As shown, if a current-limiting fuse is used, the maximum instantaneous peak current is limited to a small fraction of the peak current that could possibly flow if the fuse were not used. The current-limiting fuse link melts and clears the circuit in less than 0.0083 or 0.01 seconds for a 60Hz or 50Hz system respectively. The area under the curve is known as the I^2t let-thru energy of the fuse. The lower the I^2t is, the lower the destructive energy is that passes through the circuit before it is interrupted.

The Short Circuit Current Rating (SCCR) refers to the maximum current, usually expressed in kA at a specified voltage, that a device or system can safely withstand for a specified time (such as 0.05 seconds), or until a specified fuse or circuit breaker opens and clears the circuit (Littlefuse, 2007). It is important to point out that the SCCR of

components or panels is expressed in rms kA and not in instantaneous peak current (I_{peak}). Root-Mean-Squared current is an expression of effective current over a period of time. As already discussed, if a short circuit occurs, the instantaneous peak current can be up to 2.3 times the available rms current at the point of the fault. In other words, if the available rms short circuit current were 10 kA, the I_{peak} could be 23 kA. Conversely, if the I_{peak} of a current-limiting fuse is 23 kA, the equivalent or apparent rms value is 0.435 times the I_{peak} , or 10 kA. When properly applied, current-limiting fuses will limit the I_{peak} and apparent rms short circuit current to a level that the rest of the panel can safely handle.

However, fuse has the following shortcomings: it is technically restricted to below 40kV nominal voltages and 200A nominal currents. Fuse must be replaced, following every interruption and as such, may not be used when high speed auto-reclosing is required (Fahnoe, 1970).

2.3.4 Short Circuit Current Limiter (I_s -Limiter)

The trend towards higher line kVA ratings and the growing intermeshing of power systems are increasing the likelihood that distribution switchboards will be subjected to unacceptably high short circuit currents. Reliable and economic protection against these surge currents is provided by the I_s -limiter. This fast-acting switching device triggers a small charge to open the main conductor, which is designed to carry high operating currents. The current commutates to a parallel fuse with high breaking capacity, which limits the short circuit current during the first rise (Hartung, 2017). Such a fast switching device caters for a variety of applications which cannot be fulfilled by conventional switches.

2.3.5 Power System Reconfiguration

This approach is, to some extent, empirical. There is no definite rule for this method. In other words, it is case dependent. It also depends on parameters such as creativity and familiarity of the engineer with the system under study. In many cases, it may result in considerable reduction of fault current level. Moreover, it may improve transient stability and voltage stability of the system (Seyedi and Barzan, 2012).

2.3.6 Bus Bar Splitting Techniques in the Substations

In this approach, in order to reduce fault current level, bus section or/and bus coupler circuit breakers are opened. Power system operators are seriously opposed to this approach. Their disagreement is mainly due to the fact that bus bar splitting significantly reduces the reliability of the substation. Moreover, it affects the integrity of the system, which may result in lower transient stability and voltage stability margins. However, from the short circuit reduction point of view, this method is more effective than CLR. This is due to the fact that bus bar splitting is equivalent to application of a CLR with infinite reactance. Meanwhile, this method may be considered as a temporary strategy which is acceptable only in emergency situations (Frontin et al, 1982).

2.3.7 Application of High Impedance Transformers

Using high impedance transformers may result in the considerable reduction of fault current level. However, the undesired effects on transient stability and voltage stability might be significant (Seyedi and Barzan, 2012).

2.3.8 High Voltage Direct Current (HVDC) Links

Replacement of the lines with HVDC links will diminish inter-area short circuit currents. This will, obviously, restrict fault current levels. However, in most cases, this method is not economically justified (Zhang et al, 2006).

2.3.9 Higher Voltage Transmission Networks

Here, the existing power system is split to several islands. Afterwards, a higher voltage system is designed and then the islands are reconnected through the higher voltage network (Nasiri and Barahmandpour, 2006), (Gilany and Al-Hasawi, 2009). This method does not seem to be practical, as it is both complicated and costly.

2.3.10 Application of Neutral Reactor

Reactors applied in the neutral of transformers limit the earth fault current level. As the majority of faults include ground, this method may be considered as an effective approach (Nasiri and Barahmandpour, 2006).

2.3.11 Disconnection of some Lines from the Critical Substation

In this technique, in order to reduce bus bar short circuit level, two transmission lines are disconnected from the bus bar. Afterwards, these lines are reconnected together, outside the substation. This technique, like the bus bar splitting method, is not acceptable, from the power system operation point of view. This approach has the disadvantages of undesired effects on the reliability, transient stability and voltage stability of power system (Seyedi and Barzan, 2012).

2.4 Adapter

An adapter is a connector for joining parts or devices having different sizes, designs, etc., to enabling them to be fitted or to work together. An electrical adapter or adaptor on the other hand is a device that converts attributes of one electrical device or system to those of an otherwise incompatible device or system. Some modify power or signal attributes, while others merely adapt the physical form of one electrical connector to another. Put in another way, it is a device used to connect an electrical appliance to a power source with a different voltage or a different plug shape, or to connect several appliances to one outlet.

Adapters are used virtually in all fields of engineering and can be used to couple a circuit breaker and current limiting reactor connected in parallel with a conducting bar. Here, this is made possible by modifying the circuit breaker terminal to a relay operated adaptive terminal. This shall be presented latter in this work (Wikipedia, 2017).

2.4.1 Power System Protection using Adaptive Circuit Breaker (CB) Terminals

In addition to generators, transformers, and transmission lines, other devices are required for the satisfactory operation and protection of a power system (Saadat, 2002). The use of adapters in the CB terminals requires the protective system.

A protective system is formed by the Current Transformers (CTs), Voltage Transformers (VTs), Protective Relays, and Circuit Breakers etc. The functions of protection are performed by the teamwork of the following components as summarized in Table 2.1 (Uppal and Rao, 2012).

Table 2.1: Components of the Protective System and their Functions

S/N	Equipment	Location	Function
1.	Protective relays	On control panels in the control room.	To sense the fault and close trip-circuit of Circuit Breakers.
2.	Control cables	Between the Current Transformers (CTs)/Voltage Transformers (VTs) in switchyard and control panels.	For protective circuits between CTs/VTs and relays.
3.	Trip-circuit cables	Between battery room, control boards and CBs in the switchyard.	For trip-circuit between protective relays and Circuit Breaker trip coil.
4.	Circuit breakers	In outdoor yard and also in auxiliary switchgear room.	Opening and fault clearing.

Source: Uppal and Rao, (2012)

2.5 Review of Related Literature

2.5.1 Circuit Breaker Contacts in Medium and High Voltage Systems

Nasrallah et al, (2007) and Zensol, (2007) who worked on the Make/Break Contacts in Circuit Breakers towards ensuring that they withstand the Arc's heat without excessive damage and as well have good conduction to Electricity flow, combined the properties of tungsten and tungsten alloys that have good resistance-to-arc properties but less conductivity as well as copper and silver that have great conductivity but relatively poor resistance-to-arc properties. Also, because the contacts have to overcome the deposition of

by-products that may become a problem if not wiped off before an insulating layer is built; their work resulted in sliding contacts with the moving contact being straight.

The moving contact and the stationary contact touch on closing and slide into each other to a certain distance before stopping at closed position. On opening, they slide out until their separation and the arc's ignition. This is as shown in figure 2.12. The sliding action helps to wipe off the deposited by-products, to make better contact on closing. This type of contact usually separates the resistance-to-arc role from the current carrying role by using tungsten alloy based contacts called arcing contacts that are meant to close first on closing and separate last on opening and are submitted to the arc. The current carrying role is attributed to copper or silver plated copper contacts called main contacts. These contacts are not subjected to the arc and therefore not eroded by it.



Figure 2.12: Tulip Contacts in Dell-Alsthom air-blast Circuit Breaker (Nasrallah et al, 2007).

2.5.2 Arc Control in Circuit Breakers

Schaad (1980), Bachofen (1980) and Studyelectrical, (2014) in their work on Sulphur Hexafluoride (SF₆) gas Circuit Breakers, used peculiar characteristic of Sulphur Hexafluoride (SF₆) gas to achieve rapid arc extinction. Under high pressure flow the gas rapidly absorbs the free electrons in the arc path to form immobile negative ions which are ineffective as charge carriers. In the closed position of the circuit breaker, the contacts remain surrounded by sulphur hexafluoride gas at a pressure of about 2.8 kg/cm². When the circuit breaker operates, the moving contact is pulled apart

and an arc is struck between the contacts. The movement of the moving contact is synchronized with the opening of a valve which permits sulphur hexafluoride gas at 14 kg/cm^2 pressure from the reservoir to the arc interruption chamber. The result is that the medium between the contacts quickly builds up high dielectric strength and causes the extinction of the arc.

Christie and Pelleymounter, (2013) in their work on arc inhibition, arc quenching, and dissipation of energy stored in output cables, used voltage reversal principle to inhibit arc formation and to swiftly quench arcs when they do occur. To suppress arc formation, voltage is reversed on a periodic basis, dissipating energy buildup in insulating materials deposited on the target surface during reactive sputtering.

According to Carter, (2007) and Carter et al, (2007), to quench arcs, voltage reversal temporarily removes energy in response to process conditions that indicate an arc event. It reduces arc events occurring even on metal targets by an order of magnitude or more. This lowers arc energy typically to below 1 mJ/kW , which significantly decreases particulate generation and film damage (Scholl, 1994).

Geoff Drummond of Advanced Energy authored the patent for this technique, “Thin-Film DC Plasma Processing System.” This patent describes the invention of voltage reversal with pulsed DC, with time frames and reversal magnitudes that enable practical industrial reactive sputtering processes (Drummond, 1995).

A power supply with voltage reversal capability periodically reverses target voltage to about one-tenth of the operating target voltage, which is generally slightly more positive than the plasma potential. This dissipates energy buildup on insulating regions on the target, in the plasma, on the magnetron, and in the power supply’s output stage and cabling, while maintaining plasma stability. During the reversal, electrons are delivered to the target surface, which discharges ions on any insulating layers (Belkind et al, 2000).

According to Gupta, (2012), the rate of change of current when operating a CB ($\frac{di}{dt}$), plays a key role in the management of arc/heat energy generated. This is explained below:

When contacts of circuit breakers are opened in medium and high voltage systems, the voltage drop during arc formation is in phase with the arc current since the arc path is

purely resistive. Current interruption at natural zero of current wave adopted in A.C circuit breakers can be explained using Figure 2.13.

The current passes through the zero point on the current wave shown in Figure 2.13 one hundred times per second for a 50Hz system. If the interruption is done when the current is at the zero point in the waveform, no arc shall be encountered. In between these zero limits in current wave, the current rises to maximum and drops back to zero. Due to the restriking voltage, energy is generated between the two contacts of the circuit breaker. This energy is in the form of heat. Measures should be provided to take care of this heat either by cooling or by air blasting. If the rate of cooling is faster than the rate of heat generation, the arc is extinguished; otherwise, the arc re-strikes in another half cycle. The voltage across the circuit breaker contacts at the instant of an arc being extinguished is called the restriking voltage and is shown in Figure 2.13.

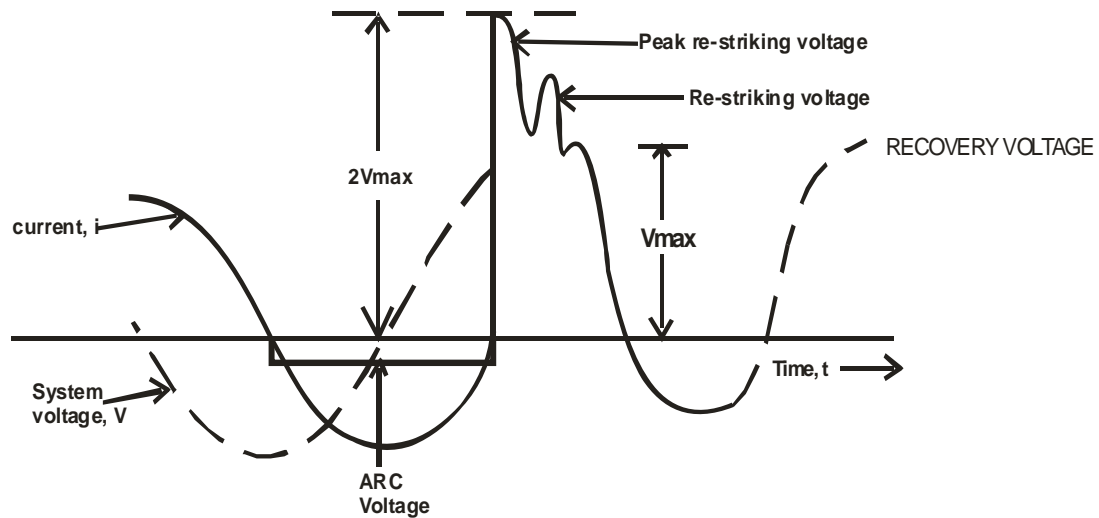


Figure 2.13: Waveforms of short circuit current and system voltage when operating a CB
(Gupta, 2012)

Before opening the circuit breaker;

The interrupted currents = 0

And

$$t = 0,$$

$$V = V_{max} \cos \omega t$$

$$I = \frac{V_{max}}{\omega L} \sin \omega t$$

$$\frac{dI}{dt} = \frac{V_{max}}{\omega L} \omega \cos \omega t$$

And at $t = 0$:

$$\frac{dI}{dt} = \frac{V_{max}}{L} \tag{2.1}$$

From Figure 2.6 in section 2.2.7, with the contacts opened and the arc broken, the current, I , is diverted through the capacitor C , so that the voltage, V , which has so far been effective only across the inductance, L , is suddenly applied to the inductance, L , and capacitance, C in series, which form an oscillatory circuit having a natural frequency:

$$f_n = \frac{1}{2\pi} \sqrt{\frac{1}{LC}} \text{ Hz} \tag{2.2}$$

The initial charging current surge tends to carry the voltage across the capacitor and therefore the circuit breaker contacts to double its equilibrium value, i.e. $2V_{max}$. This is the restriking voltage transient.

When the arc finally extinguishes at some current zero in the current waveform shown in Figure 2.13 following the opening of the circuit breaker contacts, a voltage, v , is suddenly applied across the capacitor, and therefore across the circuit breaker contacts. The current, I , which would flow to the fault, is now injected in the capacitor and inductor (Gupta, 2012). Thus:

$$I = I_L + I_C$$

Or

$$I = \frac{1}{L} \int v dt + C \frac{dv}{dt}$$

$$\therefore \frac{dI}{dt} = \frac{v}{L} + C \frac{d^2v}{dt^2} \tag{2.3}$$

Substituting $\frac{V_{max}}{L}$ for $\frac{dI}{dt}$ as given in (2.1) into (2.3), gave

$$\frac{V_{max}}{L} = \frac{v}{L} + C \frac{d^2v}{dt^2}$$

Or

$$V_{max} = v + LC \frac{d^2v}{dt^2} \quad (2.4)$$

Solving (2.4) by Laplace transforms (Stroud, 2005),

$$LCS^2v(s) + v(s) = \frac{V_{max}}{s}$$

$$v(s)[LCS^2 + 1] = \frac{V_{max}}{s}$$

Or

$$v(s) = \frac{V_{max}}{s[LCS^2 + 1]}$$

Or

$$v(s) = \frac{V_{max}}{LCS\left(s^2 + \frac{1}{LC}\right)} \quad (2.5)$$

But

$$\omega_n = \frac{1}{\sqrt{LC}}$$

Such that

$$\omega_n^2 = \frac{1}{LC}$$

So that (2.5) is written as

$$v(s) = \frac{\omega_n^2 V_{max}}{s(s^2 + \omega_n^2)}$$

Or

$$v(s) = \frac{\omega_n V_{max}}{s} \left(\frac{\omega_n}{s^2 + \omega_n^2} \right) \quad (2.6)$$

The inverse Laplace transform of (2.6) is

$$\begin{aligned} v(t) &= \omega_n V_{max} \int_0^t \sin \omega_n t dt \\ &= \omega_n V_{max} \left[\frac{-\cos \omega_n t}{\omega_n} \right]_0^t \\ &= V_{max} \left[1 - \cos \frac{t}{\sqrt{LC}} \right] \end{aligned}$$

Or

$$v = V_{max} (1 - \cos \omega_n t) \quad (2.7)$$

This is the expression for restriking voltage

Where:

$$\omega_n = \frac{1}{\sqrt{LC}} = \text{Angular natural frequency}$$

V_{max} = Peak value of recovery voltage (phase-to-neutral),

t = Time in seconds,

L = Inductance in henries,

C = Capacitance in farads and,

v = Restriking voltage in volts.

Restriking voltage has a maximum value of $2V_{max}$ and occurs at

$$t = \frac{\pi}{\omega}$$

Or

$$t = \pi\sqrt{LC}$$

For restriking voltage having a maximum value of $2V_{\max}$ means that examining (2.1), it can be inferred that with high value of the interrupted current (I), the restriking voltage will be high. So, limiting the anticipated fault current with the CLR does very well in reducing the restriking voltage of the arc.

The Rate of Rise of Restriking Voltage (RRRV) is an important characteristic of restriking voltage which affects the performance of a circuit breaker. The rate of rise of restriking voltage (RRRV) is the slope of the steepest tangent to the restriking voltage curve, expressed in kV/ μ s (Gupta, 2012).

$$RRRV = \frac{dv}{dt}$$

Where

v = Restriking Voltage.

From (2.7)

$$v = V_{\max}(1 - \cos \omega_n t)$$

So that

$$RRRV = \frac{dv}{dt}$$

Or

$$RRRV = \frac{V_{\max}}{\sqrt{LC}} \sin \frac{t}{\sqrt{LC}} \quad (2.8)$$

Where:

$$\omega_n = \frac{1}{\sqrt{LC}}$$

Maximum value of RRRV occurs when

$$\sin \frac{t}{\sqrt{LC}} = 1$$

Or

$$t = \frac{\pi}{2} \sqrt{LC}$$

Such that:

$$RRRV_{max} = \frac{V_{max}}{\sqrt{LC}} \quad (2.9)$$

It can again be seen from (2.1) and (2.9) that with high value of the interrupted current (I), the RRRV will be high. So, limiting the anticipated fault current with the CLR does very well in reducing the RRRV of the arc.

2.5.3 Operating Mechanism Energy of Circuit Breakers

Circuit Breakers require operating mechanism energy to accelerate the moving parts of the circuit breaker and to create the requisite pressure for arc quenching. The level of arc anticipated determines the size of the operating mechanism stored energy. This energy, in a pneumatic operating mechanism circuit breaker, is stored in a gas container; in a spring operating mechanism circuit breaker, it is stored in the springs; in a hydraulic operating mechanism circuit breaker, this energy is stored in the hydraulic pump, while in a power electronic based operating mechanism type circuit breaker, it is stored in a capacitor bank.

Bachofen et al, (1982), in their work on Circuit Breakers of High Rated Capability with Low Operating Mechanism Energy, identified the kinetic energy requirement, W_{KIN} , the blast pressure, ΔP , necessary for arc quenching and the moving contact cross-sectional area, A , as the key parameters that determine the operating mechanism energy of Circuit

Breakers, such that their reduction leads to reduction in the Operating Mechanism Energy of the circuit breaker.

2.5.4 Resistance Switching

Gupta, (2012), who worked on Resistance Switching in circuit breakers used a deliberate connection of a resistor in parallel with the contact space (or arc) in circuit breakers having high post zero resistance of contact space (i.e. air-blast circuit breakers).

On occurrence of fault, the contacts of the circuit breaker open and an arc is struck between the contacts. With the arc shunted by the resistor, a part of the arc current is diverted through this resistor. This results in the decrease of the arc current and an increase in the rate of deionization of the arc path. Thus the arc resistance is increased leading to a further increase in the current through the shunt resistance. This build up process continues until the current becomes so small that it fails to maintain the arc. The arc is then extinguished and the current gets interrupted. Alternatively, for an axial blast circuit breaker, the resistor can be automatically switched-in by transference of the arc from the main contacts to the probe contact. The time required for this action is very small (usually less than one half-cycle of the current wave). The effect of the shunt resistor R is to prevent the oscillatory growth of restriking voltage and cause it to grow exponentially up to recovery voltage. This is being most effective when the value of R is so chosen that the circuit is critically damped. The value of R that gives critical damping

$$\text{is } 0.5\sqrt{\frac{L}{C}}.$$

2.5.5 Limiting Short Circuit Current via Short Circuit Current Limiters (I_s-Limiters)

The I_s-limiter is an improved version of the fuse. During normal operation of this device, major portion of current passes through a path parallel with the fuse. When short circuit occurs, the parallel part is opened using electro-dynamic forces of fault current. Consequently, the fault current is commuted to the fuse. This way, the problem associated with the limited nominal current of fuse is resolved. I_s-Limiter is claimed to be capable of interrupting fault currents up to 5kA within 1 millisecond after occurrence of the fault. However, it is still limited to 40kV rated voltage (Hartung, 2002)

Hartung, (2017), who worked on the applications of the I_s -Limiter to reduce high short circuit currents, noted that the trend towards higher line kVA ratings and the growing intermeshing of power systems are increasing the likelihood that distribution switchboards are subjected to unacceptably high short circuit currents. He affirmed that reliable and economic protection against these surge currents can be provided by the I_s -limiter.

2.5.6 Limiting Short Circuit Levels with Current Limiting Reactors

Gupta, (2012), worked on the application of series reactors to limit short circuit current and concluded that series current limiting reactors can be employed on feeders to reduce short circuit level considerably such that circuit breakers of lesser breaking capacity would be needed. However, the reactors under this arrangement carry the full load current and so, constitute enormous constant power losses in the system.

Malik, (2017) and Klaus et al, (2009) in their work on the use of reactors on the power system concluded that series reactors on feeders are necessary to reduce the flow of current into a short circuit so as to protect the power system apparatus (especially, the circuit breaker) and parts of the system from excessive mechanical stress and overheating, and to localize the faults by limiting the current that flows into the fault from other healthy feeders or part of the system.

Nair, (2016) also affirmed that to reduce the duty imposed on switching equipments namely: the circuit breaker, during short circuits, series current limiting reactors are needed

2.5.7 Parallel Operation of Short Circuit Current Limiters (I_s -Limiters) and Reactors

Dreimann et al, (1994) in their work on avoiding the constant power losses incurred when current limiting reactors are used, and Brandt et al, (2012) in their work on Limitation of Short-circuit Currents for Maximum Economic Benefits, employed parallel operation of I_s -Limiter and reactor method such that if system components are not to be totally isolated in the case of a short circuit, but further supplied via a short circuit current limiting reactor, the reactor can be bridged by an I_s -limiter in normal operation, so as to avoid the copper losses, voltage fluctuations which would otherwise occur

during load changes and the electro-magnetic influences caused by the reactor. I_s -limiter and a reactor connected in parallel are as shown in Figure 2.14.

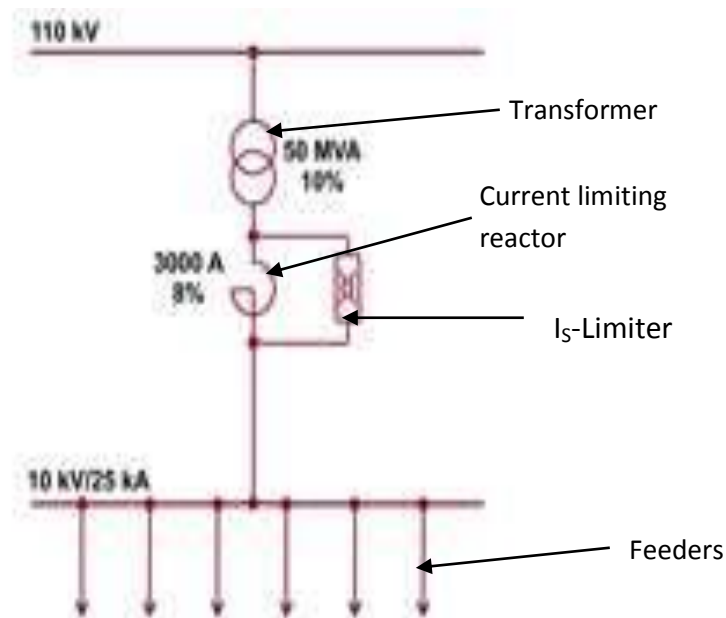


Figure 2.14: I_s -limiter and reactor connected in parallel (Brandt et al, 2012)

2.5.8 Relay Co-ordination

GEC, (1987) in the work on Protective Relay Application, affirmed that correct current relay application requires knowledge of the fault current that can flow in each part of the network. Since large scale tests are normally impracticable, system analysis must be used. It is generally sufficient to use machine transient reactance, X_d and to work on the instantaneous symmetrical current.

The basic rules for correct relay co-ordination can generally be stated as follows (GEC, 1987):

- (1) Whenever possible, use relays with the same operating characteristics in series with each other.
- (2) Make sure that the relay farthest from the source has current setting equal to or less than the relays behind it. That is, the primary current required to operate the relay in front is always equal to or less than the primary current required for operating the relay behind it.

2.6 Summary of the Reviewed Works

- (a) Limiting fault current lowers arc energy in circuit breakers.
- (b) Limiting fault current lowers the restriking voltage in circuit breakers.
- (c) Current limiting reactor technique is the most practical technique for limiting fault current.
- (d) In resistance switching, the value of the resistance 'R' is limited by the circuit inductance 'L' and the capacitance 'C', since 'R' must be $0.5\sqrt{L/C}$ for critical damping.
- (e) Straight moving contacts are used in existing circuit breaker designs. This means that if current limiting reactors will be used on our systems, they must be permanently connected in series.
- (f) The energy required for closing/opening operation (i.e. the operating mechanism energy) of a circuit breaker is directly proportional to the fault current rating of the circuit breaker.

2.7 Research Gaps

Based from the reviewed literature, it is seen that several advances have been made towards controlling arc in medium and high voltage systems. Substantial achievements have been made but the following gaps still need to be bridged:

- (1) The magnitude of arc generated when operating a CB needs to be reduced.
- (2) The power losses incurred when current limiting reactors are use on feeders need to be mitigated.
- (3) The heat generated when operating a circuit breaker needs to be reduced.
- (4) The operating mechanism energy requirement of a CB has to be reduced.
- (5) The increase in the reactive voltage drop when reactors are used on feeders during healthy system condition needs to be avoided.
- (6) The decreased power factor when reactors are used on feeders during healthy system condition needs to be avoided

Forked Moving Contact circuit breakers and the Relay Operated Adapters in coupling Current Limiting Reactors (CLRs) and Circuit Breakers (CBs) can be used to solve the above problems. The Forked Moving Contact circuit breakers and the Relay Operated Adapters provide means of connecting CBs and CLRs in a parallel arrangement in the circuit during healthy system condition (i.e. CB in closed position) and allow the CLR turn

in series arrangement during CB opening operation. This way, no power flows through the CLR during healthy system condition and so constitutes no constant power losses. This work is therefore targeted at modifying circuit breaker contacts and terminals and the design of Relay Operated Adapter, to solve the above problems.

CHAPTER THREE

METHODOLOGY

3.1 Methodology

The use of CLR for limiting short circuit currents is not new in the power industry. It is in fact the best available means for short circuit currents limitation. However, its use has not been properly harnessed due to the constant power losses it poses on the system since it can only be connected serially in the network. This serial connection is the only available way to connect the CLR because of the way and manner the contacts and terminals of the existing CBs are made. The existing CB by design has a straight moving contact and must be connected in series with the network to achieve its primary goal in the network, which is current interruption. The CLR also must be connected in series with the network before it can do the work of current limitation in the circuit. But the CLR must not be connected in series in the network when it is not required to limit any current; else it constitutes constant power losses.

This dissertation proffered ways to mitigate the enormous constant power losses encountered during implementation of Current Limiting Reactors (CLRs) in medium and high voltage systems. Two methods were used to achieve the objectives. One method involves circuit breaker contacts design modification - modifying the straight moving contact to forked moving contact and the other - the design of adapters for coupling CLRs and circuit breakers.

The forked moving contact has two prongs of unequal lengths. The longer prong provides a parallel path where the CLR can be connected to remain in parallel with the shorter prong through which current flows in the system when the CB is in closed position. The adapter on the other hand provides the parallel paths for current flow and CLR connection for an existing CB which has already been built with a straight moving contact.

The mathematical analysis done was verified by MATLAB codes while the power flow was simulated in POWERWORLD environment.

3.1.1 Measurement Environment

Measurements were taken at Nkalagu 132/33kV Transmission Station and Abakaliki 132/33kV Transmission Station, both in the Transmission Company of Nigeria (TCN).

3.1.2 Measurement Instrument

The following instruments were used for measurements:

1. SIEMENS 7SJ8011 current meter
2. SIEMENS SIPROTEC 7UT61 current meter
3. EDMII-MK6E Energy meter
4. ACE6000 ITRON Energy meter
5. Thread
6. Meter rule

3.1.3 Experimental Measurement and Data Collection from TCN

Items measured and their values are:

1. 132kV CB moving contact: Length = 1.2m (i.e. 120cm), Cross sectional area = $9.61 \times 10^{-4} \text{m}^2$ (i.e. 9.61cm^2)
2. Internal diameter of 132kV CB interrupter unit = 0.24m (i.e. 24cm)
3. Diameter of the circumscribing circle on 132kV CB post insulator = 0.3m (i.e. 30cm)
4. Load current on Nkalagu – Abakaliki 132kV line = 280A
5. Power factor for residential customers = 0.94
6. Power factor for commercial customers = 0.79
7. Percentage of total load current consumed by residential customers = 30%
8. Percentage of total load current consumed by commercial customers = 70%

Data collected include:

- A. Nkalagu – Abakaliki 132kV line
 1. Voltage rating = 132kV
 2. Current rating = 400A

3. Line length = 50 km
4. Positive sequence impedance (Ω/km) $Z_1 = R_1 + jX_1$

$$0.008389744435 + j0.01646580057$$

$$= 0.01848 \Omega/\text{km}$$

5. Zero sequence impedance (Ω/km) $Z_0 = R_0 + jX_0$

$$0.01775380209 + j0.06191486584$$

$$= 0.06441 (\Omega/\text{km})$$

6. Frequency = 50 Hz
7. Conductor size = 250 mm^2

B. Transformers T1 and T2 at Abakaliki 132/33kV Transmission Station

1. 30MVA 132/33kV Transformer T1 with percentage impedance of 12.3%
2. 60MVA 132/33kV Transformer T2 with percentage impedance of 10.07%

C. Electricity tariff for Enugu Electricity Distribution Company

1. Residential tariff = ₦30.93 per kWh
2. Commercial tariff = ₦45.24 per kWh

D. 132kV CB and Current Transformer (CT) data

1. CT Ratio = 500/1
2. Maximum Current setting = 400 Amperes
3. CB Relay operating time = 0.2 seconds
4. CB operating time = 0.3 seconds

3.2 System Modeling

3.2.1 Power Loss Reduction

The mathematical models for calculating the constant power losses when operating a CB in series with a CLR are as follows (Gupta, 2012):

$$P = \sqrt{3} I^2 Z_{CLR} \cos \phi \text{ Watts} \quad (3.1)$$

Or

$$P = \frac{\sqrt{3} I^2 Z_{CLR} \cos \phi}{1000} \text{ kW} \quad (3.2)$$

$$\text{kWh per month} = \frac{\sqrt{3} I^2 Z_{CLR} \cos \phi \times 24 \times 30}{1000}$$

Or

$$\text{kWh per month} = 1.25 I^2 Z_{CLR} \cos \phi \quad (3.3)$$

$$\text{kWh per annum} = 15 I^2 Z_{CLR} \cos \phi \quad (3.4)$$

Where:

I = Load Current in amperes

Z_{CLR} = Impedance of the CLR in series with the CB moving contact

$\cos \phi$ = Power Factor

P = Total Power losses in watts

Hours per day = 24

Days in a month = 30

Months in a year = 12

For power loss reduction, the CB and the CLR are connected in parallel and for the line feeding many groups of customers (i.e. many feeders with different tariff classes, for example residential feeders, commercial feeders, etc), (3.2) has been modified as (3.5), (3.3) modified as (3.6) and (3.8), while (3.4) has been modified as (3.7) and (3.9). That is:

$$P = \frac{\sqrt{3}}{1000} I^2 Z_{CB} \sum_{i=1}^n f_{di}^2 \cos \phi_i \text{ (kW)} \quad (3.5)$$

$$\text{kWh per month} = 1.25 I^2 Z_{CB} \sum_{i=1}^n f_{di}^2 \cos \phi_i \quad (3.6)$$

$$\text{kWh per annum} = 15I^2 Z_{CB} \sum_{i=1}^n f_{di}^2 \cos\phi_i \quad (3.7)$$

$$\text{Losses per month} = 1.25I^2 Z_{CLR} \sum_{i=1}^n f_{di}^2 T_i \cos\phi_i \quad (\text{naira}) \quad (3.8)$$

$$\text{Losses per annum} = 15I^2 Z_{CLR} \sum_{i=1}^n f_{di}^2 T_i \cos\phi_i \quad (\text{naira}) \quad (3.9)$$

Where:

T_i = Tariff for customer group i in naira

f_{di} = Percentage of total load current supplied to the feeder for customer group i

$\cos\phi_i$ = Power factor for the load for customer group i

Z_{CB} = Impedance of the CB moving contact in parallel with the CLR

Equation numbers (5), (6) and (7) are the models for power loss reduction in kW, kWh per month and kWh per annum respectively for the improved CB with CLR, where the CLR impedance (Z_{CLR}) is very much greater than the CB moving contact impedance (Z_{CB}), while (8) and (9) are the models for calculating the power losses in monetary terms per month and per annum respectively.

3.2.2 The Heat generated when operating a CB

When a current I passes through an area A that has a resistance R, the Energy E absorbed by A is:

$$E = I^2 R t \quad (3.10)$$

Where:

E = Heat energy generated

R = Resistance of the material

I = Current through the material

t = Time duration of I

A's temperature T is directly related to E by the following equation (Zensol, 2007):

$$T = \frac{E}{\lambda} \quad (3.11)$$

Where

λ = the function of the heat dissipation rate.

(3.10) gives the heat generated when operating a CB (Zensol, 2007).

From (3.10), with the material resistance R taken to be constant since contacts are usually fabricated with identical materials (Mechprod, 2012) and the time duration of current t being constant as well, then (3.10) can be written as:

$$E = KI^2 \quad (3.12)$$

Where:

$K = Rt$ is the constant term.

From (3.12), the model for the corresponding reduction in the generated heat energy for a given reduction in the interrupted current when operating a circuit breaker is:

$$E\% = [1 - (1 - I\%)^2] \times 100 \quad (3.13)$$

Where:

$I\%$ = Percentage reduction in the interrupted current

$E\%$ = Corresponding percentage reduction in the generated heat energy.

(3.13) is the model for reduced heat generation when operating a CB.

3.2.3 Connecting CB and CLR in parallel

Improvement on the existing circuit breaker contacts and terminals provides a suitable way to connect the current limiting reactor such that:

- (1) At healthy condition when the CB is in closed position, the current limiting reactor remains in parallel with the feeder circuit break.
- (2) At fault condition, just before the CB contacts totally separate, the current limiting reactor becomes in series with the feeder circuit breaker.

Parallel operation of the I_s -limiter and the CLR should have perfectly mitigated the constant power losses in the use of CLR on the existing CBs if not for the following shortcomings:

- (1) No matter how good the I_s – Limiter Technique is, it can only serve for systems below 40kV.
- (2) When the current Limiter operates, the copper bar and fuse in the phases that are triggered are destroyed. They must be replaced before the current limiter can be energized again.
- (3) The replacement of these components is another shortcoming of the I_s – Limiter. For instance, even when used in systems of below 40kV, the time wasted and the cost for replacing the destroyed copper bars and the fuses in event of a transient fault is of serious concern when considering the system down time.

Two possible ways to mitigate this problem are:

- (1) The use of forked moving contacts in circuit breakers. Here, the moving contact of the circuit breaker provides the path parallel to the current limiting reactor.
- (2) The use of adapters to couple current limiting reactors and circuit breakers. Here, the conducting path parallel to the current limiting reactor is provided by the adapter.

3.2.3.1 Modifying the CB Moving Contact

The modification is done with a 132kV straight moving contact rod. The dimension of the moving contact is as shown in Table 3.1. The measurement was taken in Nkalagu 132/33kV Transmission Sub-station in Transmission Company of Nigeria (TCN).

Table 3.1: Measured dimension for 132kV CB Moving Contact at TCN Nkalagu Transmission Station

S/N	Item measured	Value
1.	Moving contact length	1.2 meters
2.	Moving contact cross-sectional area	$9.61 \times 10^{-4} \text{m}^2$

Important parameters considered in the design of CB moving contact rod are:

- (1) The maximum anticipated fault current I to be interrupted
- (2) The cross sectional area A , of the moving contact.
- (3) The length l , of the moving contact

3.2.3.1.1 The Maximum Anticipated Fault Current I

A typical network: Nkalagu-Abakaliki 132kV line in the Transmission Company of Nigeria (TCN) is considered here to better appreciate this work. From Nkalagu, a 100MVA 132kV 0.62% impedance source feeds Abakaliki Transmission station via an overhead line with the data given in Table 3.2.

Table 3.2: Nkalagu-Abakaliki 132kV line data

S/N	Description	Value
1.	Voltage rating	132kV
2.	Current rating	400A
3.	Line length	50 km
4.	Positive sequence impedance (Ω/km) $Z_1 = R_1 + jX_1$	$0.008389744435 + j0.01646580057$ $= 0.01848 \Omega/\text{km}$
5.	Frequency	50 Hz
6.	Conductor size	250 mm^2

Source: Transmission Company of Nigeria (TCN), Enugu Sub-Region

The data for the transformers at Abakaliki Transmission Station is as given in Table 3.3.

Table 3.3: Transformer data at Abakaliki Transmission station

S/N	Transformer	Rating in MVA	Voltage rating (kV)	%Z
1.	T ₁	30	132/33	12.3
2.	T ₂	60	132/33	10.07

Source: Transmission Company of Nigeria (TCN), Abakaliki 132/33kV Sub-Station

From Tables 3.2 and 3.3 and other available information given earlier, the network is represented as shown in Figure 3.1.

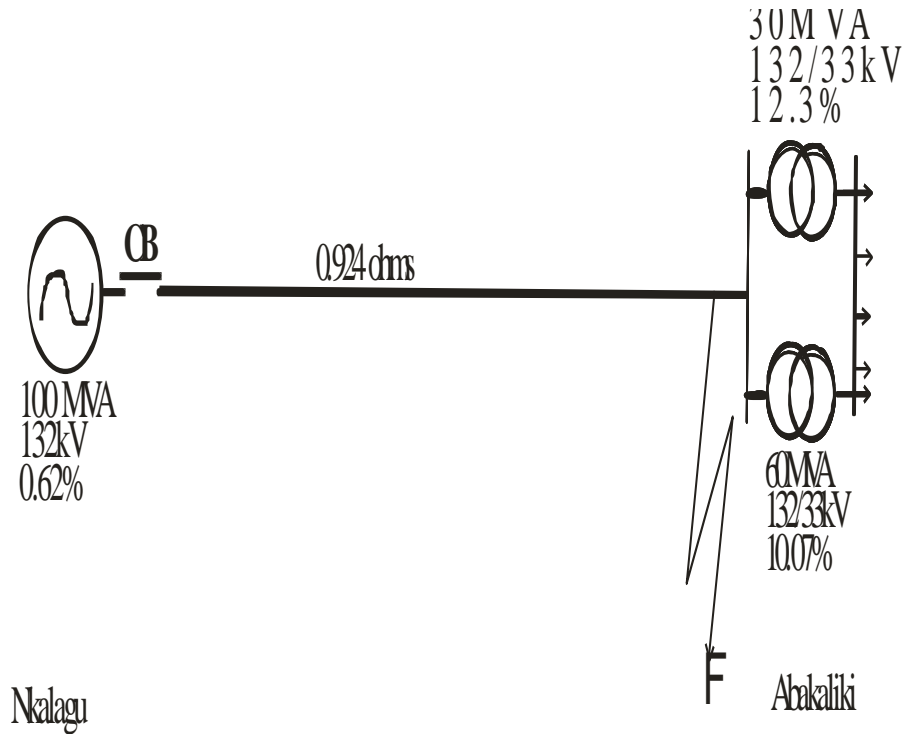


Figure 3.1: Nkalagu-Abakaliki 132kV line with the existing CB without CLR

Good idea of percentage impedance is important at this point. Percentage impedance is the voltage drop across the given impedance expressed as percentage of normal voltage when carrying full load current pertaining to normal rating, i.e.,

$$\%Z = \frac{IZ}{V} \times 100 \quad (3.14)$$

Where:

Z = Impedance in ohms

I = Full load Current

V = Rated Voltage.

According to GEC (1987), the percentage impedance affects short-circuit level in the following way:

$$MVA_f = \frac{MVA_G}{\%Z} \quad (3.15)$$

Where:

MVA = Mega-Volt-Amperes

MVA_f = Fault level in MVA which a generating source can supply to a Fault Point

MVA_G = Generating source rating in MVA

$\%Z$ = Total percentage impedance from the generating source to the fault point.

The following are standard equations for fault current calculations:

$$MVA = \frac{(kV)^2}{Z} \quad (\text{Gupta, 2012}) \quad (3.16)$$

$$kA = \frac{MVA}{\sqrt{3} \times kV} \quad (\text{GEC, 1987}) \quad (3.17)$$

$$Z = \frac{\%Z \times (kV)^2}{100 \times MVA_B} \quad (\text{Gupta, 2012}) \quad (3.18)$$

$$MVA = \frac{MVA_B}{\%Z} \quad (\text{GEC, 1987}) \quad (3.19)$$

Where:

MVA = The fault level

kV = System voltage in kilo volts

Z = System impedance from source to the fault point, in ohms

kA = Fault Current in kilo amperes

MVA_B = Base MVA

$\%Z$ = Percentage Impedance

Using (3.18), the 0.924 ohms overhead conductor results in the following percentage impedance on 100MVA base:

$$\frac{0.924 \times 100}{132^2} \times 100 = 0.53\% \text{ impedance on 100MVA}$$

For a fault F, occurring on the line just before the 132kV bus at Abakaliki Transmission Station end as shown, the total impedance from source to fault point is:

$$\begin{aligned} &0.62 + 0.53 \\ &= 1.15\% \text{ on 100 MVA base.} \end{aligned}$$

This means that the maximum fault level the system protection at Nkalagu Transmission Station sees at that point using (3.19) for 100MVA base is:

$$\begin{aligned} &\frac{100}{1.15\%} \text{ MVA} \\ &= 8696 \text{ MVA} \end{aligned}$$

Using (3.17), the maximum fault current I_f is:

$$\frac{8696}{\sqrt{3} \times 132} = 38 \text{ kA}$$

With the two transformers at Abakaliki Transmission Station connected to a common 33kV bus as shown in Figure 3.1, a fault at this bus is seen by the CB at Nkalagu Transmission Station as follows:

12.3% impedance on 30MVA transformer becomes:

$$\begin{aligned} &\frac{12.3 \times 100 \times 100}{100 \times 30} \\ &= 41\% \text{ impedance on 100MVA base} \end{aligned}$$

10.07% impedance on 60MVA transformer becomes:

$$\frac{10.07 \times 100 \times 100}{100 \times 60}$$

= 16.78% impedance on 100MVA base.

But the two transformers are in parallel, so the combined percentage impedance is:

$$\frac{41 \times 16.78}{41 + 16.78} \%$$

= 11.91% impedance on 100MVA base.

The percentage impedance from source to the fault point at the 33kV bus at Abakaliki Transmission Station is thus:

$$0.62 + 0.53 + 11.91$$

= 13.06% on 100MVA base.

This means that the minimum fault level the system protection at Nkalagu Transmission Station sees (i.e. for the fault at that 33kV bus) is:

$$\frac{100}{13.06\%} \text{ MVA}$$

= 765.7MVA

The minimum fault current I_f is:

$$\frac{765.7}{\sqrt{3} \times 132}$$

= 3.35 kA at 132kV

Or

$$\frac{765.7}{\sqrt{3} \times 33}$$

= 13.4 kA at 33kV

The required circuit breaker that will be used at Nkalagu Transmission Station for controlling the arc must be that capable of interrupting 38kA shown above, hence, the breaker short circuit interrupting capacity, giving 5% allowance, is 40kA.

To lower the above 40kA fault current to ensure that a lower arc that will be easier to control is developed during the interruption; the impedance from source to the fault point can be increased. This can be done by installing a series current limiting reactor on the Nkalagu – Abakaliki 132kV line shown in Figure 3.1, preferably close to the CB.

As seen from Figure 3.1 and the calculation that followed it, the total percentage impedance from the supply source to the fault point is 1.15%. The ohmic value of this 1.15% impedance using (3.18) is:

$$\frac{1.15 \times 132^2}{100 \times 100}$$

$$= 2.0 \text{ ohms}$$

The question now is; what shall be the reactance in ohms of this current limiting reactor appropriate to give a good result?

As stated earlier in chapter 2, in any given system under consideration, the reactance of the CLR is not arbitrarily chosen. There is the efficiency limit consideration. As the inductance L (and thus the reactance) of the reactor increases, the slope of the $I_{SC} - \omega L$ curve decreases until the efficiency limit is reached, beyond which variation of L will not significantly change the short circuit current (I_{SC}). From the short circuit reduction point of view, this efficiency limit is an effective value for reactance in ohms.

Substituting for MVA with $\frac{(kV)^2}{Z}$ as given in (3.16) into (3.17) for values of Z between 2Ω and 14Ω on 132kV and using the MATLAB codes given in Appendix A to generate Fault current – Reactance curve for this particular case, where the fault current is given in kA and the line Reactance in ohms, Figure 3.2 and Table 3.4 were obtained.

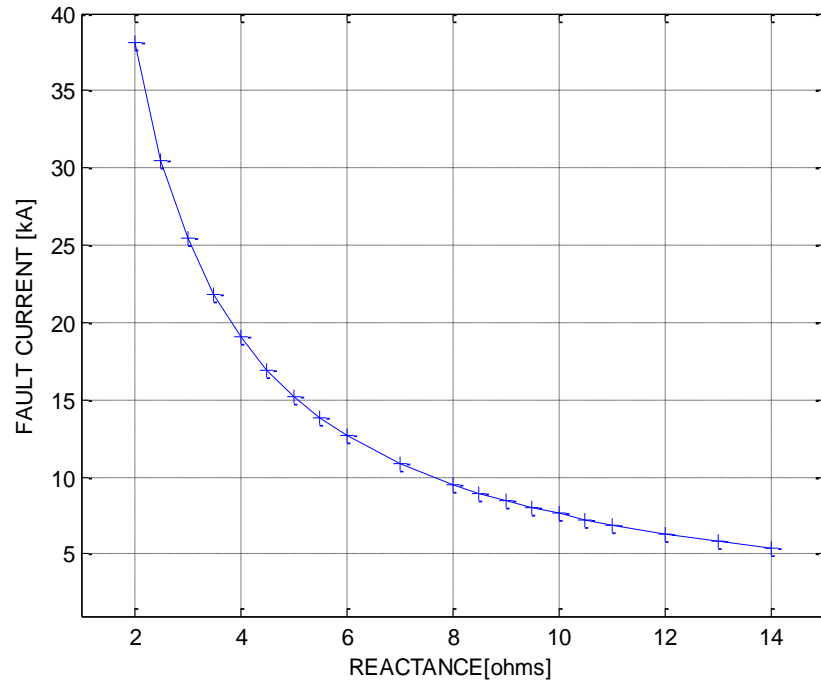


Figure 3.2: Effect of CLR reactance on fault current level

Table 3.4: Effect of CLR reactance on fault current level

S/N	Line Reactance in ohms	Fault current in kA	$dx =$ increase in line reactance	$dy =$ reduction in fault current	$\frac{dy}{dx}$	Difference between successive $\frac{dy}{dx}$
1.	2.0000	38.1062	-	-	-	-
2.	2.5000	30.4850	0.5	7.6212	15.2424	-
3.	3.0000	25.4042	0.5	5.0808	10.1616	5.0808
4.	3.5000	21.7750	0.5	3.6292	7.2584	2.9032
5.	4.0000	19.0531	0.5	2.7219	5.4438	1.8146
6.	4.5000	16.9361	0.5	2.1170	4.2340	1.2098
7.	5.0000	15.2425	0.5	1.6396	3.3872	0.8468
8.	5.5000	13.8568	0.5	1.3857	2.7714	0.6158
9.	6.0000	12.7021	0.5	1.1547	2.3094	0.4620

10.	7.0000	10.8875	1.0	1.8146	1.8146	0.4948
11.	8.0000	9.5266	1.0	1.3609	1.3609	0.4537
12.	8.5000	8.9662	0.5	0.5604	1.1208	0.2401
13.	9.0000	8.4681	0.5	0.4981	0.9962	0.1246
14.	9.5000	8.0224	0.5	0.4457	0.8914	0.1048
15.	10.0000	7.6212	0.5	0.4012	0.8024	0.0890
16.	10.5000	7.2583	0.5	0.3629	0.7258	0.0766
17.	11.0000	6.9284	0.5	0.3299	0.6598	0.0660
18.	12.0000	6.3510	1.0	0.5774	0.5774	0.0824
19.	13.0000	5.8625	1.0	0.4885	0.4885	0.0889
20.	14.0000	5.4437	1.0	0.4188	0.4188	0.0697

It can be observed from Figure 3.2 and Table 3.4 that as the reactance of the line increases, the slope of the fault current – Line reactance curve decreases until the efficiency limit is reached (4.0 ohms in this case). Beyond this limit, variation of the reactance no longer significantly changes the fault current. This is clearly seen in the column with the heading: “Difference between successive $\frac{dy}{dx}$ ” in Table 3.4. Since the system impedance from supply source to fault point in Figure 3.1 is 2.0 ohms, the efficiency limit of the CLR required on this network is 2.0 ohms. This is shown in Figure 3.3 for the existing CB.

With the addition of this 2.0 ohms CLR reactance in the network as shown in Figure 3.3, the maximum anticipated fault current is calculated thus:

Percentage impedance of this 2.0 ohms reactance on 100MVA base using (3.18) is:

$$\frac{2 \times 100 \times 100}{132^2}$$

$$= 1.15\%$$

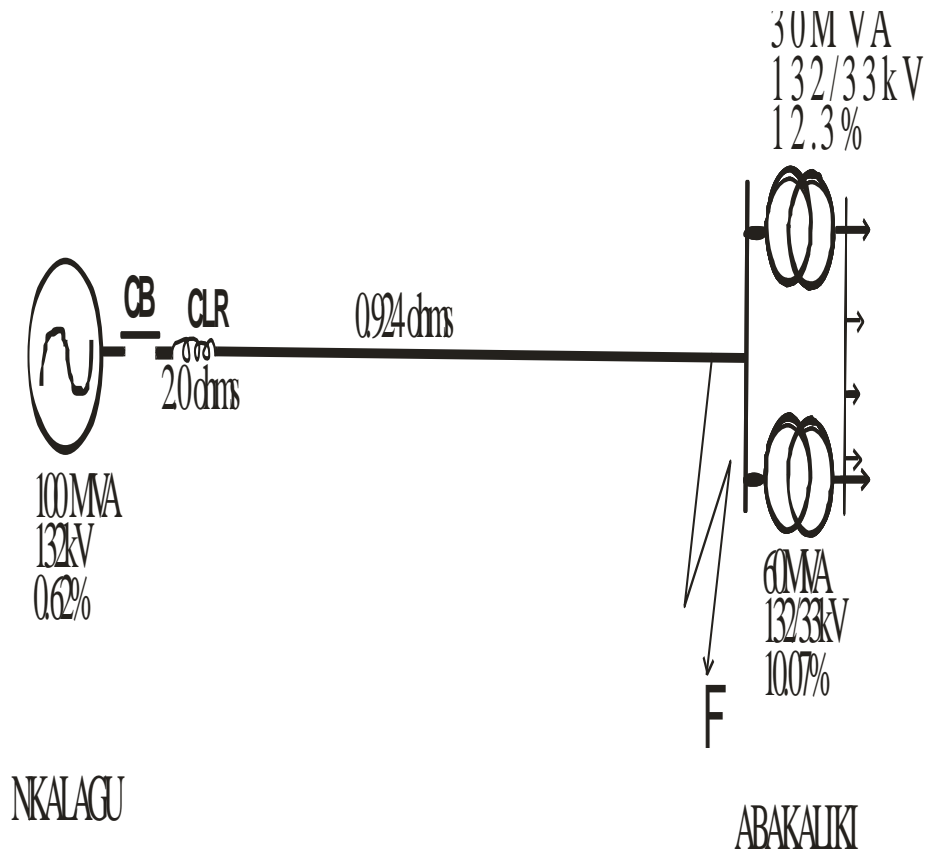


Figure 3.3: Nkalagu-Abakaliki 132kV line with existing CB in series with 2.0 ohms CLR

Total percentage impedance from source to the fault point is:

$$(0.62 + 1.15 + 0.53)\%$$

$$= 2.3\%$$

The fault MVA, using (3.19) is:

$$\frac{100}{2.3\%}$$

$$= 4347.83\text{MVA.}$$

Using (3.17), the maximum anticipated fault current I is:

$$\frac{4347.83}{\sqrt{3} \times 132}$$

$$= 19.02\text{kA on 132kV level.}$$

With the two transformers at Abakaliki Transmission Station as shown in Figure 3.3 connected to a common 33kV bus, a fault at this bus is seen by the CB at Nkalagu Transmission Station as follows:

$$0.62 + 1.15 + 0.53 + 11.91 = 14.21\% \text{ on } 100\text{MVA base}$$

This means that the minimum fault level the system protection at Nkalagu Transmission Station sees (i.e. for the fault at that 33kV bus) is:

$$\frac{100}{14.21\%} \text{ MVA}$$

$$= 704\text{MVA}$$

The minimum fault current I_f is:

$$\frac{704}{\sqrt{3} \times 132} = 3.1 \text{ kA}$$

Hence, the breaker short circuit interrupting capacity, giving 5% allowance is $19.02\text{kA} \times 1.05$. This is therefore 20kA.

3.2.3.1.2 The Cross Sectional Area A , of the Moving Contact

The area of the moving contact is of paramount importance in its current carrying capability. For a contact of uniform resistivity, ρ , the area A is given as:

$$A = \frac{\rho L}{R} \tag{3.20}$$

Where:

L = the length of the contact

R = resistance of the contact material

L can be made as short as possible in order to reduce the resistance R. So, for a given amount of current that the contact should carry, L and R should be selected to avoid overheating of the contact. The moving contact cross sectional area must be capable of

carrying the anticipated fault current magnitude I , for 3 seconds without melting. Hence, the moving contact area (A) has a direct relationship with the anticipated fault current magnitude I (Bachofen et al, 1982), i.e.:

$$A \propto I \quad (3.21)$$

Where:

A = Moving contact cross sectional area

I = anticipated fault current magnitude

The moving contact cross sectional area A has inverse relationship with the square root of the circuit breaker pressure P (Bachofen et al, 1982), i.e.:

$$A \propto \frac{1}{\sqrt{P}} \quad (3.22)$$

Where:

A = Moving contact cross sectional area

P = Circuit breaker pressure

Combining (3.21) and (3.22) gives:

$$A \propto \frac{I}{\sqrt{P}} \quad (3.23)$$

The blast pressure ΔP , which is necessary to warrant reliable arc quenching under short-line fault condition (Bachofen et al, 1982) is:

$$\Delta P \propto \left[\frac{dI}{dt} \right]^a \quad (3.24)$$

Where:

$\frac{dI}{dt}$ = The Current slope

$a =$ Constant term

$\Delta P =$ The blast pressure

The effect of the number of breaks N (i.e. the number of fold movements the pivoting links of the moving contact can make to either completely close or open), of a circuit breaker on ΔP can be obtained as follows (Bachofen et al, 1982):

$$\Delta P \propto I^a N^{-(a/n)} \quad (3.25)$$

Where:

$I =$ The interrupted current

$N =$ The number of breaks (i.e. the number of fold movements the Pivoting

Links of the moving contact can make to either completely close or open)

$n =$ Constant term

$a =$ Constant term

The values for the constant terms a and n depend on the filling Pressure P_o in the circuit breaker. Filling pressure in circuit breakers ranges between: 5.0kg/cm^2 to 8.0kg/cm^2 (Cigre, 1996). In this work, the filling pressure for the circuit breaker in consideration is 7.0kg/cm^2 . For a filling pressure of 7.0kg/cm^2 , the values for the constant terms are:

$$a = 1.4$$

$$n = 5$$

Substituting the above values of a and n into (3.25), results in the following:

$$\Delta P \propto I^{1.4} N^{-0.28}$$

Or

$$\Delta P = k I^{1.4} N^{-0.28} \quad (3.26)$$

Where k is the proportionality constant with its value as $2.77\text{kg}/(\text{cm}^2\text{-amps})$.

But,

$$P = P_0 + \Delta P \quad (3.27)$$

Where:

$P_0 =$ Circuit breaker filling pressure

And for large blast pressure, ΔP is very much greater than P_0 (Bachofen et al, 1982), such that:

$$P \approx \Delta P \quad (3.28)$$

Substituting (3.26) into (3.23) for $\Delta P = P$ as shown in (3.28)

$$A \propto \frac{I}{\sqrt{kI^{1.4}N^{-0.28}}}$$

i.e.:

$$A \propto k^{-(1/2)} I^{[1 - (\frac{1}{2} \times 1.4)]} N^{-\frac{1}{2} \times (-0.28)}$$

Meaning that:

$$A \propto k^{-(1/2)} I^{0.3} N^{0.14}$$

This implies that:

$$A = k_1 k^{-(1/2)} I^{0.3} N^{0.14}$$

i.e.:

$$A \propto I^{0.3} N^{0.14}$$

Or for $N=2$

$$A = 1.1K I^{0.3} \quad (3.29)$$

Where $K = k_1 k^{-1/2}$ is the proportionality constant with its value as $3.64 \times 10^{-5} \text{ m}^2/\text{ampere}$ and the number of breaks, N , is 2 in present CB designs (Bachofen et al, 1982). Substituting the values of K and N in (3.29) gives:

$$A = 3.64 \times 10^{-5} \times 2^{0.14} \times I^{0.3}$$

Or:

$$A = 4.0 \times 10^{-5} \times I^{0.3} \quad (\text{in m}^2) \quad (3.30)$$

To determine the actual value of the moving contact cross sectional area A , the value of I is substituted in (3.30). With I equal to 20kA (i.e. 20000 amperes) on 132kV level,

$$\begin{aligned} A &= 4.0 \times 10^{-5} \times 20000^{0.3} \\ &= 7.8 \times 10^{-4} \text{ m}^2 \end{aligned}$$

Using square cross section for the moving contact, the width (w) and thickness (th) are the same and thus:

$$\begin{aligned} w &= \sqrt{A} \\ &= 2.79 \times 10^{-2} \text{ meters} \end{aligned}$$

And

$$\begin{aligned} th &= \sqrt{A} \\ &= 2.79 \times 10^{-2} \text{ meters} \end{aligned}$$

Where:

W = Moving Contact width

th = Moving Contact thickness

3.2.3.1.3 The Length l , of the Moving Contact

The length L , of the moving contact is standardized, depending on the system voltage. For 132kV system being considered, $l = 1.2$ meters (NERC, 2010).

The parameters for the modified CB moving contact are as given in Table 3.5

Table 3.5: Calculated dimension for modified CB Moving Contact

S/N	Item measured	Value
1.	Moving contact length	1.2 meters
2.	Moving contact width	2.79×10^{-2} meters
3.	Moving contact thickness	2.79×10^{-2} meters
4.	Moving contact cross-sectional area	$7.8 \times 10^{-4} \text{m}^2$

3.2.3.1.4 Modifying the Moving Contact to two pronged forked moving contact

As stated earlier, one of the ways to mitigate the enormous constant power losses in the use of CLR on feeder CBs is the use of forked moving contacts in circuit breakers. In modifying the moving contact to two pronged moving contact, the length must be maintained at 1.2 meters for 132kV CB. The 1.2 meters length is divided into two parts, the straight part and the forked part. The dimensions for the straight part are as given in Table 3.6.

Table 3.6: Dimension for straight part of Forked Moving Contact

S/N	Item	Value
1.	Length	1.15 meters
2.	Width	2.79×10^{-2} meters
3.	Thickness	2.79×10^{-2} meters
4.	Cross-sectional area	$7.8 \times 10^{-4} \text{m}^2$
5.	Diameter of circumscribed circle	3.94×10^{-2} meters

As seen from Table 3.6, one part measuring 1.15 meters in length, 2.79×10^{-2} meters width and 2.79×10^{-2} meters thick is left straight as shown in Figure 3.4. The diameter of the circumscribing circle on the cross section of this straight part is 3.94×10^{-2} meters as shown in Figure 3.5.



Figure 3.4: Straight part of the Forked Moving Contact

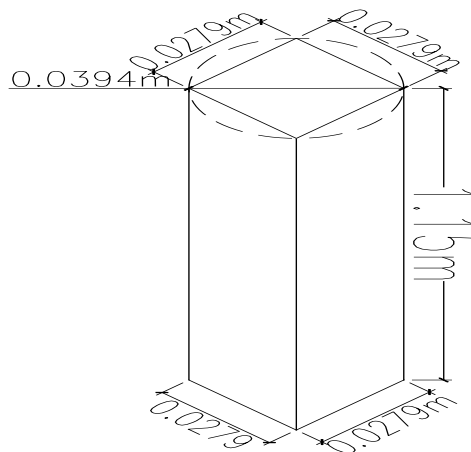


Figure 3.5: Diameter of the Circumscribing Circle on the Straight part of Moving Contact

The remaining length of 0.05 meters is modified to two prongs of unequal lengths separated by 3mm gap. The cross-sectional area of each of these prongs must agree with the calculated value of $7.8 \times 10^{-4} \text{m}^2$ in section 3.2.3.1.2, in line with the anticipated fault current I , hence, choosing the prong width as 4.1×10^{-2} meters the thickness is:

$$\frac{7.8 \times 10^{-4}}{4.1 \times 10^{-2}} = 1.9 \times 10^{-2} \text{ meters.}$$

The dimensions for the longer prong are as given in Table 3.7.

Table 3.7: Dimension for the Longer Prong of Forked Moving Contact

S/N	Item	Value
1.	Length	0.05 meters
2.	Width	4.1×10^{-2} meters
3.	Thickness	1.9×10^{-2} meters
4.	Cross-sectional area	$7.8 \times 10^{-4} \text{m}^2$

The longer prong is 0.05 meters in length, which when added to the straight part makes the maximum length equal to 1.2 meters. This is as shown in Figure 3.6.

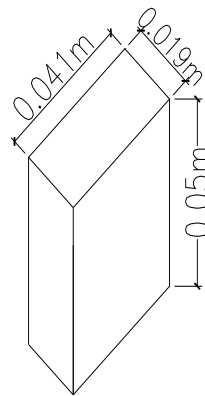


Figure 3.6: Longer Prong of the Forked Moving Contact

The shorter prong of the forked moving contact is 10mm shorter than the longer prong. The reason for this difference in the prong lengths is to ensure that during CB opening process, power flow is first broken from the shorter prong so as to cause arc to develop only via the longer prong when it finally pulls out from the fixed contact. The dimensions for the shorter prong are as given in Table 3.8.

Table 3.8: Dimension for the shorter Prong of Forked Moving Contact

S/N	Item	Value
1.	Length	0.04 meters
2.	Width	4.1×10^{-2} meters
3.	Thickness	1.9×10^{-2} meters
4.	Cross-sectional area	$7.8 \times 10^{-4} \text{m}^2$

The cross sectional area of this prong as seen from Table 3.8 must also agree with the calculated value of $7.8 \times 10^{-4} \text{m}^2$ in line with the anticipated fault current I, hence, the width is 4.1×10^{-2} meters and the thickness is 1.9×10^{-2} meters. This is as shown in Figure 3.7.

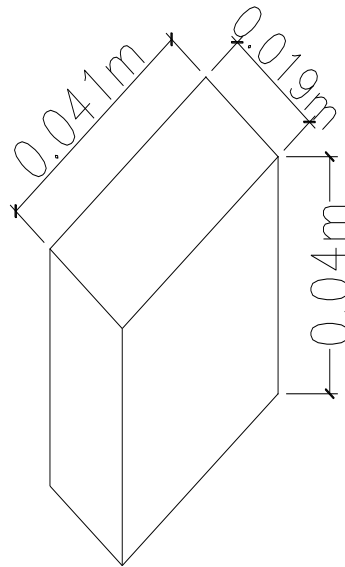


Figure 3.7: Shorter Prong of the Forked Moving Contact

The two pronged forked moving contact is as shown in Figure 3.8. The diameter of the circumscribing circle on the cross section of the prongs separated by 3mm is 5.8×10^{-2} meters as shown in Figure 3.9.

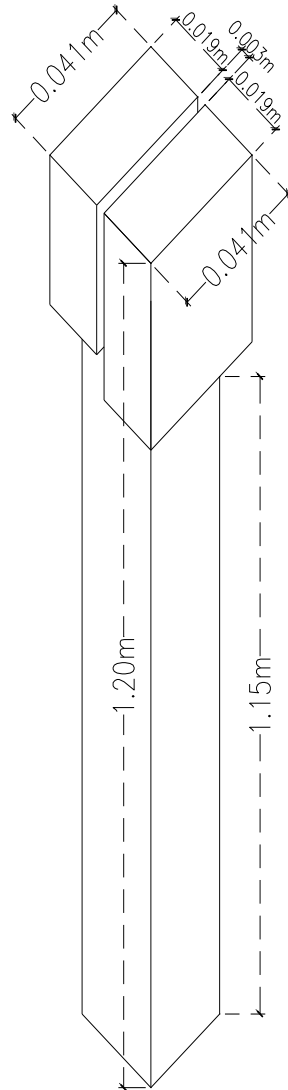


Figure 3.8: The Forked Moving Contact

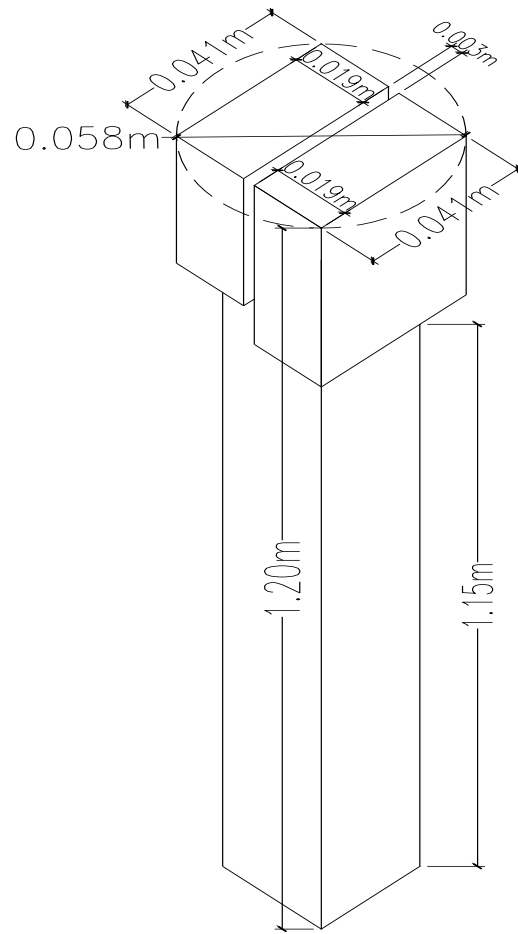


Figure 3.9: Diameter of the Circumscribing Circle on the Forked Moving Contact prongs

The dimensions for the modified moving contact are as summarized in Table 3.9.

Table 3.9: Summary of the calculated Dimension for the Forked Moving Contact

S/N	Item	Value
1.	Prong Width	4.1×10^{-2} meters
2.	Prong Thickness	1.9×10^{-2} meters
3.	Prong separation	3.0×10^{-3} meters
4.	Cross-sectional area of each prong	$7.8 \times 10^{-4} \text{m}^2$

5.	Length of longer prong	0.05 meters
6.	Length of shorter prong	0.04 meters
7.	Length of straight part of forked contact	1.15 meters
8.	Width of straight part of forked contact	2.79×10^{-2} meters
9.	Thickness of straight part of forked contact	2.79×10^{-2} meters
10.	Cross-sectional area of straight part of forked contact	$7.8 \times 10^{-4} \text{ m}^2$
11.	Length of contact (shorter side)	1.19 meters
12.	Length of contact (longer side)	1.2 meters
13.	Overall Length of moving contact (i.e. Length of straight part of forked contact + Length of longer prong + Length of shorter prong)	1.24 meters
14.	Diameter of circumscribed circle on straight part cross section	3.94×10^{-2} meters
15.	Diameter of circumscribed circle on the cross section of the prongs separated by 3mm	5.8×10^{-2} meters
16.	Volume of the Forked Moving Contact	$9.67 \times 10^{-4} \text{ m}^3$
17.	Mass of the Forked Moving Contact	8.67kg

Some key parameters of the modified CB moving contact compared with the moving contact for the existing CB is summarized in Table 3.10.

Table 3.10: Summary of the existing CB and the modified CB compared

S/N	Item considered	Existing CB	Modified CB
1.	Effective Length of the CB moving contact	1.2 meters	1.2 meters
2.	Overall Length of the CB moving contact	1.2 meters	1.24 meters
3.	Cross-sectional area of the CB moving		

	contact	$9.61 \times 10^{-4} \text{m}^2$	$7.8 \times 10^{-4} \text{m}^2$
4.	Moving contact resistance (Z_{CB}) (in ohms)	2.15×10^{-5}	2.73×10^{-5}
5.	Moving Contact Mass	10.33kg	8.67kg
6.	Maximum diameter of circumscribed circle on moving contact cross section	4.38×10^{-2} meters	5.8×10^{-2} meters

3.2.3.1.5 The CB Terminals

The CB has two terminals per pole as shown in Figure 3.10. The terminals are usually such that the choice of most engineers installing it in the utility company had been to connect the load to the upper terminal and the supply source to the lower terminal, or vice versa, based on some peculiarities on ground.

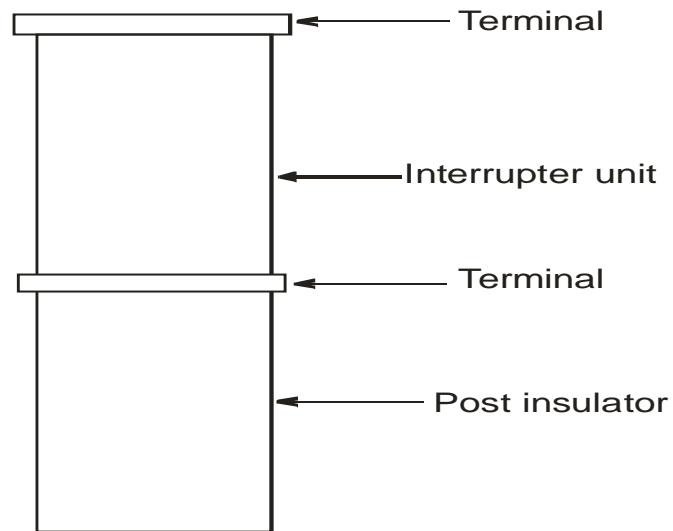


Figure 3.10: Post Insulator/Interrupter unit of an existing CB showing its terminals.

To achieve the desired aim, the load must always be connected on the lower terminal. The upper terminal is split into two and separated for:

- (1) Connecting the CLR and
- (2) Connecting the CLR bypass bar.

This is shown in Figure 3.11.

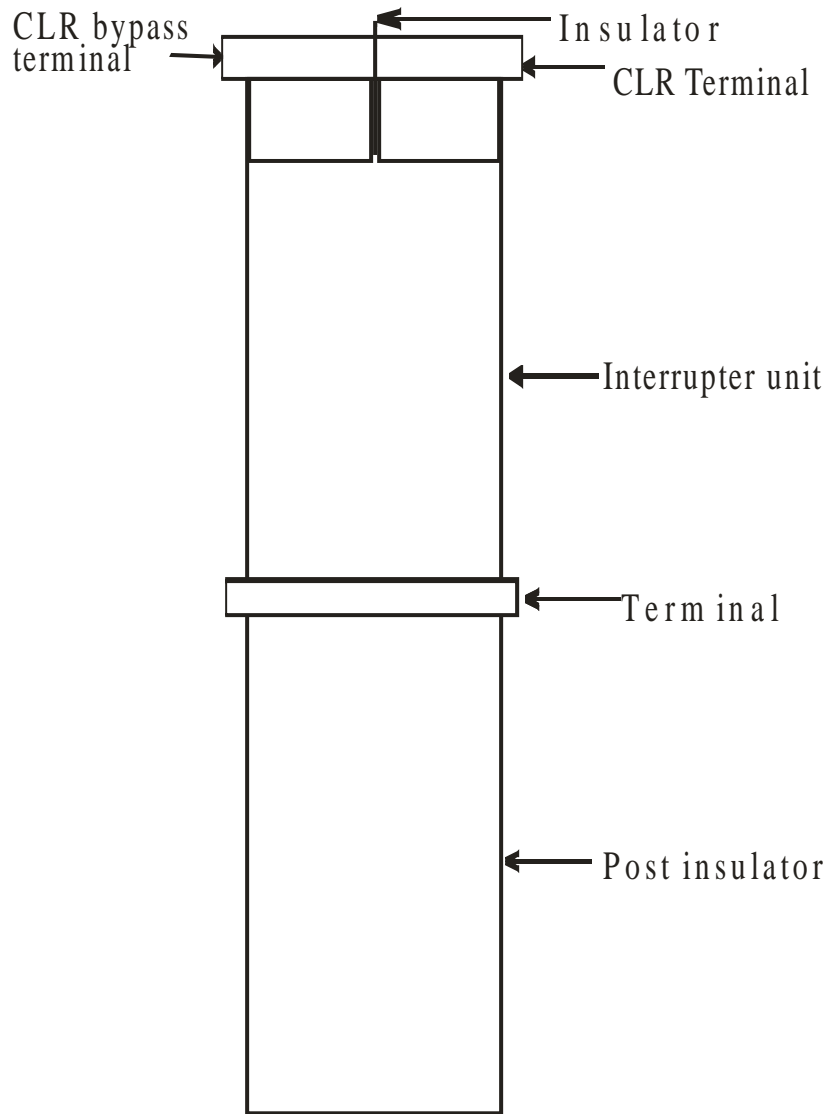


Figure 3.11: Post Insulator/Interrupter unit of a CB showing the modification on the fixed contact terminal.

The prototype connection that gives the CLR and CB moving contact parallel connection is shown in Figure 3.12.

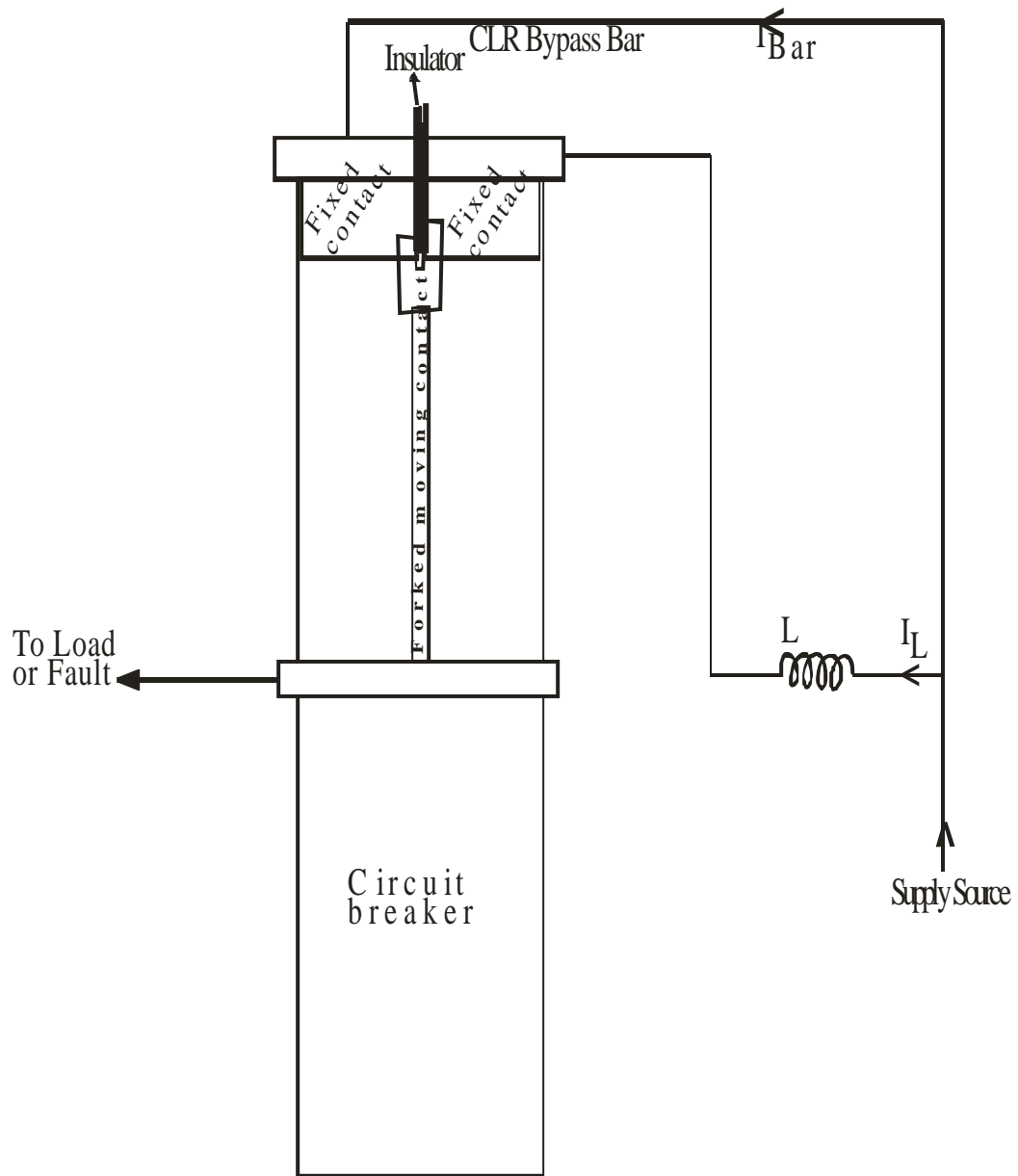


Figure 3.12: CLR/CB prototype connection for forked moving contact

Legend to Figure 3.12:

L = The CLR

I_L = The current through the CLR

I_{Bar} = The current through the CLR bypass bar.

3.2.3.2 The adapter

The adapter for fitting on an existing circuit breaker terminal is as shown in Figure 3.13. This is meant for the existing circuit breakers shown in Appendix B (i.e. circuit breakers with straight moving contacts) when due to increased demand for energy and network expansion, short circuit level grows beyond the rating of the circuit breaker. It is for coupling CLR and existing CB to achieve CLR and CB moving contact parallel connection. The adapter is spring operated and comprises two supply contacts B to CB terminal, two springs E and D, a CLR bypass bar, and a moveable (sliding) contact rod S. The moveable (sliding) rod is enclosed in an insulated casing and has two parts – a conducting part and a non-conducting part.

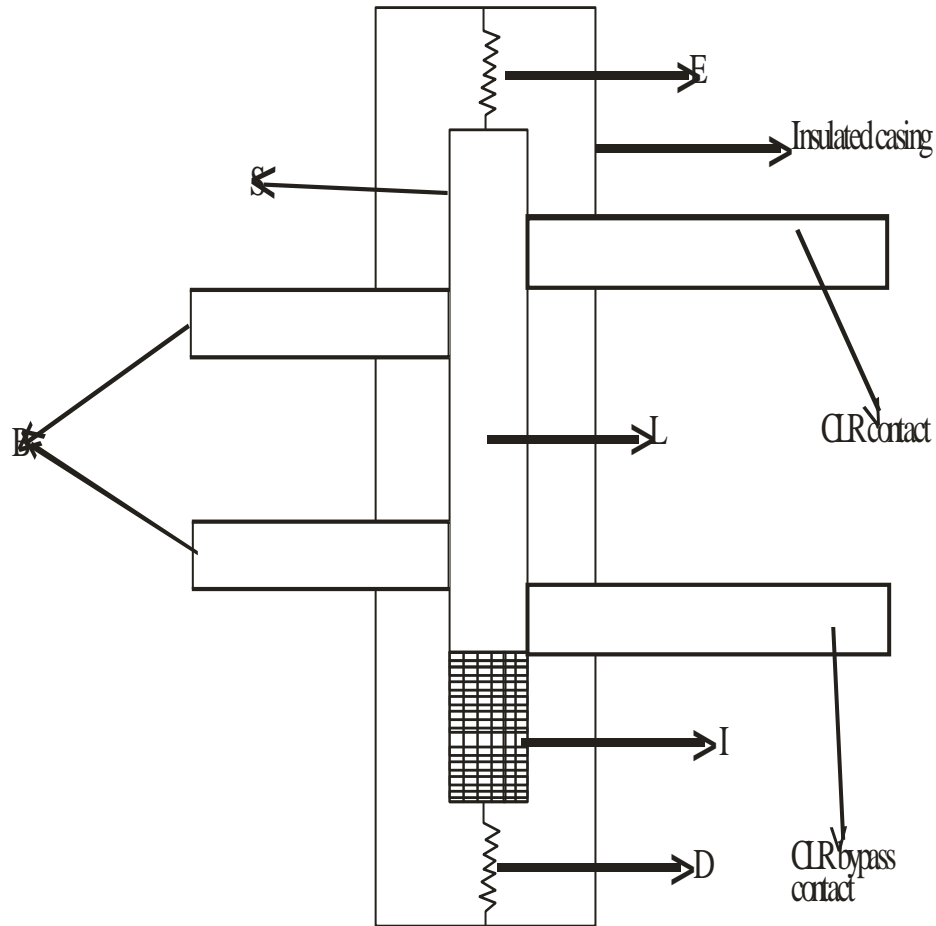


Figure 3.13: The adapter

Legend to Figure 3.13:

B = supply contact to CB terminal

S = Moveable (sliding) contact rod

L = Conducting part of S

I = Non-conducting part of S

D = spring (discharges to open-circuit CLR bypass bar i.e. pushes S to bring I part of S in contact with CLR bypass bar)

E = spring (discharges to close CLR bypass bar back to circuit after fault is cleared)

If for instance, due to increased energy demand and network expansion at Abakaliki end in Figure 3.1, the supply source at Nkalagu end is increased. If this increase goes beyond the 40kA rating of the CB at Nkalagu Transmission Station as seen in section 3.2.3.1.1, the adapter can be used to couple the CLR and the CB such that the maximum allowable fault current I through the CB is maintained at 40kA when breaking. With the contacts and sliding rod in the adapter made of copper, and I known to be 40kA, the contacts and sliding rod in the adapter automatically assume the same measured cross sectional area as the moving contact of the existing CB. This should be so since their current densities should be the same (Kraus and Fleisch, 1999), (Cathy, 2001). However, since the supply contacts to the CB terminal share the current to the CB equally, the cross sectional area of each is half that of the CB moving contact.

The length of the sliding rod should not be more than the measured diameter of the CB pole to ensure adequate clearance between phases. For the 132kV CB considered,

Measured pole diameter = 0.3m

The lengths for the sliding rod, CLR contact, CLR bypass contact and the supply contacts to the CB terminal are therefore all chosen to be 0.3m to ensure adequate clearance between phases.

The cross-sectional area of the sliding rod must agree with the measured value seen to be $9.61 \times 10^{-4} \text{ m}^2$ in section 3.1.3 for the existing CB, hence, choosing the thickness as 5.0×10^{-2} meters the width is:

$$\frac{9.61 \times 10^{-4}}{5.0 \times 10^{-2}} = 1.922 \times 10^{-2} \text{ meters.}$$

The CLR contact cross-sectional area must also agree with the measured value seen to be $9.61 \times 10^{-4} \text{ m}^2$ in section 3.1.3 for the existing CB, hence, choosing the thickness as 2.0×10^{-2} meters the width is:

$$\frac{9.61 \times 10^{-4}}{2.0 \times 10^{-2}} = 4.81 \times 10^{-2} \text{ meters.}$$

The CLR bypass contact cross-sectional area must also agree with the measured value seen to be $9.61 \times 10^{-4} \text{ m}^2$ for the existing CB, hence, choosing the thickness as 2.0×10^{-2} meters the width is:

$$\frac{9.61 \times 10^{-4}}{2.0 \times 10^{-2}} = 4.81 \times 10^{-2} \text{ meters.}$$

Since there two supply contacts on the adapter to the CB terminals, they share the current to the CB equally, such that the cross sectional area of each is half that of the existing CB moving contact. That is:

$$\frac{9.61 \times 10^{-4}}{2} = 4.81 \times 10^{-4} \text{ m}^2.$$

Choosing the supply contact thickness as 2.0×10^{-2} meters the width is:

$$\frac{4.81 \times 10^{-4}}{2.0 \times 10^{-2}} = 2.405 \times 10^{-2} \text{ meters.}$$

The dimensions for the adapter parts are as shown in Table 3.11 and Figure 3.14.

Table 3.11: Summary of the calculated Dimensions for the adapter parts

S/N	Item	Value
1.	Sliding rod length	0.3 meters
2.	Sliding rod width	1.922×10^{-2} meters
3.	Sliding rod thickness	0.05 meters
4.	Sliding rod cross-sectional area	$9.61 \times 10^{-4} \text{m}^2$
5.	CLR contact length	0.3 meters
6.	CLR contact width	0.0481 meters
7.	CLR contact thickness	0.02 meters
8.	CLR contact cross-sectional area	$9.61 \times 10^{-4} \text{m}^2$
9.	CLR bypass contact length	0.3 meters
10.	CLR bypass contact width	0.0481 meters
11.	CLR bypass contact thickness	0.02 meters
12.	CLR bypass contact cross-sectional area	$9.61 \times 10^{-4} \text{m}^2$
13.	Supply contact to CB terminal length	0.2 meters
14.	Supply contact to CB terminal width	0.02405 meters
15.	Supply contact to CB terminal thickness	0.02 meters
16.	Supply contact to CB terminal cross-sectional area	$4.81 \times 10^{-4} \text{m}^2$

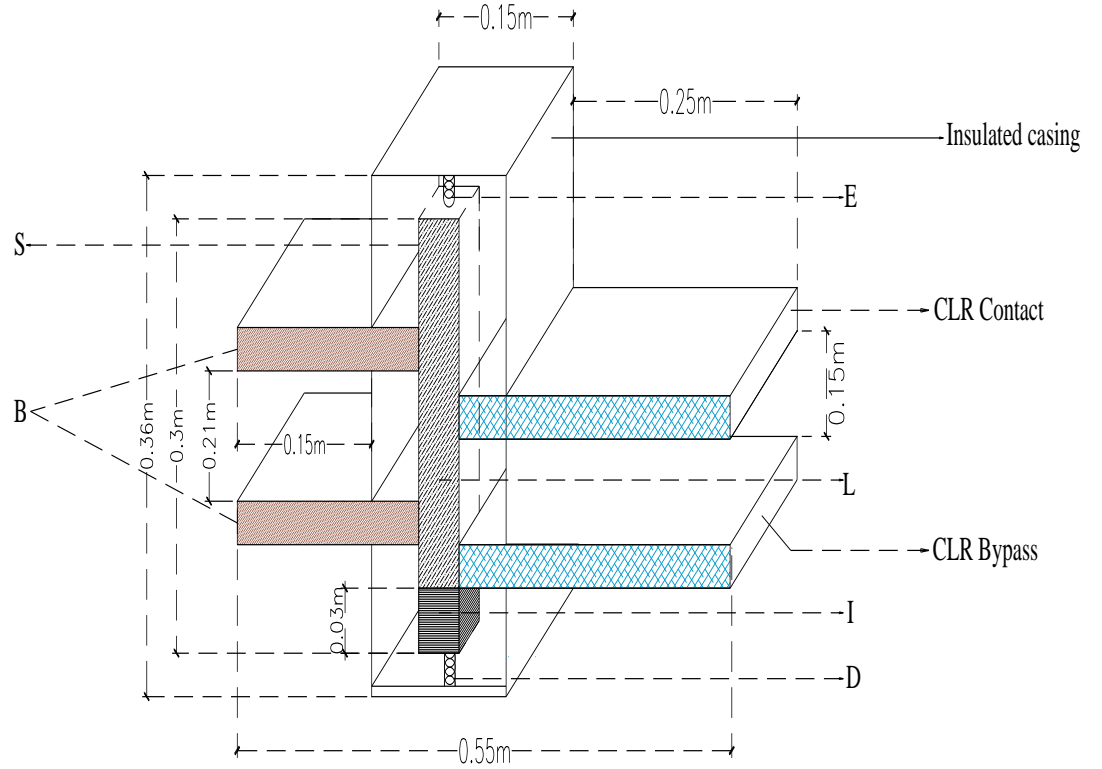


Figure 3.14: Dimensions for the adapter

The prototype connection for the adapter on the existing CB is as shown in Figures 3.15 and 3.16.

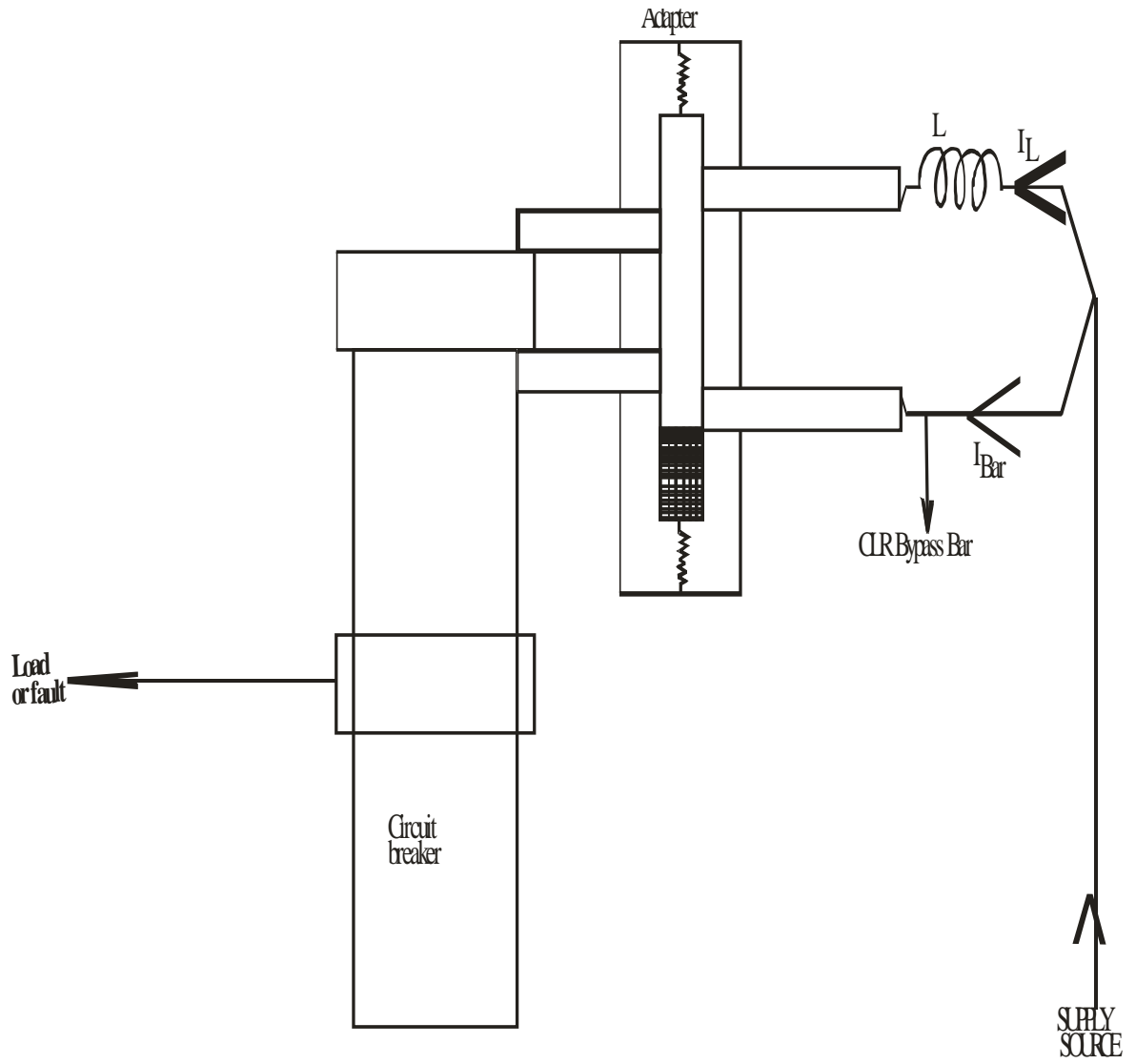


Figure 3.15: CLR/Adapter/CB prototype connection

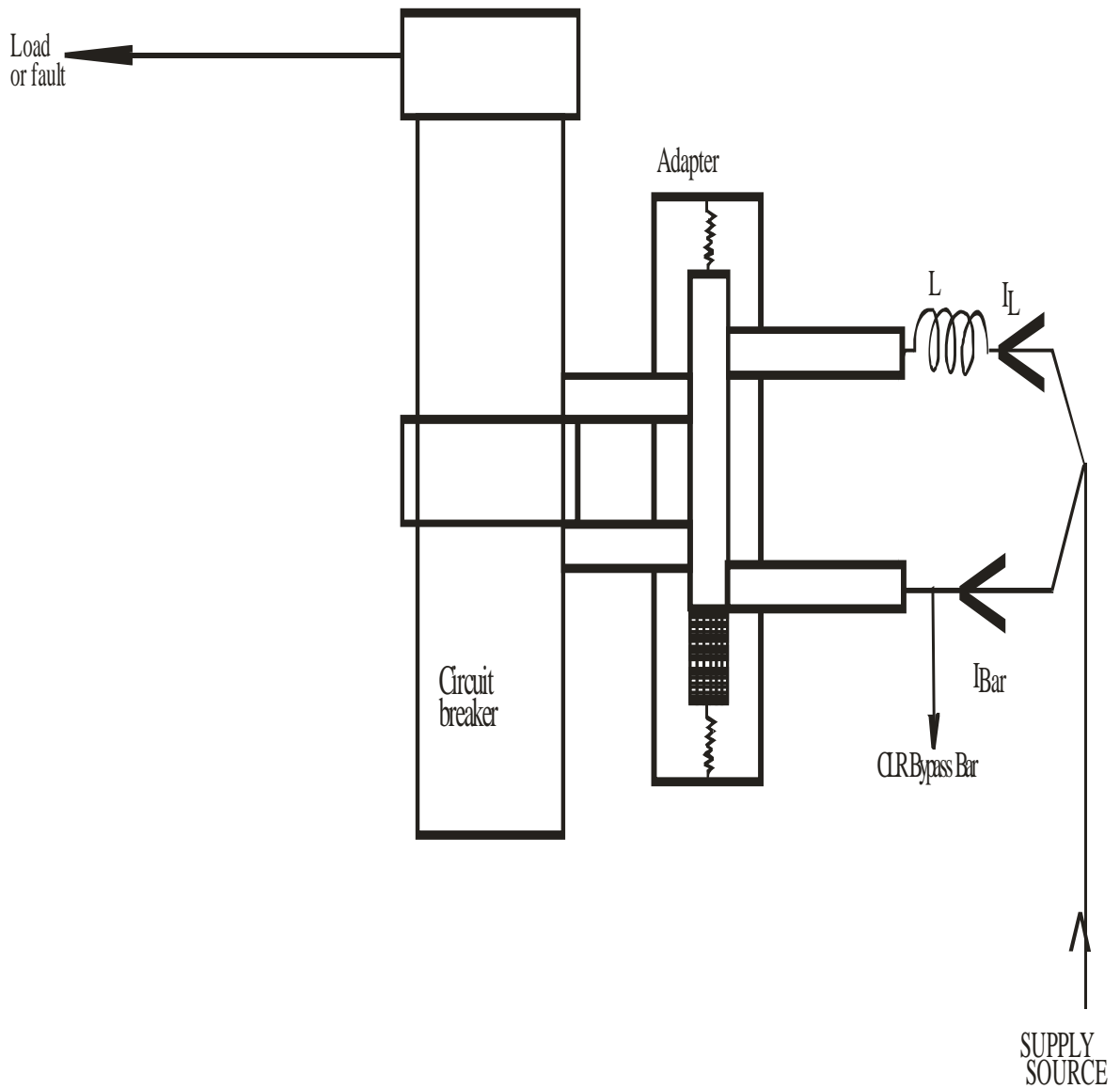


Figure 3.16: CLR/Adapter/CB prototype connection

This can be implemented on an existing circuit breaker contact shown in appendix B when there is increased short circuit level beyond the existing breaker rating, resulting from network expansion.

3.2.3.2.1 Operation of the Adapter and the CB

Open circuiting and closing the CLR by-pass bar is triggered by a relay different from the relay for tripping the feeder CB. However, the relays must be fed the same current

quantity from the same current transformer (CT). The relays are located in the control room, while the CTs, the circuit breaker and the current limiting reactor are located in the switch yard as shown in the block diagram of Figure 3.17.

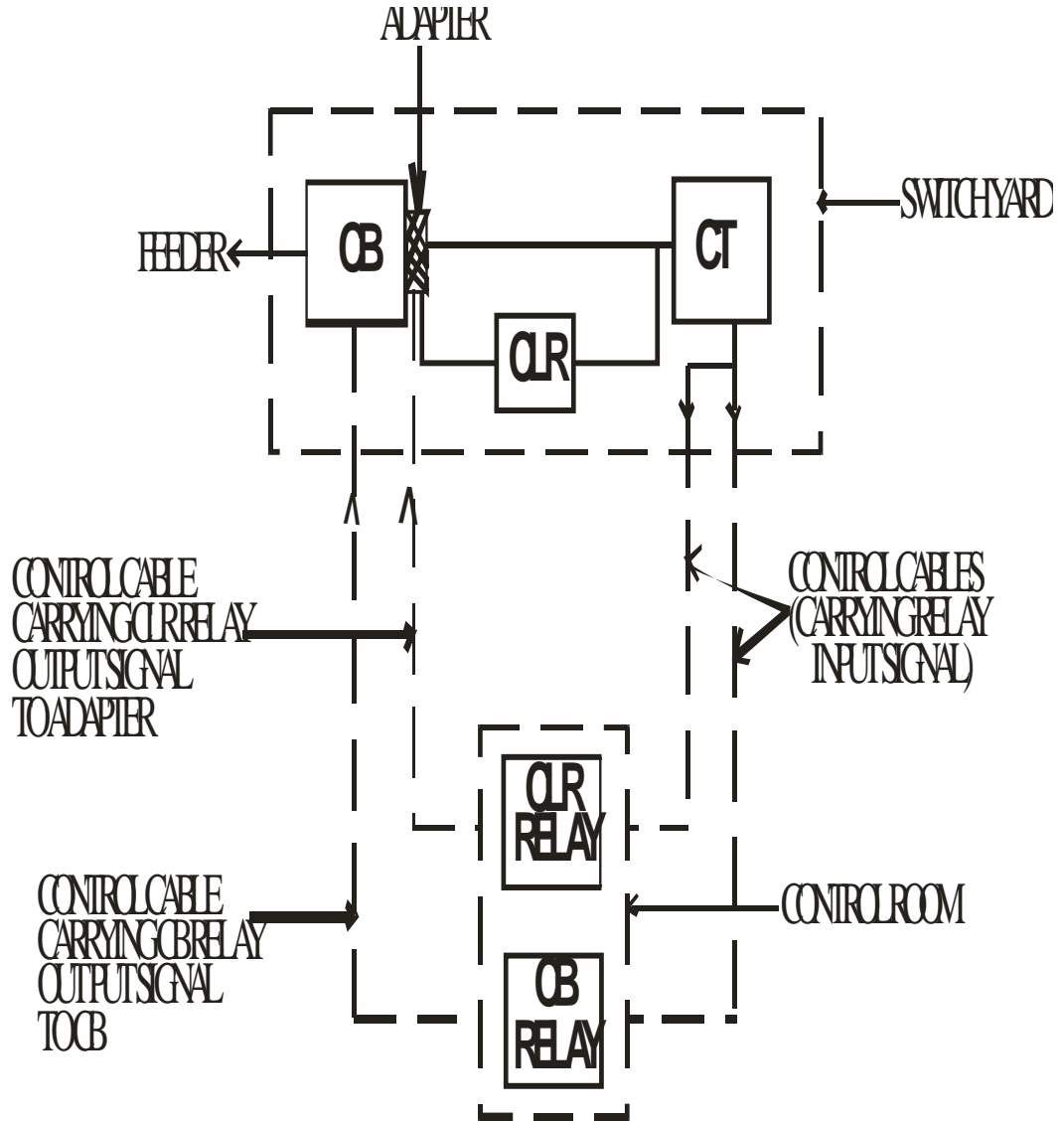


Figure 3.17: Block diagram showing the locations of CB, Adapter, CLR, CT and Relays.

Since two relays are involved in the adapter usage, and because the two relays are fed the same current quantity from the same current transformer while they are not expected to operate at the same time, the two relays must be appropriately coordinated. One relay is the usual relay for initiating trip signal to the circuit breaker while the second relay is for the operation of the adapter to couple the current limiting reactor in the circuit. The two

relays are in the same relaying station and are fed with the same input quantities but, by relay co-ordination, the relay for coupling the current limiting reactor in the circuit must operate first, thereafter the circuit breaker relay operates after a pre-determined time delay achieved using an appropriate relay coordination principle.

3.2.3.3 CB/CLR Relay Coordination

Co-ordination by time alone is all that is required between the CLR relay and the feeder CB relay since both are in the same place and fed by the same current transformer, CT, (meaning they see the same fault level and the same impedance value at any instant). However, if the feeder relay has to co-ordinate with the relays behind it in the system, there should first be discrimination between the feeder CB relay and the relays behind it by inverse time over current principle, since discriminating these relays by time alone, means longest fault clearing time for faults closest to the power source. After discriminating these relays, the feeder CB relay time should then be reduced by 0.05s and assigned to the CLR relay.

There are two basic adjustable settings on all inverse time relays. One is the time multiplier setting (TMS), shown with an electromechanical relay in Appendix C and the other is the current plug setting multiples (PSM), shown also with an electromechanical relay in Appendix D. What the time multiplier setting actually does is to adjust the time of operation of the relay so as to either increase or reduce the time. This is achieved with electromechanical relay by adjusting the distance between the making contacts as can be seen in Appendix C. As per British Standard, there are two types of Inverse Definite Minimum Time (IDMT) relays, namely: 3.0 seconds and 1.3 seconds relays (NAPTIN, 2010). This only means that with $TMS = 1.0$ and $PSM = 10$, the relay operates at the time of 3.0 seconds or 1.3 seconds as the case may be. The current/time tripping characteristics of IDMT relays may need to be varied according to the tripping time required and the characteristics of other protection devices used in the network. For this purpose, International Electro-technical Commission (IEC) 60255 defines a number of standard characteristics as shown in Tables 3.12 and 3.13.

Table 3.12: Relay characteristics

S/N	Relay Type	Characteristic
1.	Standard Inverse	$t = TMS \times \frac{0.14}{I_r^{0.02} - 1}$
2.	Very Inverse	$t = TMS \times \frac{13.5}{I_r - 1}$
3.	Extremely Inverse	$t = TMS \times \frac{80}{I_r^2 - 1}$
4.	Long time standard inverse	$t = TMS \times \frac{120}{I_r - 1}$

Source: National power training institute of Nigeria (NAPTIN), (2010)

For the relay Characteristic given in Table 3.12,

I_r = Multiples of Plug Setting

I = Value of Short Circuit Current at the secondary side of Current Transformer

I_s = Relay Setting Current

TMS = Required Time Multiplier Setting to give the desired Time of Operation of the Relay

t = Required Time of operation of the Relay.

Table 3.13: North American IDMT relay characteristics

S/N	Relay Type	Characteristic
1.	IEE Moderately Inverse	$t = \frac{TD}{7} \left(\frac{0.0515}{I_r^{0.02} - 1} + 0.114 \right)$
2.	IEE Very Inverse	$t = \frac{TD}{7} \left(\frac{19.61}{I_r^2 - 1} + 0.491 \right)$

3.	Extremely Inverse	$t = \frac{TD}{7} \left(\frac{28.2}{I_r^2 - 1} + 0.1217 \right)$
4.	US CO8 Inverse	$t = \frac{TD}{7} \left(\frac{5.95}{I_r^2 - 1} + 0.18 \right)$
5.	US CO2 Short Time Inverse	$t = \frac{TD}{7} \left(\frac{0.02394}{I_r^{0.02} - 1} + 0.01694 \right)$

Source: National power training institute of Nigeria (NAPTIN), (2010)

For the relay Characteristic given in Table 3.13, for IEE Moderately Inverse relay,

$$t = \frac{TD}{7} \left(\frac{0.0515}{I_r^{0.02} - 1} + 0.114 \right) \quad (3.31)$$

Where:

I_r = Multiples of Plug Setting

I = Value of Short Circuit Current at the secondary side of Current Transformer

I_S = Relay Setting Current

TD = Required Time Dial Setting to give the desired Time of Operation of the Relay

t = Required Time of operation of the Relay.

Relay time - current characteristic curves for a standard 3.0 seconds Inverse Time relay CDG11 for 50Hz and 60Hz (British Standard (BS) 142) is as shown in Appendix E and relay discrimination curves shown in Appendix F.

For the network under consideration (i.e. Nkalagu – Abakaliki 132kV line) the data for the protective system is as shown in Table 3.14.

Table 3.14: Data for the protective system for Nkalagu – Abakaliki 132kV line

S/N	Item	Value
1.	Current Transformer Ratio	500/1
2.	Maximum Load Current	400 Amperes
3.	CB Relay operating time t	0.2 seconds

Source: TCN, Nkalagu 132/33 kV Transmission Station

From Table 3.12,

$$t = TMS \times \frac{0.14}{I_r^{0.02} - 1} \quad (3.32)$$

Where:

$$I_r = MPS = \frac{I}{I_S}$$

MPS = Multiples of Plug Setting

I = Value of Short Circuit Current at the secondary side of Current Transformer

I_S = Relay Setting Current

TMS = Required Time Multiplier Setting to give the desired Time of Operation of the Relay

t = Required Time of operation of the Relay.

With 2.0 ohms CLR installed on the network as shown in Figure 3.3, the maximum and minimum fault current the protection at Nkalagu Transmission Station sees are 19.02kA and 3.1kA respectively.

The value of the load current of 400A given in Table 3.14, at the secondary side of the Current Transformer is:

$$400 \times \frac{1}{500}$$

$$= 0.8 \text{ amperes}$$

With 100% relay current setting,

$$I_S = 0.8A$$

Maximum value of Short Circuit Current I at the secondary side of Current Transformer is:

$$I = 19020 \times \frac{1}{500}$$

$$= 38.04A$$

$$\text{MPS} = \frac{38.04}{0.8}$$

$$= 47.55$$

Using (3.32) for time of CB relay operation for maximum fault current being 0.2 seconds,

$$\text{TMS} = \frac{0.2 \times 47.55^{0.02} - 1}{0.14}$$

$$= 0.11$$

As stated earlier, giving the CLR relay, the CB relay time reduced by 0.05 seconds means that the CLR relay operation time for maximum fault current shall be 0.15 seconds. This is achieved by setting CLR relay TMS using (3.32) as:

$$\text{TMS} = \frac{0.15 \times 47.55^{0.02} - 1}{0.14}$$

$$= 0.09$$

Minimum value of Short Circuit Current I at the secondary side of Current Transformer is:

$$I = 3100 \times \frac{1}{500}$$

$$= 6.2A$$

$$\text{MPS} = \frac{6.2}{0.8}$$

$$= 7.75$$

CB relay operation time for minimum fault current of 3.1kA using (3.32) is:

$$t = 0.11 \times \frac{0.14}{7.75^{0.02} - 1}$$

$$= 0.37 \text{ seconds}$$

Similarly, the time of CLR relay operation for minimum fault current of 3.1kA using (3.32) is:

$$t = 0.09 \times \frac{0.14}{7.75^{0.02} - 1}$$

$$= 0.3 \text{ seconds}$$

The CB/CLR relay coordination is therefore as summarized in Table 3.15.

Table 3.15: Summary of CB/CLR relay Coordination

S/N	Description	CB relay	CLR relay
1.	TMS	0.11	0.09
2.	Operation time for maximum fault current in seconds	0.2	0.15
3.	Operation time for minimum fault current in seconds	0.37	0.3

3.2.3.4 Principle of operation of the Modified CB Contacts

The existing CB/CLR was connected as shown in the single line diagram of Figure 3.18. As seen from Figure 3.18, the Current Limiting Reactor (CLR) is permanently in series, meaning that it carries the full load current under normal system condition. The CLR carrying the full load current under normal system condition as stated earlier, causes enormous constant power losses.

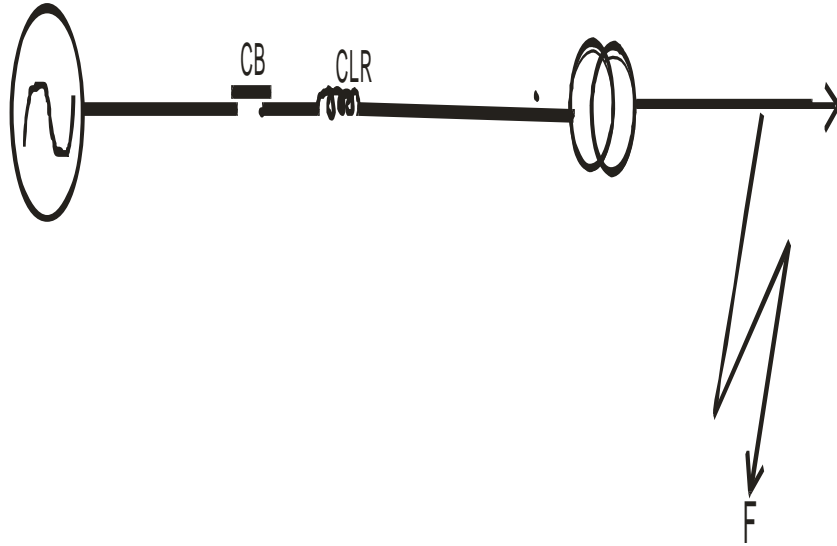


Figure 3.18: Single line diagram of CLR implementation on the existing feeder CB

This work is targeted at reconnecting Figure 3.18 as shown in Figure 3.19.

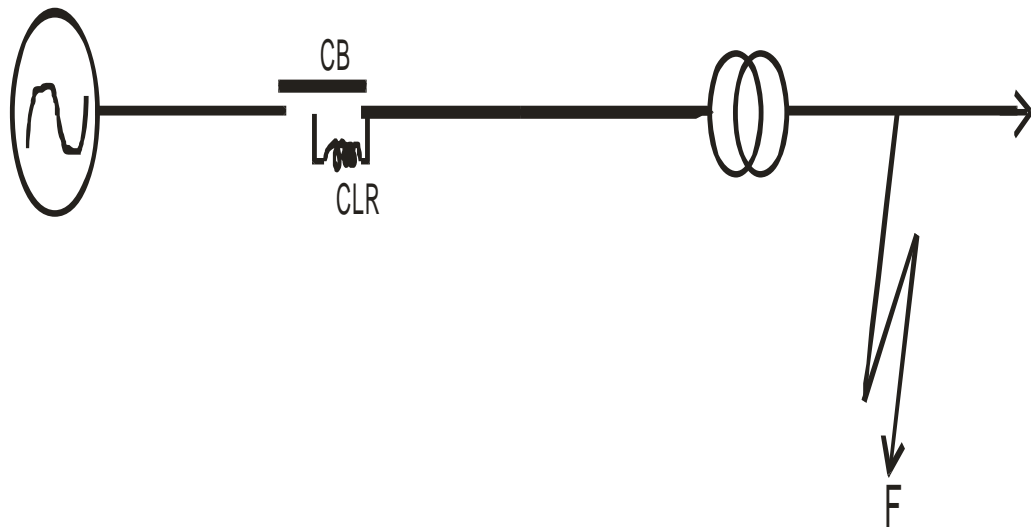


Figure 3.19: Single line diagram of CLR implementation on a Modified feeder CB

It can be seen from Figure 3.18 that the existing CB has contacts and terminals that permit the CB and CLR connection in series alone. The modified CB gives the CB and CLR connection in parallel when the CB is in closed position as shown in Figure 3.20. During CB opening operation, the CLR automatically becomes serially connected in the circuit just before the CB contacts finally separate, as shown in Figure 3.21. The modified CB in open position is as shown in Figure 3.22.

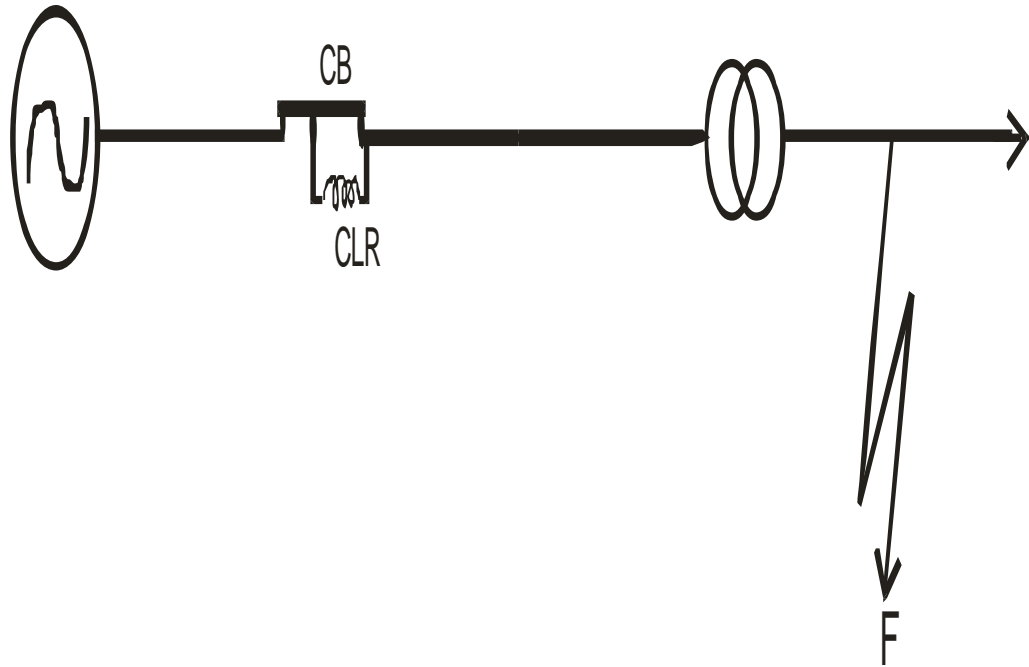


Figure 3.20: CB/CLR in parallel when the modified CB is in closed position

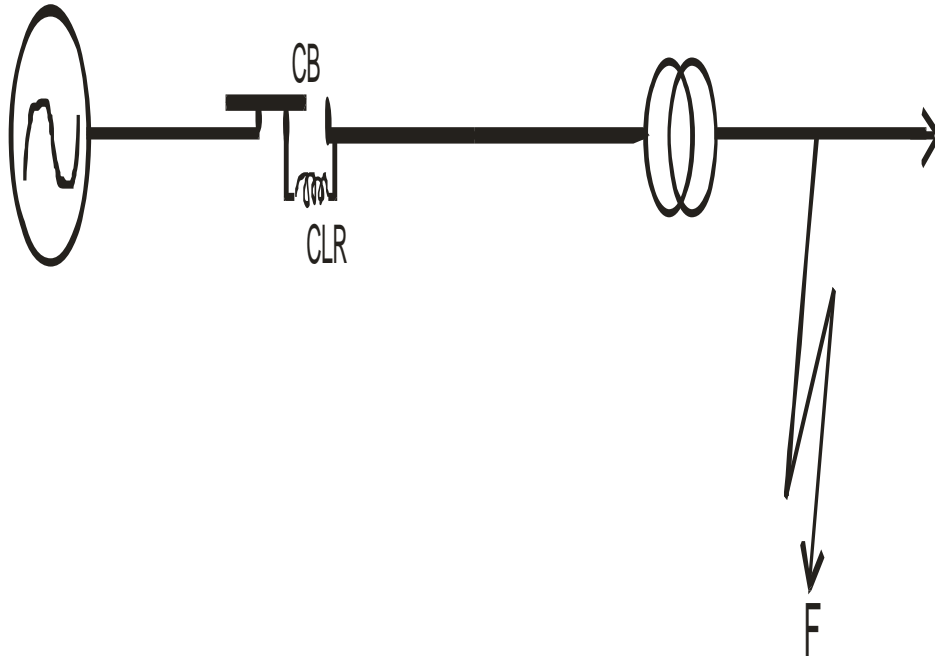


Figure 3.21: CB/CLR in series before the modified CB contacts separate during opening

Operation

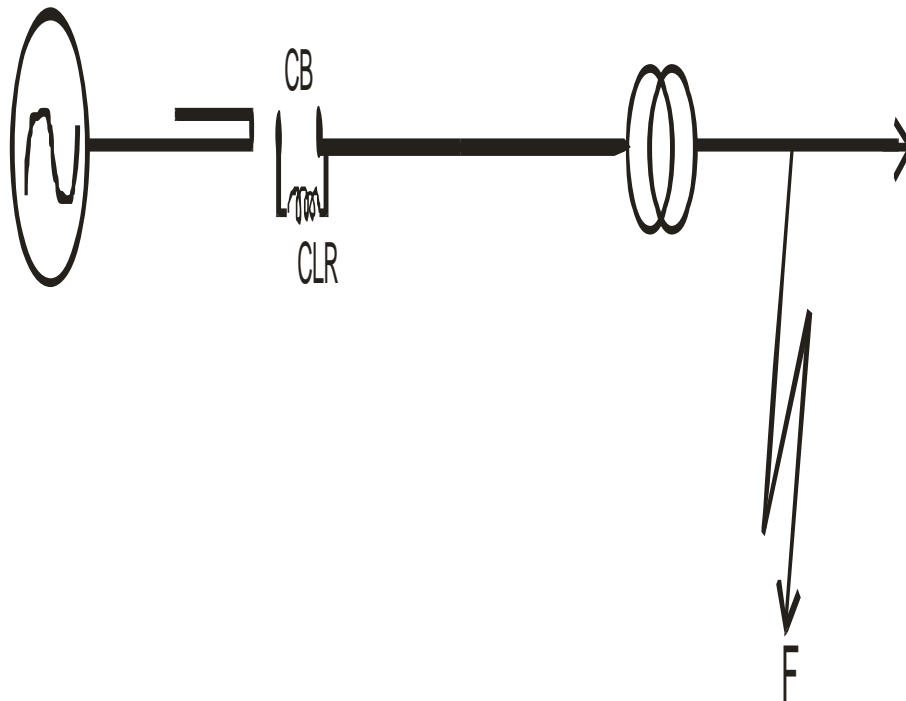


Figure 3.22: The modified CB in open position

3.2.4 Circuit Breaker Cost Parameters

The costs of circuit breakers can be reduced via reduction in the values of the key parameters that determine the operating mechanism energy requirement of circuit breakers, namely:

- (1) The kinetic energy requirement, W_{KIN}
- (2) The blast pressure, ΔP , necessary for arc quenching
- (3) The moving contact cross-sectional area, A

3.2.4.1 Kinetic Energy Requirement (W_{kin}) of Circuit Breakers

The kinetic energy requirement (W_{KIN}) of circuit breakers is influenced by the total break time (t_0) of the circuit breaker, the minimum arc-gap distance and the mass of the moving contact rod of the circuit breaker. Pflaum and Muller, (1974) affirmed that the reliability of circuit breakers is directly related to the number of moving parts. Switching of high short circuit currents involves high reliability and shortest operating times. A short break time as well as short make/break time is necessary to reduce the electro-dynamic stresses on switchgears and generators.

If the total break time (t_0) of a circuit breaker is reduced, the minimum arc-gap distance would have to be attained in an approximately reduced duration. The breaker ready time (t_{BR}), relates with the total break time (t_0) of a circuit breaker as follows (Bachofen et al, 1982):

$$t_{BR} = t_0 - (2f)^{-1} \quad (3.33)$$

Where:

f = System Frequency

t_{BR} = Breaker Ready Time

t_0 = Total Break Time

Since the speed of contact travel increases in inverse proportion to the breaker ready time, t_{BR} , the velocity, V , of the contact travel relates with the minimum arc-gap distance and the breaker ready time, t_{BR} , as follows:

$$V = \frac{\text{Minimum arc gap distance}}{t_{BR}} \quad (3.34)$$

$$W_{KIN} = \frac{1}{2} MV^2 \quad (3.35)$$

Where:

W_{KIN} = CB Kinetic Energy Requirement

M = Mass of the moving contact rod of the CB

V = Velocity of the moving contact.

From (3.35),

$$W_{KIN} \propto V^2 \text{ (The mass } M \text{ being constant)}$$

For ease of calculation, since only the proportion of change in quantities is being investigated, the constant term is taken as unity. This is appropriate since in a given equation, no matter the value of the constant term, the variable term determines the proportion of change in the value. From (3.34), with minimum arc-gap distance being constant,

$$V \propto \frac{1}{t_{BR}}$$

Or

$$V^2 \propto (t_{BR})^{-2}$$

Such that:

$$V^2 = k(t_{BR})^{-2} \quad (3.36)$$

Where the constant term $k = 1 \text{ meter}^2$ and,

Hence,

$$W_{KIN} = k_1(t_{BR})^{-2}$$

Where the constant $k_1 = \frac{1}{2} Mass$

$$= 1\text{kg (for ease of calculation)}$$

Such that applying (3.33):

$$W_{KIN} = k_1[t_0 - (2f)^{-1}]^{-2} \quad (3.37)$$

To examine how the variations in the total break time (t_0) can affect the kinetic energy requirement (W_{KIN}), breaker ready time (t_{BR}) is generated using (3.33) and then (3.37).

If for instance, the mass of the moving contact M is no longer constant but increasing,

$$W_{KIN} \propto M(t_{BR})^{-2}$$

And (3.37) becomes:

$$W_{KIN} = M[t_0 - (2f)^{-1}]^{-2} \quad (3.38)$$

However, from the expression:

$$\text{Mass} = \text{volume (i.e. area x length) x density}$$

Mass is proportional to area, A , i.e.

$$M \propto A$$

And from (3.35), for constant velocity and varying mass,

$$W_{KIN} \propto M \quad (3.39)$$

Such that

$$W_{KIN} \propto A \quad (3.40)$$

3.2.4.2 The Blast Pressure (ΔP), Necessary for Arc Quenching

As already shown in (3.26) in section 3.2.3.1.2

$$\Delta P \propto I^{1.4} N^{-0.28}$$

Or

$$\Delta P = k I^{1.4} N^{-0.28} \text{ kg/cm}^2$$

Where:

k = Proportionality constant with its value as 2.77×10^{-4} kg/(cm²-amps) at 20°C (Bachofen et al, 1982)

I = The Interrupted Short Circuit Current

N = The number of breaks (i.e. the number of fold movements the Pivoting

Links of the moving contact can make to either completely close or open). Its value is 2 (Bachofen et al, 1982), such that:

$$\Delta P = 2.27 \times 10^{-4} I^{1.4} \text{ kg/cm}^2$$

3.2.4.3 The Circuit Breaker Moving Contact Cross-sectional Area, A .

This also is already shown in (3.29) in section 3.2.3.1.2 to be:

$$A \propto N^{0.14} I^{0.3} \text{ (m}^2\text{)}$$

Or

$$A = K N^{0.14} I^{0.3} \text{ (m}^2\text{)}$$

Where:

I = The Interrupted Short Circuit Current

K = Proportionality constant with its value as $3.64 \times 10^{-5} \text{ m}^2/\text{ampere}$ (Bachofen et al, 1982)

N = The number of breaks (i.e. the number of fold movements the Pivoting

Links of the moving contact can make to either completely close or open). Its value is 2 such that:

$$A = 4.0 \times 10^{-5} \times I^{0.3} \text{ (m}^2\text{)}$$

3.2.4.3.1 The Effect of Overall Length of Forked Moving Contact on its Mass

The mass of the copper moving contact, M , is the product of its volume, v , and the density, d . i.e.

$$M = dv$$

But

$$v = hA$$

Where

h = The Length of the Moving Contact

A = The Cross sectional area of the Moving Contact.

But from (3.29),

$$A = 1.1KI^{0.3}$$

Such that:

$$M = 1.1KdhI^{0.3} \text{ (kg)} \tag{3.41}$$

3.2.4.4 The Compression Work Requirement of the Circuit Breaker

The relationship between blast pressure ΔP and compression work, W_{COMP} , is not simple since one part of the blast pressure is produced by the arc through heating up. Assuming a

linear relationship as a rough approximation, ΔP relates to the compression work, W_{COMP} thus (Bachofen et al, 1982):

$$W_{COMP} \propto N \cdot A \cdot \Delta P \quad (3.42)$$

But from (3.40),

$$W_{KIN} \propto A$$

Such that the compression work requirement of a CB, W_{COMP} as given in (3.42) is the cost determinant for a CB.

Substituting (3.26) and (3.30) into (3.42) gives

$$W_{COMP} \propto N \cdot N^{0.14} I^{0.3} I^{1.4} N^{-0.28}$$

OR

$$W_{COMP} \propto N^{0.86} I^{1.7} \quad (3.43)$$

Again, taking the value of the total number of breaks, N, to be 2 in (3.43)

$$W_{COMP} \propto 1.8 I^{1.7}$$

Or

$$W_{COMP} = K 1.8 I^{1.7} \text{ Newton} \quad (3.44)$$

Where:

K= Proportionality constant

I = The Interrupted Short Circuit Current

(3.44) is the mathematical model for determining the cost of circuit breakers in monetary terms as the cost of CBs is proportional to the compression work capacity. Any measure or technique that lowers the value of the interrupted short circuit current I as shown in (3.44), results in the reduction of the CB cost.

3.3 System Simulations

A very significant objective of the improved circuit breaker contacts and terminals in this dissertation is ensuring minimal constant power losses when Current Limiting Reactors (CLRs) are used for arc control in medium and high voltage systems. With the CB and CLR connection as shown in Figure 3.20, the power flow in the network (Nkalagu – Abakaliki 132kV line) was simulated in POWERWORLD environment to prove that indeed the result is minimal constant power losses. The simulation captured four different states of the network namely:

- (1) The network with the existing CB without CLR, as shown in Figure 3.1
- (2) 2 ohms CLR used on the network with the modified CB in closed position as shown in Figure 3.20
- (3) 2 ohms CLR used on the network with the modified CB during opening operation (before the contacts separate) as shown in Figure 3.21.
- (4) The network with the existing CB with 2 ohms CLR, as shown in Figure 3.3

The impedance (Z) of a conductor is the square root of the absolute value of the sum of the squares of the resistance (R) and reactance (X) (Theraja and Theraja, (2012). That is:

$$Z = \sqrt{|R^2 + jX^2|} \quad (3.45)$$

Hence the data in Appendices H, I, J, K, L, L1, M and M1 are the simulation results, while the data in Appendix G is the Nkalagu – Abakaliki 132kV Line reactance obtained from TCN and given in Table 3.2 as $0.008389744435 + j0.01646580057$, the calculated existing CB moving contact impedance of 2.15×10^{-5} ohms given in Table 3.10 (which is the same as $0.00001 + j0.00002$) and the calculated value of CLR of 2.0 ohms in section 3.2.3.1.1 (which is the same as $0.00552 + j0.01083$).

3.3.1 Power Flow on Nkalagu – Abakaliki 132kV Line with the Existing CB without CLR

The network model is as shown in Figure 3.23. The power flow is as shown in Figure 3.24, while the input parameters, branch state (i.e. the flow from source to the load) and the bus records are respectively shown in Appendices G, H and I.

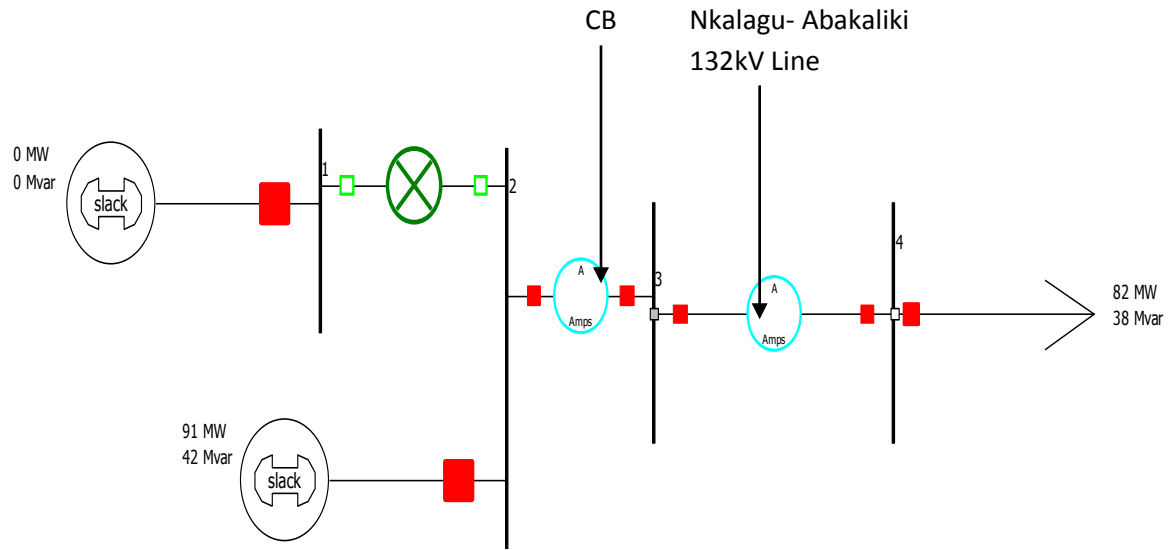


Figure 3.23: Network Model for Nkalagu – Abakaliki 132kV Line with the existing CB without CLR

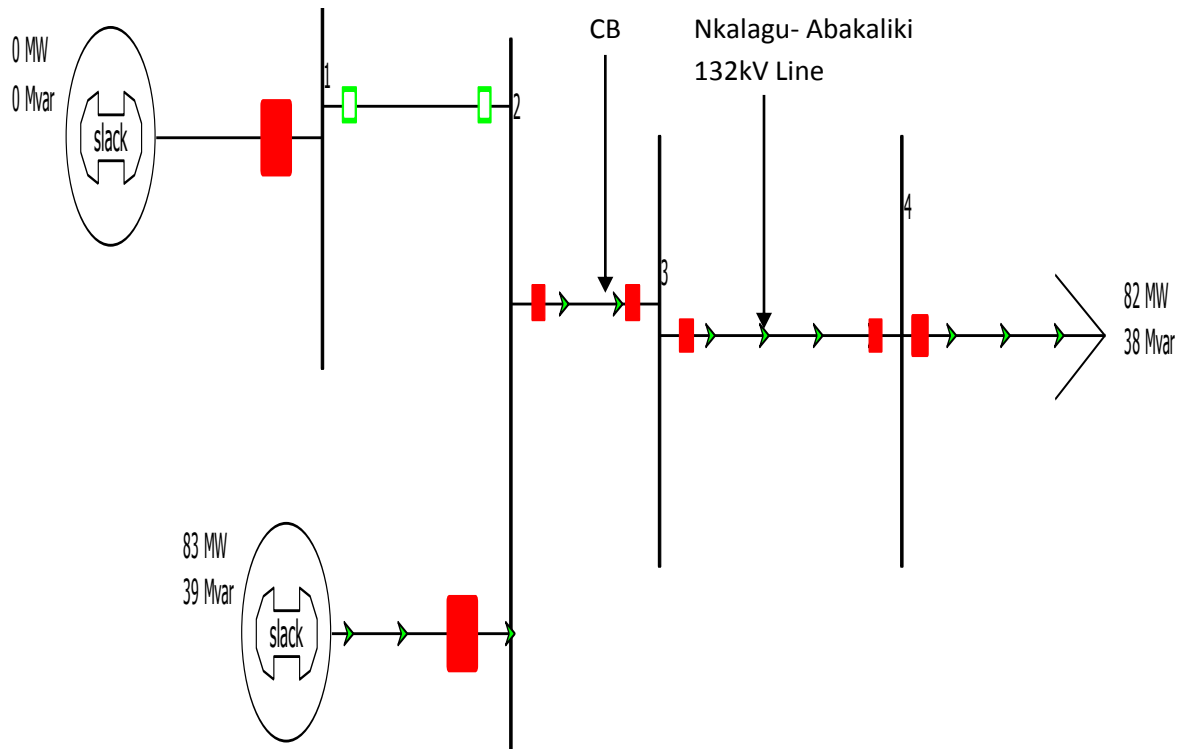


Figure 3.24: The power flow on Nkalagu – Abakaliki 132kV Line with the existing CB without CLR

3.3.2 Power Flow on Nkalagu – Abakaliki 132kV Line with the modified CB and CLR in closed position connected as earlier shown in Figure 3.20

The network model is as shown in Figure 3.25. The power flow is as shown in Figure 3.26, while the input parameters, branch state (i.e. the flow from source to the load) and the bus records are respectively shown in Appendices G, J and K.

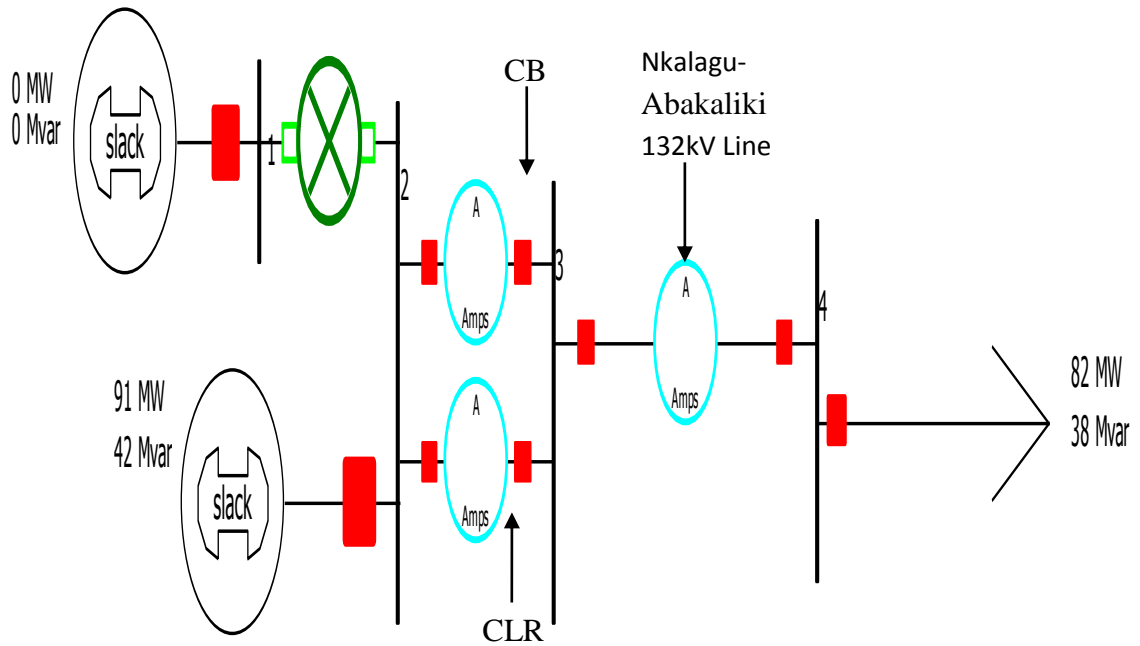


Figure 3.25: Network Model for Nkalagu – Abakaliki 132kV Line with the Modified CB and a CLR of 2 ohms Impedance in closed position

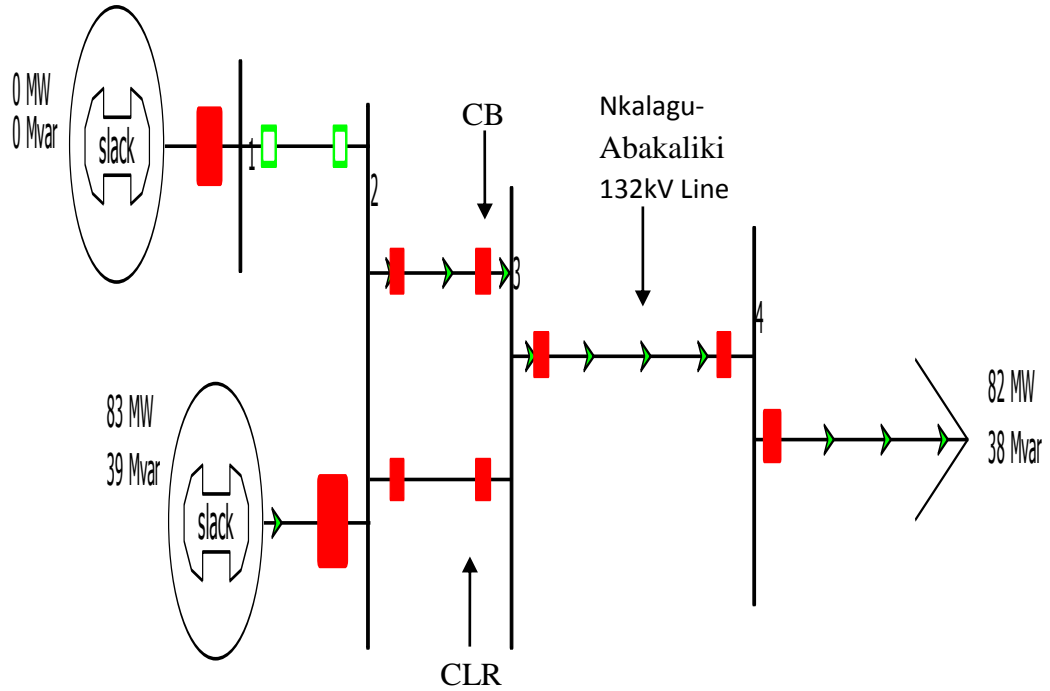


Figure 3.26: The power flow on Nkalagu – Abakaliki 132kV Line with the Modified CB in closed position and a CLR of 2 ohms Impedance

3.3.3 Power Flow on Nkalagu – Abakaliki 132kV Line with the modified CB and a CLR during opening operation as earlier shown in Figure 3.21

The network model is as shown in Figure 3.27. The power flow is as shown in Figure 3.28, while the input parameters, branch state (i.e. the flow from source to the load) and the bus records are respectively shown in Appendices G, L and L1.

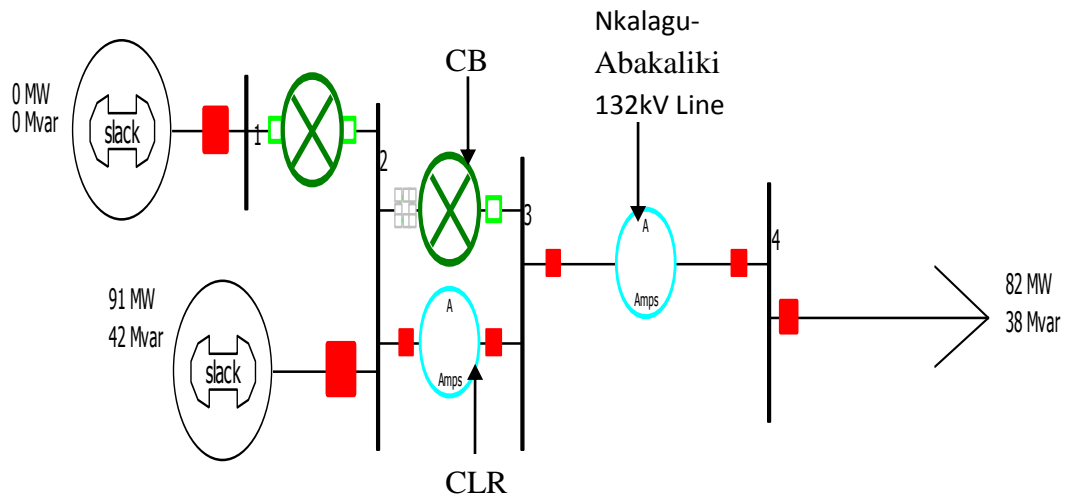


Figure 3.27: Network Model for Nkalagu – Abakaliki 132kV Line with the Modified CB and a CLR of 2 ohms Impedance during opening operation

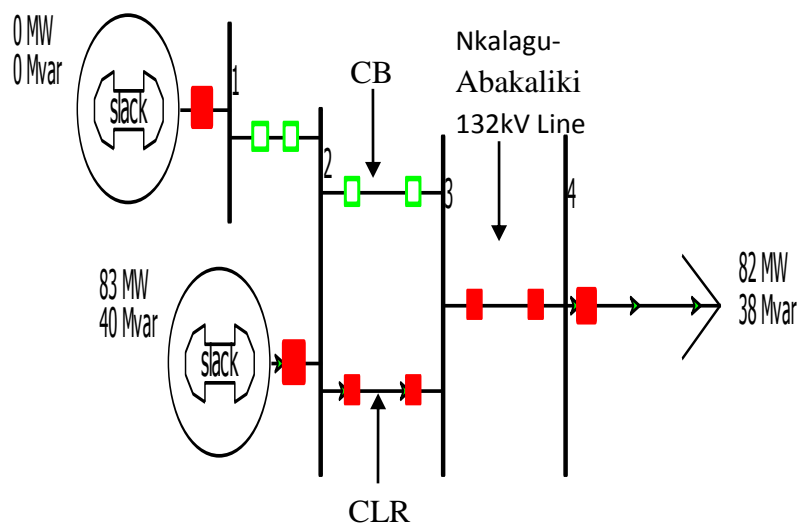


Figure 3.28: The power flow on Nkalagu – Abakaliki 132kV Line with the Modified CB and a CLR of 2 ohms Impedance during opening operation

3.3.4 Power Flow on Nkalagu – Abakaliki 132kV Line with the Existing CB with 2 ohm CLR

The network model is as shown in Figure 3.29. The power flow is as shown in Figure 3.30, while the input parameters, branch state (i.e. the flow from source to the load) and the bus records are respectively shown in Appendices G, M and M1.

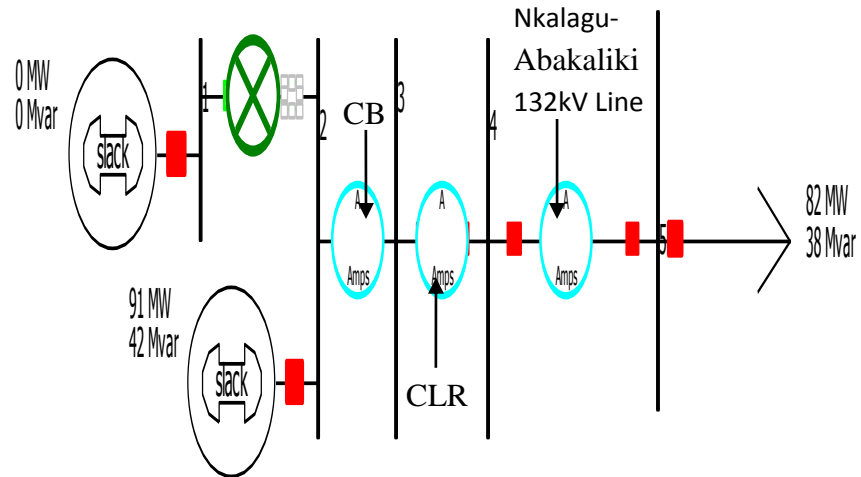


Figure 3.29: Network Model for Nkalagu – Abakaliki 132kV Line with the existing CB in series with 2.0 ohms CLR

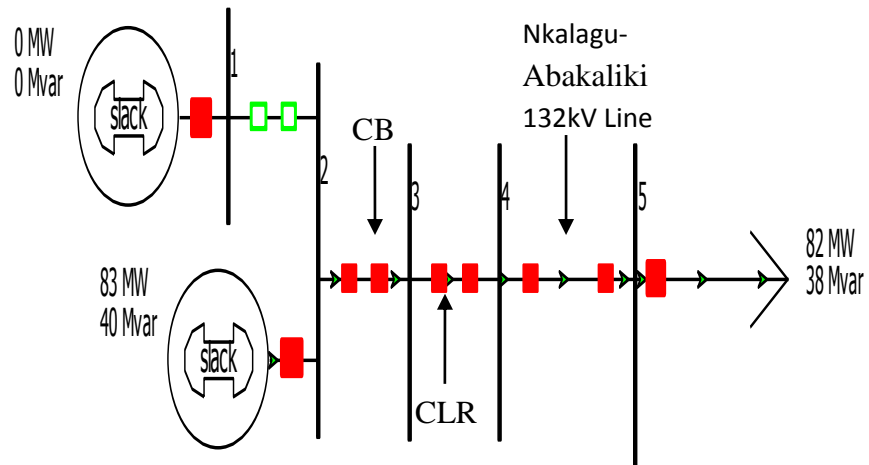


Figure 3.30: The power flow on Nkalagu – Abakaliki 132kV Line with the existing CB in series with 2.0 ohms CLR

3.4 Result Validation Models

The mathematical model for electrical power delivery in watts (Theraja and Theraja, 2012) is:

$$\sqrt{3}IV\cos\theta \quad (3.46)$$

Where:

V = voltage

I = current

θ = voltage phase angle

While the mathematical model for the power losses in an electrical conductor in watts is:

$$\sqrt{3}I^2Z / \cos \theta / \tag{3.47}$$

Where:

Z = impedance of the conductor

I = current through the conductor

θ = voltage phase angle

CHAPTER FOUR

RESULTS AND DISCUSSIONS

4.1 Power Loss Reduction

4.1.1 Forked Moving Contact and Power Loss Reduction

Some experimental measured values and data collected shown in section 3.1.3 and the calculated value for Z_{CLR} and Z_{CB} shown in section 3.2.3.1.1 and Table 3.10 respectively, are recast in Table 4.1. These data in Table 4.1 shall be used first, on the existing mathematical models for power losses namely: (3.2), (3.3) and (3.4). Thereafter, the data shall be used on the developed models for power loss reduction namely: (3.5), (3.6) and (3.7).

Table 4.1: Tariff and load data

S/N	Item	Value
1	T_1	₦30.93 per kwh
2	T_2	₦45.24 per kwh
3	f_{d1}	30% of 280A (i.e. 84A)
4	f_{d2}	70% of 280A (i.e. 196A)
5	$\cos\phi_1$ (power factor)	0.94
6	$\cos\phi_2$ (power factor)	0.79
7	I = total load current	280 amperes
8	Z_{CB}	2.73×10^{-5} ohms
9	Z_{CLR}	2.0 ohms

Source: TCN, Nkalagu Transmission Station

Where:

T_1 = Tariff for customer group 1 (naira per kWh)

T_2 = Tariff for customer group 2 (in naira per kWh)

I = Load current (in amperes)

f_{d1} = Percentage of total load current supplied to the feeder for customer group 1

f_{d2} = Percentage of total load current supplied to the feeder for customer group 2

$\cos\phi_1$ = Power factor for the load for customer group 1

$\cos\phi_2$ = Power factor for the load for customer group 2

Substituting in (3.2) gives:

$$P = \frac{\sqrt{3} \times 84^2 \times 2 \times 0.94}{1000} + \frac{\sqrt{3} \times 196^2 \times 2 \times 0.79}{1000} \text{ kW}$$
$$= 128.11 \text{ kW}$$

Substituting in (3.3) gives:

$$\text{kWh per month} = (1.25 \times 84^2 \times 2 \times 0.94) + (1.25 \times 196^2 \times 2 \times 0.79)$$
$$= 92453.2 \text{ kWh per month}$$
$$= 92.453 \text{ MWh per month}$$

Substituting in (3.4) gives:

$$\text{kWh per annum} = (15 \times 84^2 \times 2 \times 0.94) + (15 \times 196^2 \times 2 \times 0.79)$$
$$= 1109438.4 \text{ kWh per annum}$$
$$= 1109.438 \text{ MWh per annum}$$

Substituting in (3.5) gives:

$$P = \frac{\sqrt{3} \times 280^2 \times 0.0000273}{1000} \times [(0.3^2 \times 0.94) + (0.7^2 \times 0.79)]$$
$$= 0.00175 \text{ kW}$$
$$= 1.75 \text{ W}$$

Substituting in (3.6) gives:

$$\begin{aligned} \text{kWh per month} &= 1.25 \times 280^2 \times 0.0000273 \times ([0.3^2 \times 0.94] + [0.7^2 \times 0.79]) \\ &= 1.262\text{kWh per month} \end{aligned}$$

Substituting in (3.7) gives:

$$\begin{aligned} \text{kWh per annum} &= 15 \times 280^2 \times 0.0000273 \times ([0.3^2 \times 0.94] + [0.7^2 \times 0.79]) \\ &= 15.144\text{kWh per annum} \end{aligned}$$

Comparing the results above for the existing models namely: (3.2), (3.3) and (3.4) side by side with the developed models resulting from the improved contacts and terminals namely: (3.5), (3.6) and (3.7), negligible power losses were achieved. These calculated values are in agreement with the simulation result shown in Appendix J that showed the power flow through the CLR (represented with the line from bus 2 to bus 3, circuit 2) as 0.0MVA for the improved CB and CLR in closed position. This is also evident from the simulation result explained below.

From the simulation in section 3.3.2 shown in Figure 3.26, with the CLR of 2 ohms impedance connected as shown in figure 4.1, there was negligible power flow through the CLR. The result is shown in Appendix J where the simulation result shows 91.6MVA (i.e. 82.7MW, 39.4Mvar) available at bus 2 delivered at bus 3 with 91.4MVA i.e. 82.5MW, 39.3Mvar, via the CB (i.e. circuit 1) and 0.2MVA i.e. 0.2MW, 0.1Mvar via the CLR (i.e. circuit 2).

It is important to further explain here that Figure 4.1 is the same as the model shown in Figure 3.23 where the available power injected on Nkalagu – Abakaliki network at Nkalagu Transmission station is 100MVA (i.e. 91MW, 42Mvar). Severing the Nkalagu – Abakaliki network from the National grid by opening the CB between bus 1 and bus 2, the power injected at Nkalagu Transmission Station adjusted automatically from 100MVA to 91.6MVA (i.e. 82.7MW, 39.4Mvar) to supply the load of 90MVA (i.e. 82MW, 38Mvar) at Abakaliki Transmission Station as shown in the simulated power flow in Figures 3.24 and 3.26 for the existing CB without CLR and the modified CB with CLR respectively. If the

Nkalagu – Abakaliki network is not severed from the grid, 8.4MVA will be exported to the rest of the grid.

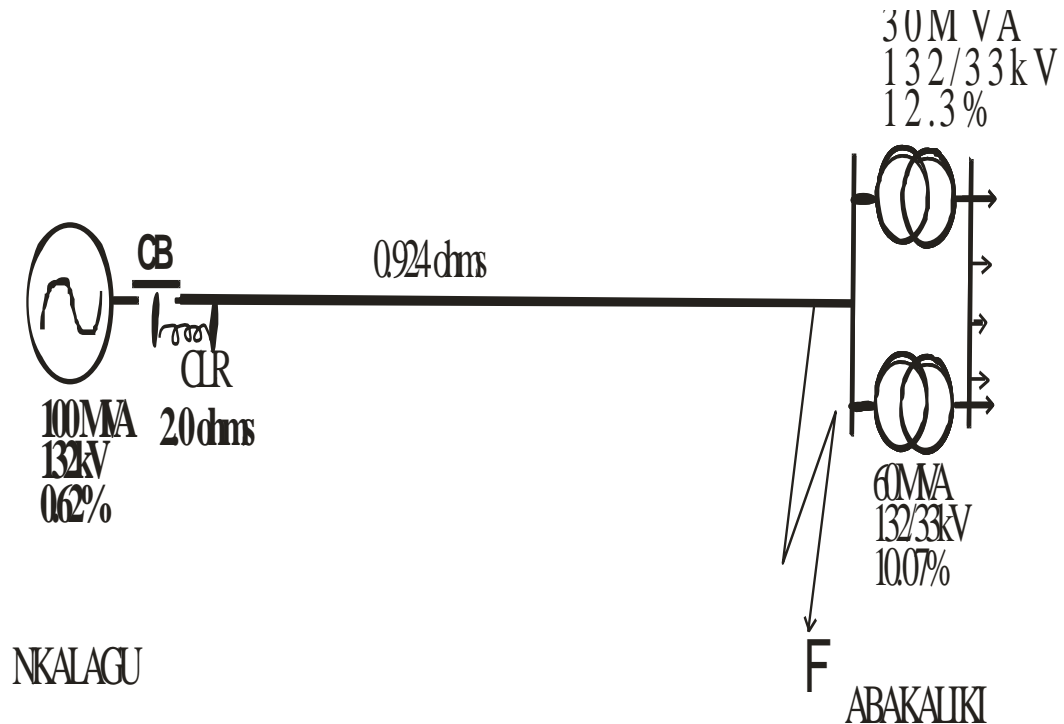


Figure 4.1: Nkalagu-Abakaliki 132kV line with the modified CB and CLR

The voltage at bus 4 from the simulation result shown in Appendix k is 130.23kV, meaning 1.3% voltage drop (from 132kV to 130.23kV). Comparing this voltage drop to the allowable voltage variation of between +9.85% and -10% (TCN, 2010), (NERC, 2010), it is very acceptable.

The advantage of the improved CB in terms of constant power losses can still be appreciated better if the loss incurred during CB opening operation which is similar to Figure 4.2 as shown in the simulation result presented in Appendices L and L1 is considered. It can be seen from Appendix L that of the 92.5MVA available at bus 2, only 91.6MVA got to bus 3 and 0.9MVA lost.

It is again important to further explain here that Figure 4.2 is the same as the model shown in Figure 3.28 where the available power injected on Nkalagu – Abakaliki network at Nkalagu Transmission station is 100MVA (i.e. 91MW and 42Mvar). Severing the Nkalagu – Abakaliki network from the National grid by opening the CB between bus 1 and bus 2,

the power injected on Nkalagu – Abakaliki network at Nkalagu Transmission Station adjusted automatically from 100MVA to 91.6MVA (i.e. 83MW, 39Mvar) to supply the load of 90MVA (i.e. 82MW, 38Mvar) at Abakaliki Transmission Station as shown in the simulated power flow in Figures 3.24 and 3.26 for the existing CB without CLR and the modified CB with CLR respectively.

However, during the opening operation of the modified CB when the CLR gets serially connected (which is equivalent to the existing CB with CLR), the power injection at Nkalagu Transmission Station adjusted a little. It maintained 83MW and 40Mvar at bus 2) and delivered 82MW, 38Mvar at Abakaliki Transmission Station as shown in the simulated power flow in Figures 3.28 and 3.30.

The voltages at buses 3 and 4 in Appendix L1 are 130.82kV and 129.04kV respectively. These are the same at buses 4 and 5 in Appendix M1. These, amount to 0.89% and 2.2% voltage drop respectively. The meaning of this is that using CLR in the existing CBs requires increased Generating capacity so as to maintain the same voltage level at both the sending bus and the receiving bus.

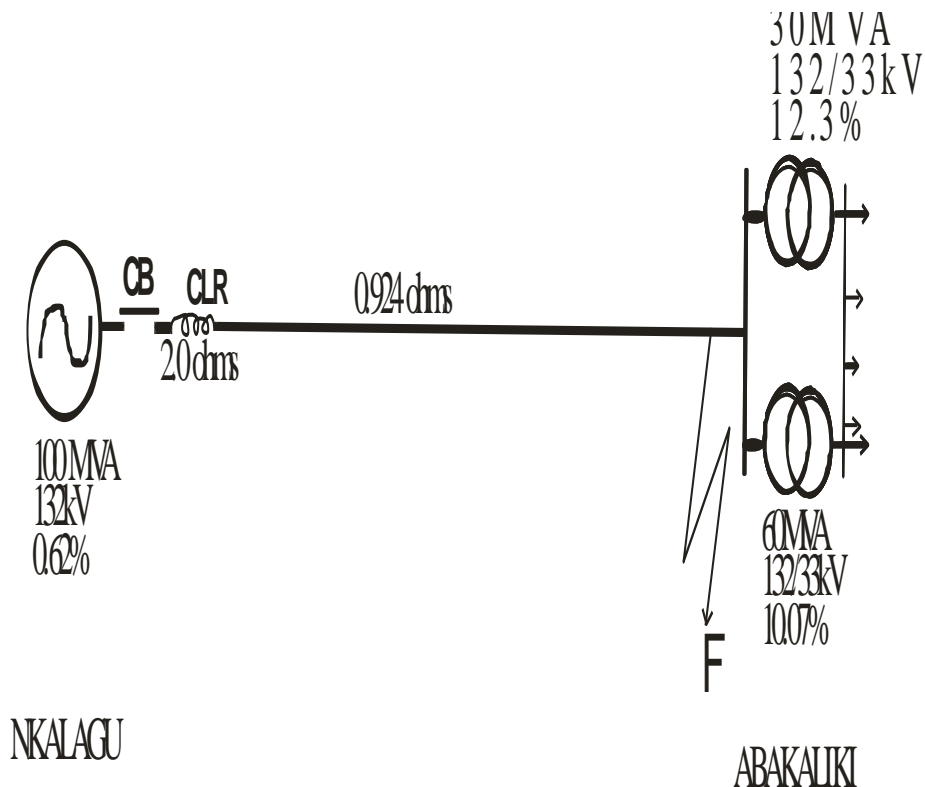


Figure 4.2: Nkalagu-Abakaliki 132kV line with the existing CB and CLR

The losses arising from the arrangement in Figure 4.2 are outrageous. The result is as summarized in Table 4.2.

Table 4.2: Summary of the Calculated/Measured result from the use of forked moving contact CB and the existing CB

S/N	Description	Existing CB with CLR (calculated/measured)	Modified CB (CB with forked moving contact) with CLR (calculated/measured)
1	Moving contact resistance (ohms)	2.15×10^{-5}	2.73×10^{-5}
2	Moving contact cross-sectional area (m ²)	9.61×10^{-4}	7.8×10^{-4}
3	CLR reactance (ohms)	2.0	2.0
4	Equivalent reactance of CLR and CB moving contact (in ohms) at normal condition	2.0	2.73×10^{-5}
5	Voltage rating (kV)	132	132
6	Available load current (amperes)	280	280
7	Rated normal current (kA)	3.15	3.15
8	Rated short circuit breaking capacity (kA)	40	40 but seen as 20 when breaking
9	Power losses (kW)	128.11	0.00175

The following are very conspicuous from Table 4.2:

- (1) 19% reduction in moving contact cross sectional area (from 9.61×10^{-4} to 7.8×10^{-4}) was achieved.
- (2) 50% reduction in short circuit level (from 40kA to 20kA) was achieved.
- (3) Negligible constant power losses (from 128.11kW to 0.00175kW) was achieved.

4.1.2 The Adapter and Power Loss Reduction

The calculated value for Z_{CLR} and Z_{CB} shown in section 3.2.3.1.1 and Table 3.10 respectively are:

$$Z_{CLR} = 2.0 \text{ ohms, and } Z_{CB} = 2.15 \times 10^{-5} \text{ ohms}$$

Where:

$$Z_{CLR} = \text{CLR reactance}$$

$$Z_{CB} = \text{CB moving contact reactance in ohms}$$

Substituting the values given in Table 4.1 for $Z_{CB} = 2.15 \times 10^{-5}$ ohms in the existing mathematical models for power losses namely: (3.2), (3.3) and (3.4) and then on the developed models for power loss reduction namely: (3.5), (3.6) and (3.7) gives the following results:

Substituting in (3.2) gives:

$$P = \frac{\sqrt{3} \times 84^2 \times 2 \times 0.94}{1000} + \frac{\sqrt{3} \times 196^2 \times 2 \times 0.79}{1000} \text{ kW}$$

$$= 128.11 \text{ kW}$$

Substituting in (3.3) gives:

$$\text{kWh per month} = (1.25 \times 84^2 \times 2 \times 0.94) + (1.25 \times 196^2 \times 2 \times 0.79)$$

$$= 92453.2 \text{ kWh per month}$$

$$= 92.453 \text{ MWh per month}$$

Substituting in (3.4) gives:

$$\text{kWh per annum} = (15 \times 84^2 \times 2 \times 0.94) + (15 \times 196^2 \times 2 \times 0.79)$$

$$= 1109438.4 \text{ kWh per annum}$$

$$= 1109.438 \text{ MWh per annum}$$

Substituting in (3.5) gives:

$$P = \frac{\sqrt{3} \times 280^2 \times 0.0000215}{1000} \times [(0.3^2 \times 0.94) + (0.7^2 \times 0.79)]$$

$$= 0.00138 \text{ kW}$$

Substituting in (3.6) gives:

$$\text{kWh per month} = 1.25 \times 280^2 \times 0.0000215 \times [(0.3^2 \times 0.94) + (0.7^2 \times 0.79)]$$

$$= 0.994 \text{ kWh per month}$$

Substituting in (3.7) gives:

$$\text{kWh per annum} = 15 \times 280^2 \times 0.0000215 \times [(0.3^2 \times 0.94) + (0.7^2 \times 0.79)]$$

$$= 11.926 \text{ kWh per annum}$$

These calculated values again are in agreement with the simulation result shown in Appendix J that showed the power flow through the CLR as 0.0MVA.

The result obtained, for the modified CB terminal (the use of adapter to couple the CLR on the existing CB) implemented on the same Nkalagu-Abakaliki 132kV line is as summarized in Table 4.3.

Table 4.3: Summary of the result from the adapter implementation on the existing CB terminal and the existing CB

S/N	Description	Existing CB with CLR (calculated/measured)	Modified CB with CLR connected with adapter (calculated/measured)

1	Moving contact resistance (Z_{CB}) (in ohms)	2.15×10^{-5}	2.15×10^{-5}
2	Moving contact cross-sectional area (m^2)	9.61×10^{-4}	9.61×10^{-4}
3	CLR reactance (Z_{CLR}) (in ohms)	2.0	2.0
4	Equivalent reactance of CLR and CB moving contact (ohms)	2.0	2.15×10^{-5}
5	Voltage rating (kV)	132	132
6	Available load current (amperes)	280	280
7	Rated normal current (kA)	3.15	3.15
8	Rated short circuit breaking capacity (kA)	40	Sees 40 as 20 and so 80 seen as 40
9	Power losses (kW)	128.11	0.00138

The following are very conspicuous from Table 4.3:

- (1) It can accommodate 100% increase in short circuit level arising from network expansion (from 40kA to 80kA) or
- (2) In the absence of increase in short circuit level arising from network expansion, offers 50% reduction in short circuit level (from 40kA to 20kA)
- (3) Negligible constant power losses (from 128.11kW to 0.00138kW was achieved).

4.2 Reduction in the Heat generated when operating a CB

Both the forked moving contact and the adapter implementation offered 50% reduction in the interrupted current. Substituting this value into the developed model for reduced heat generation namely: (3.13), gives percentage reduction in heat generated as:

$$[1 - (1 - 0.5)^2] \times 100$$

$$= 75\%$$

This means 75% reduction in the heat energy generated when operating the modified circuit breaker with the CLR in place on the network considered.

Alternatively, the mathematical model for the heat generated when operating a CB is as given in (3.10). That is: $E = I^2Rt$

From section 3.2.3.1.1, the existing CB interrupts 38kA while the improved CB interrupts 19kA (i.e. I in (3.10) = 38000A and 19000A respectively for the existing CB and improved CB). From the data obtained from TCN shown in section 3.1.3 the CB relay instructs the CB to open after 0.2 seconds from the time the fault occurred while the CB interrupts the current in 0.3 seconds. Hence, t in (3.10) is 0.5 seconds. From Table 3.10, the moving contact impedance was shown to be 2.15×10^{-5} ohms. Substituting these values into (3.10) for the existing CB for $I = 38000A$ and then for the improved CB for $I = 19000A$ gave the following result:

$$\text{For the Existing CB, heat generated} = 38000^2 \times 0.0000215 \times 0.5$$

$$= 15523 \text{ Joules}$$

$$= 15.52\text{kJ.}$$

$$\text{For the Improved CB, heat generated} = 19000^2 \times 0.0000215 \times 0.5$$

$$= 3880.75 \text{ Joules}$$

$$= 3.88\text{kJ.}$$

Percentage heat reduction can be calculated as follows:

$$\frac{\text{heat generated in the existing CB} - \text{heat generated in the improved CB}}{\text{heat generated in the existing CB}} \times 100$$

$$= \frac{15.52 - 3.88}{15.52} \times 100$$

= 75%

4.3 Technique for connecting CB and CLR in parallel

The technique for connecting CB and CLR in parallel when the CB is in closed position as shown in section 3.2.3 is by the use of forked moving contacts in CBs and the use of adapters on existing CBs. What either the forked contact as shown in the prototype connection in Figure 3.12 in section 3.2.3.1.5 or the adapter does as seen in the prototype connection in Figures 3.15 and 3.16 in section 3.2.3.1.6 is to provide a conducting path parallel to the moving contact of the CB. It is on this parallel conducting path that the CLR is connected. With the CB in closed position, the CLR remains in parallel with it thereby constituting negligible power losses through the CLR as negligible power flows through it as seen in Appendix J where only 0.2MW out of 82.7MW passed through the CLR.

During opening operation, the CLR gets serially connected as the CB moving contact (the shorter prong of the forked moving contact) separates from the fixed contact first. Due to very high impedance developed by this contact separation (open circuit impedance), automatically by current reversal, power flows through the CLR (just for about 0.3 seconds) in the circuit before the longer prong (CLR contacts) also open. This principle of operation is as shown in Figures 3.20, 3.21 and 3.22 in section 3.2.3.4. It is the improved CB's capability to connect the CB and CLR in Parallel when the CB is in closed position that guarantees negligible constant power losses in the system, while its ability to connect the CLR in series just before the CB contacts separate guarantees its role as a current limitation device for efficient arc control. These are what the forked contact and the adapter have achieved as shown with Figures 3.20, 3.21 and 3.22 in section 3.2.3.4.

4.4 Circuit Breaker Cost Reduction

4.4.1 Kinetic Energy Requirement, W_{KIN} , of Circuit Breakers

How the variations in the total break time (t_0) can affect the kinetic energy requirement (W_{KIN}), can be analyzed by generating the breaker ready time (t_{BR}) using (3.33) and then using (3.37)

Using (3.33), at $t_0 = 50\text{ms}$, $f = 50\text{Hz}$

$$t_{BR} = 50 \times 10^{-3} - (2 \times 50)^{-1}$$

$$= 0.05 - 0.01 = 40\text{ms.}$$

Using (3.37)

$$\begin{aligned} W_{KIN} &= k_1(40 \times 10^{-3})^{-2} \\ &= 625k_1 \text{ joules.} \end{aligned}$$

For $t_0 = 33.3\text{ms}$

$$\begin{aligned} t_{BR} &= 33.3 \times 10^{-3} - (2 \times 50)^{-1} \\ &= 0.0233 \\ &= 23.3\text{ms} \end{aligned}$$

$$\begin{aligned} W_{KIN} &= k_1 \times (t_{BR})^{-2} \\ &= (23.3 \times 10^{-3})^{-2}k_1 \\ &= 1842k_1 \text{ joules} \end{aligned}$$

The result gotten above means that reduction in the total break time (t_0) of the circuit breaker by a factor of 1.50 (from 50ms to 33.3ms), i.e.:

$$\frac{50}{33.3} = 1.5$$

Could result to as much as an increase in the kinetic energy requirement (W_{KIN}) of the circuit breaker by a factor of 2.947 (from 625 joules to 1842 joules), i.e.:

$$\frac{1842}{625} = 2.947$$

Using the MATLAB codes given in Appendix N and using (3.37) for a 50Hz system, the response curve of CB kinetic energy (W_{KIN}) against the total break time(t_0) is shown in Figure 4.3. The derived relationships between the total break time, (t_0) and breaker ready time, (t_{BR}); between the breaker ready time, (t_{BR}) and the kinetic energy requirement,

(W_{KIN}); and between the total break time, (t_0) and the kinetic energy requirement, (W_{KIN}) are respectively presented in Tables 4.4, 4.5 and 4.6.

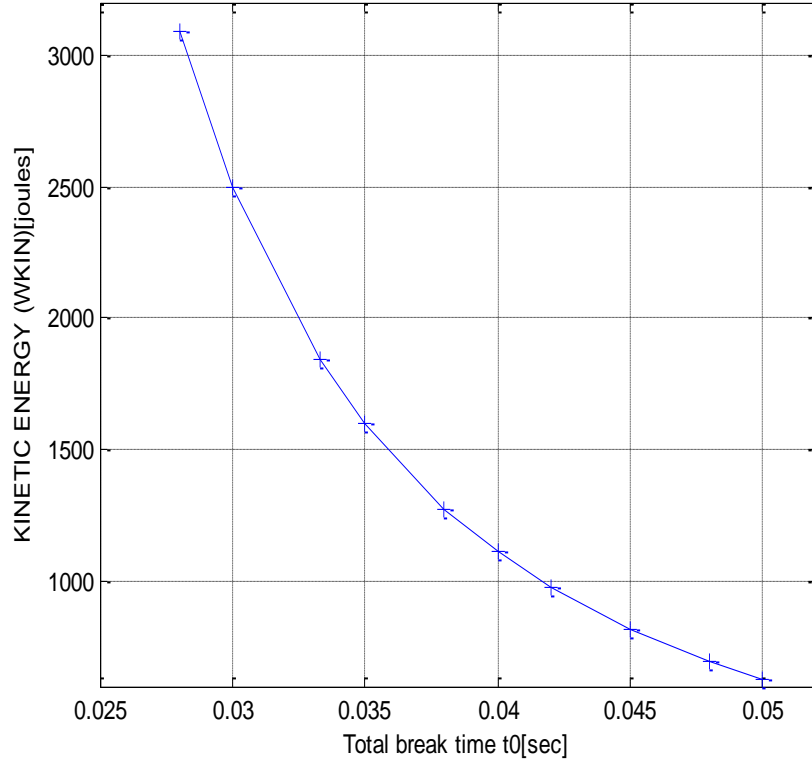


Figure 4.3: Response curve of CB total break time (t_0) against the kinetic energy requirement (W_{KIN})

Table 4.4: Total break time and the corresponding breaker ready Time for a 50Hz system

S/N	Total break time, t_0 (in seconds)	Breaker ready time, t_{br} (in seconds)
1.	0.0500	0.0400
2.	0.0480	0.0380
3.	0.0450	0.0350
4.	0.0420	0.0320
5.	0.0400	0.0300

6.	0.0380	0.0280
7.	0.0350	0.0250
8.	0.0333	0.0233
9'	0.0300	0.0200
10.	0.0280	0.0180

Table 4.5: Breaker ready time and the corresponding kinetic energy requirement for a 50Hz system

S/N	Breaker ready time, t_{BR} (in seconds)	Kinetic energy requirement, W_{KIN} (in kilo Joules)
1.	0.0400	0.6250
2.	0.0380	0.6925
3.	0.0350	0.8163
4.	0.0320	0.9766
5.	0.0300	1.1111
6.	0.0280	1.2755
7.	0.0250	1.6000
8.	0.0233	1.8420
9.	0.0200	2.5000
10.	0.0180	3.0864

Table 4.6: Total break time and the corresponding kinetic energy requirement for a 50Hz system

S/N	Total break time, t_o (in seconds)	Kinetic energy requirement, W_{KIN} (in kilo Joules)
1.	0.0500	0.6250
2.	0.0480	0.6925
3.	0.0450	0.8163
4.	0.0420	0.9766
5.	0.0400	1.1111

6.	0.0380	1.2755
7.	0.0350	1.6000
8.	0.0333	1.8420
9.	0.0300	2.5000
10.	0.0280	3.0864

Values for kinetic energy requirement of the circuit breaker at any required total break time can be read from the graph. The graph has a negative slope and clearly shows a rapid growth in kinetic energy requirement for little reduction in the total break time. Table 4.4 shows a direct relationship between circuit breaker total break time (t_o) and circuit breaker ready time (t_{BR}). However, decrease in t_o and t_{BR} cause astronomical rise in the circuit breaker kinetic energy requirement W_{KIN} . The meaning of these is that reduction in the total break time of a circuit breaker increases the cost of the circuit breaker.

Now, from (3.38), i.e. ($W_{KIN} = M [t_o - (2f)^{-1}]^{-2}$), keeping the velocity of the contact travel, V (i.e. total break time, t_o , of the circuit breaker as well as the minimum arc-gap distance), constant, while from (3.39) and (3.40), i.e. ($W_{KIN} \propto M$ and $W_{KIN} \propto A$) reducing the mass, M , of the circuit breaker moving contact, could result in the reduction of the kinetic energy requirement, W_{KIN} , of the circuit breaker of the same proportion as the proportion of reduction in the mass or the area of the moving contact.

There was 19% reduction in the moving contact area as seen in Table 4.2. Hence a reduction of 19% in W_{KIN} was achieved since no matter the value of the proportionality constant; W_{KIN} and the area A must grow or reduce in the same proportion.

The strategy here, as far as reduction in the kinetic energy requirement, W_{KIN} , of the circuit breaker is concerned, was to leave the circuit breaker to operate in the existing designed total break time, t_o , and the existing designed minimum arc-gap distance, but at a reduced mass of the moving contact via reduction in the cross sectional area of the moving contact rod.

4.4.2 Reduction in the Blast Pressure, Δp , necessary for Arc Quenching

Using the MATLAB codes presented in Appendix O and using (3.26) i.e. ($\Delta P = k \times 0.82 \times I^{1.40}$ for $N = 2$) for the value of k equal to 2.77, the response curve is as shown in figure 4.4.

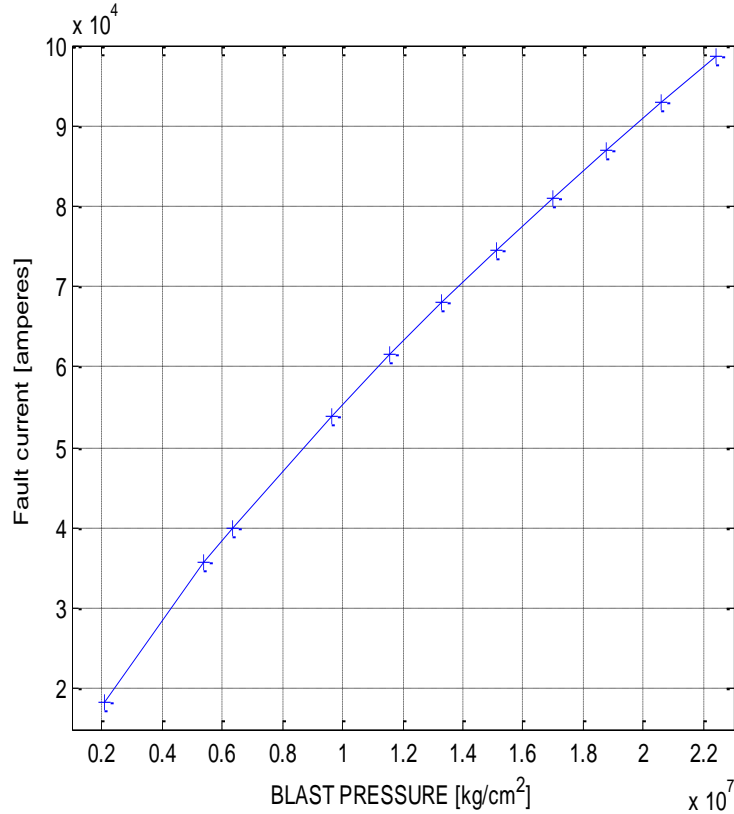


Figure 4.4: Response curve of blast pressure against fault current

Figure 4.4 has a positive slope and shows that increase in anticipated fault current results in increase in the required blast pressure necessary for arc quenching and vice versa.

To determine how the reduction in the fault current averagely affects the blast pressure of circuit breakers, (3.26) is examined, i.e.

$$\Delta P = k \times N^{-0.28} \times I^{1.40}$$

Where

$N = 2$ in recent CBs such that $N^{-0.28}$ is 0.82

ΔP = blast pressure necessary for reliable arc quenching

I = anticipated short circuit current

k = proportionality constant

On examining (3.26), it was seen that k and 0.82 (i.e. $2^{-0.28}$) are constant terms, meaning that the blast pressure ΔP is dependent on the value of the anticipated short circuit raised to power 1.4 (i.e. $I^{1.40}$).

From Tables 4.2 and 4.3, 50% reduction in short circuit level (from 40kA to 20kA) was shown to be achieved. What this means is that (3.26) can be written as:

$$\Delta P = k \times 0.82 \times (0.5I)^{1.40}$$

Or

$$\Delta P = k \times 0.82 \times (0.5)^{1.40} \times I^{1.40}$$

Where 0.82 equals $N^{-0.28}$ and $0.5I$ equals 50% reduction in fault current (I)

Rearranging gives:

$$\begin{aligned}\Delta P &= (0.5)^{1.40} [k \times 0.82 \times I^{1.40}] \\ &= 0.379[k \times 0.82 \times I^{1.40}]\end{aligned}$$

On comparing:

$$\Delta P = k \times 0.82 \times I^{1.40}$$

And

$$\Delta P = 0.379[k \times 0.82 \times I^{1.40}]$$

62.1% reduction in the blast pressure necessary for reliable arc quenching for a corresponding reduction of 50% in the interrupted current when operating the modified

circuit breaker with the CLR in place is very noticeable. This can be clearly seen from Table 4.7 generated using the MATLAB codes presented in Appendix P.

Table 4.7 Fault current and the corresponding blast pressure

Serial no.	Fault current (kA)	Blast pressure (kg/cm ²)
1.	20.00	2.397 0 x 10 ⁶
2.	35.70	5.3940 x 10 ⁶
3.	40.00	6.3250 x 10 ⁶
4.	54.00	9.6280 x 10 ⁶
5.	61.50	1.1551 x 10 ⁷
6.	68.00	1.3295 x 10 ⁷
7.	74.50	1.5108 x 10 ⁷
8.	80.00	1.6692 x 10 ⁷
9.	87.00	1.8772 x 10 ⁷
10.	93.00	2.0610 x 10 ⁷
11.	98.70	2.2399 x 10 ⁷

As can be seen in Table 4.7 every reduction of 50% in fault current results in 62.1% reduction in the blast pressure.

4.4.3 Effect of Cross-Sectional Area (A) on the CB Forked moving Contact

Using the MATLAB codes presented in Appendix Q and using (3.29) i.e. ($A = k \times 1.1 \times I^{0.3}$), for the value of k equal to 3.64×10^{-5} , the response curve is as shown in Figure 4.5.

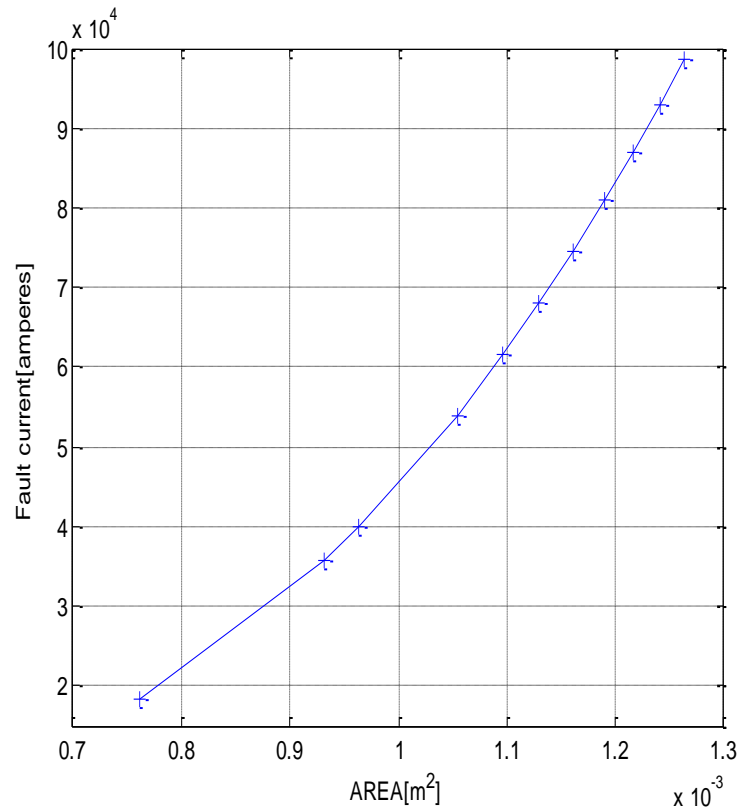


Figure 4.5: Response curve of the moving contact area against the fault current

Figure 4.5 simply shows that reduction in the anticipated fault current amounts to reduction in circuit breaker moving contact cross-sectional area.

Again, to determine how the reduction in the fault current averagely affects circuit breaker moving contact cross-sectional, (3.29) is examined i.e.

$$A = k \times 1.1 \times I^{0.3}$$

Where:

A = moving contact cross sectional area

I = anticipated short circuit current

k = proportionality constant

On examining (3.29), it can be seen that k and 1.1 are constant terms, meaning that the moving contact cross sectional area A , is dependent on the value of the anticipated short circuit raised to power 0.3 (i.e. $I^{0.3}$). From Tables 4.2 and 4.3, 50% reduction in short circuit level (from 40kA to 20kA) was shown to be achieved. What this means again is that (3.29) can be written as:

$$A = k \times 1.1 \times (0.5I)^{0.3}$$

Or

$$A = k \times 1.1 \times (0.5)^{0.3} \times I^{0.3}$$

Rearranging gives:

$$\begin{aligned} A &= (0.5)^{0.3} [k \times 1.1 \times I^{0.3}] \\ &= 0.81 [k \times 1.1 \times I^{0.3}] \end{aligned}$$

On comparing:

$$A = k \times 1.1 \times I^{0.3}$$

And

$$A = 0.81 [k \times 1.1 \times I^{0.3}]$$

19% reduction in the moving contact cross sectional area for a corresponding reduction of 50% in the interrupted current when operating the modified circuit breaker with the CLR in place can be seen. This agrees with the value gotten from Table 4.2.

4.4.4 The Compression Work Requirement of the Circuit Breaker

Using the MATLAB codes presented in Appendix R and using (3.44) i.e. ($W_{COMP} = k \times 1.8 \times I^{1.7}$) for proportionality constant k taken as unity, the response curve is shown in Figure 4.6 while some selected fault levels and the corresponding CB's compression work requirement are given in Table 4.8.

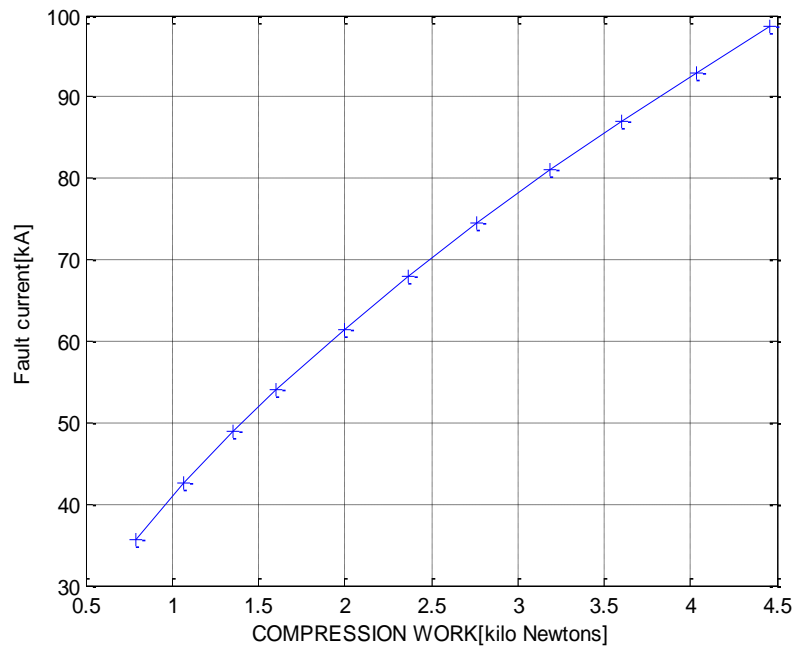


Figure 4.6: Response curve of compression work against fault current

Table 4.8: Fault current and the corresponding CB's compression work Requirement

S/N	Fault current (kA)	Corresponding CB's Compression Work Requirement (kilo Newton)
1.	35.7000	0.7914
2.	42.5000	1.0645
3.	49.0000	1.3559
4.	54.0000	1.5994
5.	61.5000	1.9951
6.	68.0000	2.3667
7.	74.5000	2.7641
8.	81.0000	3.1865
9.	87.0000	3.5981
10.	93.0000	4.0300
11.	98.7000	4.4589

Figure 4.6 and Table 4.8 show that reduction in the anticipated fault current amounts to reduction in the compression work requirement of circuit breakers.

Again, to determine how the reduction in the fault current averagely affects circuit breaker compression work requirement, (3.44) was examined i.e.:

$$W_{\text{COMP}} = k \times 1.8 \times I^{1.7}$$

Where

W_{COMP} = compression work requirement of circuit breaker

I = anticipated short circuit current

k = proportionality constant

On examining (3.44), it can be seen that k and 1.8 are constant terms, meaning that compression work requirement of circuit breaker (W_{COMP}), is dependent on the value of the anticipated short circuit current raised to power 1.7 (i.e. $I^{1.7}$).

From Tables 4.2 and 4.3, 50% reduction in short circuit level (from 40kA to 20kA) was shown to be achieved. What this means again is that (3.44) can be written as:

$$W_{\text{COMP}} = k \times 1.8 \times (0.5I)^{1.7}$$

Or

$$W_{\text{COMP}} = k \times 1.8 \times (0.5)^{1.7} \times I^{1.7}$$

Rearranging gives:

$$\begin{aligned} W_{\text{COMP}} &= (0.5)^{1.7} [k \times 1.8 \times I^{1.7}] \\ &= 0.31 [k \times 1.8 \times I^{1.7}] \end{aligned}$$

Comparing:

$$W_{\text{COMP}} = k \times 1.8 \times I^{1.7}$$

And

$$W_{\text{COMP}} = 0.31[k \times 1.8 \times I^{1.7}]$$

69% reduction in the Circuit Breaker Compression Work requirement for a corresponding reduction of 50% in the interrupted current when operating the modified circuit breaker with the CLR in place is noticed.

The followings equations are considered to buttress this point:

$$(3.26) \text{ i.e. } ((\Delta P = kI^{1.4}N^{-0.28} \text{ i.e. } \Delta P \propto I^{1.4}N^{-0.28})$$

$$(3.29) \text{ i.e. } (A \propto I^{0.3} \times N^{0.14})$$

$$(3.40) \text{ i.e. } (W_{\text{KIN}} \propto A) \text{ and}$$

$$(3.42) \text{ i.e. } (W_{\text{COMP}} \propto N.A. \Delta P)$$

It can be observed that the dependent items in (3.26) and (3.29) namely: ΔP and A , are the independent items in (3.42) and A is also the independent item in (3.40). What this means is that all the variables in the cost parameters of a circuit breaker are embedded in (3.42) and so the compression work requirement is the determinant for circuit breaker cost, such that for the fifty percent reduction in the anticipated fault current, there is a sixty-nine percent reduction in the circuit breaker cost.

4.4.5 Reduction in Circuit Breaker Size

Using the MATLAB codes presented in appendix S and using (3.41) i.e. ($M = d \times h \times k \times 1.1 \times I^{0.3}$), the effect of the increased overall length of the forked moving contact rod on its mass is shown in the response curves given in Figure 4.7. Some selected fault levels and the corresponding effect of the increased overall length of the forked moving contact rod on its mass are given using the MATLAB codes presented in Appendix T, in Tables 4.9 and 4.10.

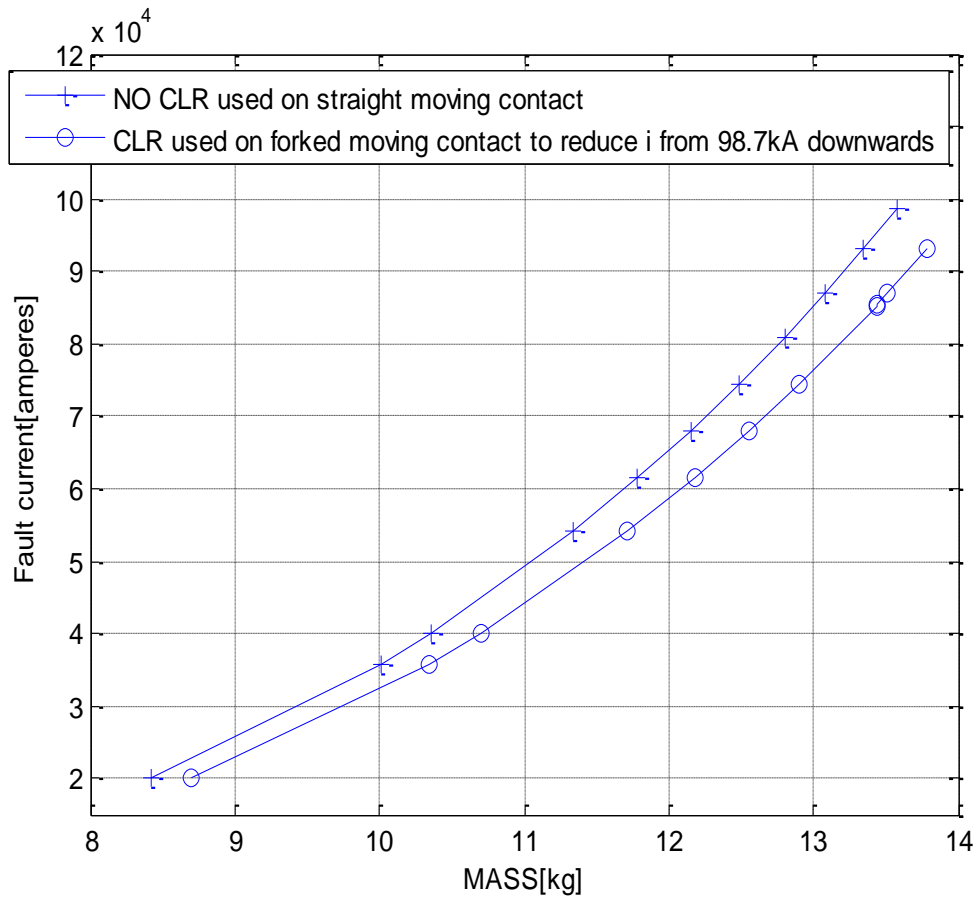


Figure 4.7 Response curve of the overall mass of the forked moving contact against the fault current.

Table 4.9: Fault current and the corresponding mass of moving contact rod (straight rod of 1.20m length)

S/N	Fault current (kA)	Mass of moving contact rod (kg)
1.	98.70	13.5841
2.	93.00	13.3438
3.	87.00	13.0795
4.	81.00	12.8021
5.	74.50	12.4848
6.	68.00	12.1475
7.	61.50	11.7868

8.	54.00	11.3358
9.	40.00	10.3598
10.	35.70	10.0123
11.	20.00	8.4148

Table 4.10: Fault current and the corresponding mass of moving contact rod (forked rod of 1.24m overall length)

S,N	Fault current (kA)	Mass of moving contact rod (kg)
1.	93.00	13.7886
2.	87.00	12.9010
3.	74.50	12.9010
4.	68.00	12.5524
5.	61.50	12.1797
6.	54.00	11.7137
7.	40.00	10.7052
8.	35.858	10.3598
9.	35.542	10.3323
10.	35.541	10.3322
11.	20.00	8.6953

It can be read from Figure 4.7 and Table 4.10 that reducing any particular fault level with the CLR does not immediately start reducing the mass of the moving contact rod. The mass is rather higher unless the fault level is reduced to a certain point before the mass begins to reduce. As seen from Tables 4.9 and 4.10, reducing 40kA even down to 35.859kA for the forked moving contact gives an increase in the mass of the moving contact (in this case, above 10.3598kg gotten for the straight moving contact meant for 40kA)

When the moving contact is forked, the overall length is slightly increased.

From the expression:

$$\text{Mass} = \text{volume (i.e. area x length)} \times \text{density};$$

it appears there could be increased mass and as such increased operating mechanism energy all round but as shown in (3.29), (3.42) and (3.44), reducing the current reduces the cross-sectional area of the moving contact rod and the compression work, 'W_{COMP}'. That is, the mass of the moving contact rod is reduced even though the length is slightly increased as can be seen in the response curve of the moving contact area against the fault current, for the values of 'I' between 20kA and 98.7kA and for number of breaks, 'N' = 2, shown in Figure 4.5.

This is clearly seen in the response curve of fault current reduction against the overall mass of the forked moving contact rod of the CB (overall length = 124cm) compared with the mass of the required (straight) moving contact rod (length = 120cm) when no CLR is used, as shown in Figure 4.7.

However, it should be noted from Figure 4.7 that the fault current must be reduced below a certain limit (the efficiency threshold) before the mass of the rod begins to decrease else, the mass is higher. Hence, in the application of CLR on the forked moving contact, the value of the CLR reactance must meet the efficiency limit criterion as stated in section 2.3.1.1 and at the same time be capable of reducing the interrupted fault current below the efficiency threshold current for the forked moving contact. This is further shown in Tables 4.11, 4.12, 4.13 and 4.14 arising from the MATLAB codes presented in Appendices U, V, W and X respectively. It should be noted from Table 4.9 that the mass of straight moving contact rod (in kg) with no CLR used for 40kA is 10.3598.

Table 4.11: The effect of the use of CLR on the overall mass of the forked CB moving contact rod

S/N	Fault current (kA) with no	Mass of straight moving contact	40kA limited downwards with	Corresponding mass of forked moving

	CLR	rod (kg) with no CLR used	CLR	contact rod (kg) with CLR used
1.	40.00	10.3598	40.00	10.7052
2.	40.00	10.3598	35.859	10.3599
3.	40.00	10.3598	35.858	10.3598
4.	40.00	10.3598	35.542	10.3323
5.	40.00	10.3598	35.541	10.3322
6.	40.00	10.3598	35.000	10.2848

Table 4.12: The effect of the use of CLR on the overall mass of the forked CB moving contact rod

S/N	Fault current (kA) with no CLR	Mass of straight moving contact rod (kg) with no CLR used	35kA limited downwards with CLR	Corresponding mass of forked moving contact rod (kg) with CLR used
1.	35.00	9.9530	35.000	10.2848
2.	35.00	9.9530	34.000	10.1957
3.	35.00	9.9530	33.700	10.1687
4.	35.00	9.9530	31.376	9.9530
5.	35.00	9.9530	31.375	9.9529
6.	35.00	9.9530	30.000	9.8200

Table 4.13: The effect of the use of CLR on the overall mass of the forked CB moving contact rod

S/N	Fault current (kA) with no CLR	Mass of straight moving contact rod (kg) with no CLR used	30kA limited downwards with CLR	Corresponding mass of forked moving contact rod (kg) with CLR used
1.	30.00	9.5032	30.000	9.8200
2.	30.00	9.5032	29.000	9.7206
3.	30.00	9.5032	26.894	9.5032
4.	30.00	9.5032	26.893	9.5031
5.	30.00	9.5032	26.655	9.4778
6.	30.00	9.5032	25.000	9.2973

Table 4.14: The effect of the use of CLR on the overall mass of the forked CB moving contact rod

S/N	Fault current (kA) with no CLR	Mass of straight moving contact rod (kg) with no CLR used	25kA limited downwards with CLR	Corresponding mass of forked moving contact rod (kg) with CLR used
1.	25.00	8.9974	25.000	9.2973
2.	25.00	8.9974	24.000	9.1841

3.	25.00	8.9974	22.4115	8.9974
4.	25.00	8.9974	22.411	8.9973
5.	25.00	8.9974	22.213	8.9734
6.	25.00	8.9974	20.400	8.7471

4.5 Simulation Result Validation

The mathematical model for electrical power delivery by an electrical system in watts is as given in (3.46). That is: $\sqrt{3}IV\cos\theta$.

The mathematical model for power losses in watts also is as given in (3.47). That is: $\sqrt{3}I^2Z / \cos\theta$

From the simulation results in Appendices L and L1 which is the result for the improved CB with CLR during opening operation, 0.47MW was lost through the 2.0 ohms CLR between bus 2 and bus 3 via circuit 2. Other needful data from Appendices L and L1 is as given in Table 4.15.

Table 4.15: Simulation result data extracted from Appendices L and L1

S/N	Item	Bus 2	Bus 3
1	V	132kV	130.82kV
2	θ	0	-0.39
3	MW	83.2	82.7

The current available at the buses can be calculated using the model in (3.46), thus:

From (3.46),

At bus 2,

$$I = \frac{83200000}{\sqrt{3} \times 132000 \times \cos 0}$$

$$= 363.9\text{A}$$

At bus 3,

$$I = \frac{82700000}{\sqrt{3} \times 130820 \times \cos 0.39}$$

$$= 365\text{A}$$

Losses through the 2.0 ohms CLR as seen at bus 3 can be validated by substituting the current at bus 2 and the data in Table 4.15 into (3.47). That is:

$$\sqrt{3} \times 363.9^2 \times 2 \times \cos 0.39$$

$$= \sqrt{3} \times 363.9^2 \times 2 \times \cos 0.39$$

$$= 458716\text{W}$$

$$= 0.46\text{MW}$$

Between 0.47MW losses gotten from simulation and 0.46MW losses gotten by substituting values in the mathematical model, the percentage error is:

$$\frac{0.47 - 0.46}{0.47} \times 100$$

$$= 2.1\%$$

From the simulation results in Appendices M and M1 which is the result for the existing CB with CLR in series, 0.47MW was lost through the 2.0 ohms CLR between bus 3 and bus 4. Other needful data from Appendices M and M1 is as given in Table 4.16.

Table 4.16: Simulation result data extracted from Appendices M and M1

S/N	Item	Bus 3	Bus 4
1	V	131.997kV	130.818kV
2	θ	0	-0.39
3	MW	83.2	82.7

The current available at the buses can again be calculated using the model in (3.46), thus:

From (3.46),

At bus 3,

$$I = \frac{83200000}{\sqrt{3} \times 131997 \times \cos 0}$$
$$= 363.9\text{A}$$

At bus 4,

$$I = \frac{82700000}{\sqrt{3} \times 130818 \times \cos 0.39}$$
$$= 365\text{A}$$

Losses through the 2.0 ohms CLR as seen at bus 4 can be validated by substituting the current at bus 3 and the data in Table 4.10 into (3.47). That is:

$$\sqrt{3} \times 363.9^2 \times 2 \times \cos 0.39$$
$$= \sqrt{3} \times 363.9^2 \times 2 \times \cos 0.39$$
$$= 458716\text{W}$$
$$= 0.46\text{MW}$$

Between 0.47MW losses gotten from simulation and 0.46MW losses gotten by substituting values in the mathematical model, the percentage error is:

$$\frac{0.47 - 0.46}{0.47} \times 100$$
$$= 2.1\%$$

Again from the simulation results in Appendices J and K which is the result for the improved CB with CLR in closed position, 0MW was lost through the 2.0 ohms CLR between bus 2 and bus 3. Other needful data from Appendices J and K with due regard to circuit 2 between bus 2 and bus 3 is as given in Table 4.17.

Table 4.17: Simulation result data extracted from Appendices J and K

S/N	Item	Bus 2	Bus 3
1	V	132kV	131.99kV
2	θ	0	0
3	MW	0.2	82.7

The current available at the buses can be calculated using the model in (3.46), thus:

From (3.46),

At bus 2 for circuit 2,

$$I = \frac{200000}{\sqrt{3} \times 132000 \times \cos 0}$$

$$= 0.875A$$

At bus 3,

$$I = \frac{82700000}{\sqrt{3} \times 131990 \times \cos 0}$$

$$= 361.75A$$

Losses through the 2.0 ohms CLR as seen at bus 3 can be validated by substituting the current at bus 2 for circuit 2 and the data in Table 4.11 into (3.47). That is:

$$\sqrt{3} \times 0.875^2 \times 2 \times \cos 0$$

$$= 2.65W$$

$$= 2.65 \times 10^{-6}MW$$

This is approximately 0MW gotten from the simulation. It is a negligible loss when compared to the 0.47 MW losses earlier seen in the use of the existing CB.

CHAPTER FIVE

CONCLUSSION AND RECOMMENDATION

5.1 Conclusion

In this work, negligible power loss across the CLR (from 128.11kW to 1.75W and 1.38W for the forked moving contact and the adapter application respectively) during healthy system condition was achieved. Nineteen percent reduction in the CB moving contact cross-sectional area (from $9.61 \times 10^{-4} \text{m}^2$ to $7.8 \times 10^{-4} \text{m}^2$), for a 40kA short-circuit current on a 132kV CB was also achieved. Fifty percent reduction in interrupted fault current (from 40kA to 20kA), sixty-nine percent reduction in the CB cost (from ₦15,000,000.00 to ₦4,650,000.00) and seventy-five percent reduction in the heat generated (from 15.52kJ to 3.88kJ) when operating the CB were equally achieved. Hence, the study has shown that improvement of circuit breaker contacts and terminals will solve the problem of enormous constant power losses, high cost of CBs, and the problem of frequent CB explosions presently experienced due to high heat generated during operation.

The results obtained showed that with the use of adapters or forked moving contacts in circuit breakers, short circuit current limiting reactors can be used on not only the critical feeders (i.e. feeders with high necessity for steady supply) but on all feeders.

5.2 Recommendation

The relay-operated adapter is highly recommended for growing power utilities like Transmission Company of Nigeria (TCN). This is so considering the case demonstrated in this work: Nkalagu-Abakaliki 132kV network; implementation of the relay-operated adapter gives room for 100% growth in short circuit level arising from network expansion without CB replacement. Replacing the 40kA rated CB with a new one rated 80kA involves the following costs:

- (1) Procurement cost for the new CB
- (2) Labour cost for dismantling the old CB
- (3) Labour cost for installing the new CB
- (4) Equipment downtime in replacing the old CB with the new one.

With the plug and play relay-operated adapter the above costs are avoidable.

The forked moving contact CBs on the other hand is recommended for all power utilities. This is so because, apart from power loss reduction which they offer, they are cheaper. From the case demonstrated in this work: Nkalagu-Abakaliki 132kV network, as much as 69% reduction in CB cost was achieved.

5.3 Contributions to knowledge

The following are contributions to knowledge arising from this work:

- (1) The application of forked moving contacts in circuit breakers for power loss reduction was achieved. The forked moving contact allows CB and CLR connection in parallel during healthy operation of the system, thereby offering negligible constant power losses compared to the enormous constant power losses encountered in the use of series current limiting reactors on the existing system.
- (2) The application of adapters on existing circuit breaker terminal to provide CB and CLR connection in parallel during healthy operation of the system which offers negligible constant power losses compared to the enormous constant power losses encountered in the use of series current limiting reactors on the existing system was developed. It also gives opportunity for continuous use of an existing circuit breaker on the same network when the network's short circuit level increases due to network expansion.
- (3) The work also proffers reduction in Circuit Breaker operating mechanism energy and thus the reduction in the Circuit Breaker costs. For the case demonstrated here, there was a reduction in the circuit breaker cost by sixty-nine percent for a corresponding reduction in the fault current by fifty percent; when reactors are applied on either forked moving contact circuit breaker or on straight moving contact circuit breaker with adapter on the terminal.
- (4) Reduced heat generated when operating a CB was also achieved. Seventy-five percent reduction was achieved in this work and more can still be achieved, depending on the system under study.

REFERENCES

- Ahmed, M.M.R., Putrus, G.A., Li, R. and Xiao, L.J. (2004). Harmonic Analysis and Improvement of a New Solid-State Fault Current Limiter. IEEE Transactions on Industry Applications. 40, (4), 1012-1019.
- Amon, J.F., Fernandez, P.C., Rose, E.H., D'Ajuz A. and Castanheira, A. (2005). Brazilian Successful Experience in the Usage of Current Limiting Reactors for Short-Circuit Limitation. Montreal: International Conference on Power Systems Transients (IPST'05). 215-220.
- Bachofen, F. (1980). A New Range of SF₆ Outdoor Circuit Breaker Type HGF 100. Paris: Sprecher News. 1-6.
- Bachofen, F., Steinegger, P. and Glauser, R. (1982). A Novel Solution for High Speed SF₆ Puffer Type Power Circuit Breakers of High Rated Capability with Low Operating Mechanism Energy. Paris: International Conference on Large High Voltage Electric Systems. Cigre WG 13-07. 1-8.
- Belkind, A., Zhao, Z., Carter, D., Mahoney, L., McDonough, G., Roche, G., Scholl, R. and Walde, H. (2000). Pulsed-DC Reactive Sputtering of Dielectrics: Pulsing Parameter Effects in Society of Vacuum Coaters, 43rd Annual Technical Conference Proceedings, 86-90.
- Brandt, A., Hartung, K.-H., Bockholt, R. and Schmidt, V. (2012). Is-limiter: Limitation of short-circuit currents for maximum economic benefits. Germany: ABB AG – 40472 Ratingen, 1-4.
- Carter, D.C. (2007). Arc Reduction in Magnetron Sputtering of Metallic Materials. Advanced Energy Industries, Inc. ENG-ArcSputmetal, 270-271.

- Carter, D.C., Arent, R.L. and Christie, D.J. (2007). Sputter Process Enhancement through Pulsed-DC Power, in Society of Vacuum Coaters, 50th Annual Technical Conference Proceedings. 210-215.
- Cathy, J.J. (2001). Electric Machines: Analysis and Design Applying Matlab. New York: McGraw-Hill Companies, Inc.
- Cbi-electric (2012). What is Current Limitation & How Does Current Limitation Increase Short-Circuit Current Ratings? (Online), Available: http://www.cbi-electric.com.au/technical_news/innovation_and_technical_advancement/What-Is-Current-Limitation-&-How-Does-Current-Limitation-Increase-Short-Circuit-Current-Ratings?.pdf. Accessed on 17th January, 2017.
- Chao, T. (1995). Electronically Controlled Current Limiting Fuses. Proceedings of 1995 IEEE Annual Pulp and Paper Industry Technology Conference, Vancouver, Canada. pp. 10-17.
- Choi, H.S. and Lim, S.H. (2007). Operating Performance of the Flux-Lock and the Transformer Type Superconducting Fault Current Limiter Using the YBCO Thin Films. IEEE Transactions on Applied Superconductivity. 17, (2), 1823-1826.
- Christie, D.J. and Pellemounter, D. (2013). Voltage Reversal: Multi-Level Arc Management for Magnetron Sputtering - Proven technique for arc inhibition, arc quenching, and dissipation of energy stored in output cables. U.S.A: Advanced Energy Industries, Inc. 1-8.
- Cigre (1996). Studies on the Reliability of Single Pressure SF₆-Gas High-Voltage Circuit Breakers. Paris: International Conference on Large High Voltage Electric Systems. WG 13-06, 1-7.
- Claessens, M.S., Drews, L., Govindarajan, R., Holstein, M., Lohrberg, H. and Robin-Jouan, P. (2006). Advanced Modeling Methods for Circuit Breakers. Paris: International Conference on Large High Voltage Electric Systems Report, 1-8.

- Coil Innovation (2011). Current Limiting Reactors. (Online), Available:
<http://www.coilinnovation.com/products/current-limiting-reactors/?L=1>. Accessed on 17th January, 2017.
- Cooperindustries (2016). Inrush Current-limiting Reactor. (Online), Available:
http://www.cooperindustries.com/Cooper-Power-Systems/Inrush_Current-limiting_Reactor. Accessed on 25th July, 2016.
- Detlev, K. and Herbert, P. (2015). Superconducting and Solid-State Electronic Fault Current Limiter Technologies – The shift from demonstration projects to Business - as-usual Solutions. USA: Hannover Fair, 1-18.
- Dreimann, E., Grafe, V. and Hartung, K.H. (1994). Protective device for limiting short-circuit currents. Germany: ABB AG, 1, (15), 492-494.
- Drummond, G. (1995). Thin-Film DC Plasma Processing System. U.S.A: Advanced Energy Industries, Inc, US Patent 5,427,669.
- Electricalbaba (2017). Circuit Breaker and Arc Phenomena. (Online), Available:
<http://www.electricalbaba.com/circuit-breaker-and-arc-phenomenon/#content>. Accessed on 18th September, 2017.
- Electricaltechnology, (2016). Superconductor Current Limiting Reactor. (Online), Available: <http://www.electricaltechnology.org/Superconductor-Current-limiting-Reactors>. Accessed on 25th July, 2016.
- Energysiemens (2014). High Voltage Circuit Breakers. (Online), Available:
http://www.energy.siemens.com/high-voltage-circuit-breaker/portfolio_en/High-Voltage-CircuitBreakers-Siemens. Accessed on 24th July, 2014.
- Fahnoe, H.H. (1970). Taking Advantage of High Voltage Fuse Capabilities for System Protection. IEEE Transactions on Industry and General Applications, IGA-6, (5), 463-471.

- Fedasyuk, Serdyuk, P., Semchyshyn, Y. and Lviv Polytechnic National University (2008). Resistive Superconducting Fault Current Limiter Simulation and Design. Poznan: 15th International Conference Report, 349-353.
- Frontin, S.O., Morais, S.A., Nora, D. and Salgado, F.M. (1982). Limitation of Short-Circuit Stresses Applied to Switchgear on the Brazilian South-East System. Paris: International Conference on Large High Voltage Electric Systems. CIGRE WG 13-02, 1-6.
- Fuchsle D. and Heinemann, L. (2009). Hydro-Mechanical Spring Operating Mechanism – The Ultimate Solution to Operate High Voltage Circuit Breakers. Paris: International Conference on Large High Voltage Electric Systems. CIGRE Colloquium, South Africa, 1-9.
- GEC (1987). Protective Relay Application Guide. England: GEC Measurements Plc. 129 – 134.
- Geng, Z. X., Lin, X., Xu, J.Y. and Tian, C. (2008). Effects of Series Reactor on Short-circuit Current and Transient Recovery Voltage. Chongqing: International Conference on High Voltage Engineering and Application. 2008 Report, 524-526.
- Gert, R. (1968). Interrupting Short-Circuits in Power Transformer Circuits. Paris: Electrical Review Conference. 1968 Report, 198-201.
- Gert, R. and Valasek, J. (1982). Stresses Imposed on Medium Voltage Generator Circuit Breakers and on Breakers Connected to the Tertiary Windings of Large Power Transformers by the Transient Recovery Voltage Occurring in Service. Paris: International Conference on Large High Voltage Electric Systems. CIGRE WG 13-05 Report, 1-6.
- Gilany, M. and Al-Hasawi, W. (2009). Reducing the Short-Circuit Levels in Kuwait Transmission Network (A Case Study). Kuwait: World Academy of Science,

- Engineering and Technology. 53, 592-596.
- Gupta, B.R. (2012). Generation of Electrical Energy. New Delhi: Eurasia Publishing House (P) Ltd. 1-106.
- Gupta, J.B. (2012). A Course in Power Systems (Switchgear and Protection). New Delhi: S.K. Kataria & Sons.
- Hartung, K.H. (2002). I_s -Limiter, the Solution for High Short-Circuit Current Applications. ABB Calor Emag. 12-18.
- Hartung, K.H. (2017). Is-Limiter applications to reduce high short-circuit currents. ABB Calor Emag. 1-4.
- Heinemann, L. and Besold, F. (2009). Compact and Reliable, decades of Benefits of Gas-insulated switchgear from 52 to 1,100 kV. Germany: ABB Review. pp. 12-18.
- Heinemann, L. and Glock, J. (2010). Online Condition Monitoring System for Three Phase Encapsulated Gas-Insulated Switchgear. New Orleans: IEEE T&D Show & Conference, 1-7.
- Heinemann, L., Huanxin, C. and ABB AG (2014). Technology Benchmark of Operating Mechanisms for High Voltage Switchgear. Germany: ABB AG. 1-8.
- Holaus, W. and Stucki, F. (2008). Ultra-High-Voltage-Switchgear to Power China. Germany: ABB Review. Special Report, Dancing with the Dragon. pp. 19-26.
- Janowski, T., Kozak, S., Malinowski, H., Wojtasiewicz, G., Kondratowicz-Kucewicz, B. and Kozak, J. (2003). Properties Comparison of Superconducting Fault Current Limiters with Closed and Open Core. IEEE Transactions on Applied Superconductivity, 13, (2), 851-854.
- Karady, G.G. (1992). Principles of Fault Current Limitation by a Resonant LC Circuit.

- IEEE Proceedings-C, 139, (1), 1-6.
- Khorrami, M., Nader, M.S. and Nejhad, N.K. (2010). Short Circuit current Level Control and Its Effects on Circuit Breakers Transient Studies. India: Journal of Electrical Engineering: Theory and Application. 1, (1), 4-17.
- Klaus, D., Wilson, A., Dommerque, R., Bock, J., Creighton, A., Jones, D. and McWilliam, J. (2009). Fault Limiting Technology Trials in Distribution Networks. Prague, United Kingdom, 1-38.
- Kopplin H. (1980). Study of the Arc and of the Interaction Between Arc and Operating Mechanism in SF₆ Puffer Breakers. IEEE Transactions on Plasma Science, PS-8, (4), 331-338.
- Kraus, J.D and Fleisch, D.A. (1999). Electromagnetics with Applications. New York: WCB/McGraw-Hill Companies, Inc. 68-79.
- Lee, B.W., Sim, J., Park, K.B. and Oh, I.S. (2008). Practical Application Issues of Superconducting Fault Current Limiters for Electric Power Systems. IEE Transactions on Applied Superconductivity, 18, (2), 620-623.
- Lin, Y., Majoros, M., Coombs, T. and Campbell, A.M. (2007). System Studies of the Superconducting Fault Current Limiter in Electrical Distribution Grids. IEEE Transactions on Applied Superconductivity, 17, (2), 2339-2342.
- Littlefuse (2007). Using Current Limiting Fuses to Increase Short-circuit Current Ratings of Industrial Control Panels. (Online), Available:
<http://www.littlefuse.com/Using-Current-limiting-Fuses-to-Increase-Short-Circuit-Current-Ratings-of-Industrial-Control-Panels>. Accessed on 17th January, 2017.
- Malik B. (2017). Why reactors are used in power system and their types. Microcontrollers Lab. pp. 1-6. Retrieved 30th January, 2017.
- Mechprod (2012). Contacts and Contact Dynamics in Circuit Breakers. (Online),

Available: <http://www.mechprod.com/blog/bid/318509/Contacts-and-Contact-Dynamics-in-Circuit-Breakers-Contact-Resistance>. Accessed on 12th September, 2017.

Michael, A.L. and Richard, T. (2001). A Revolution in Circuit-Breaker Operating Mechanism Technology. Ludvika: ABB Switchgear AB, 1-5.

Mkireps (2016). Air Core Dry Type Reactors. (Online), Available: <http://www.mkireps.com/Air-core-dry-type-reactors>. Accessed on 25th July, 2016.

Nagrath, I.J. and Kothari, D.P. (2004). Power System Engineering. New Delhi: Tata McGraw-Hill Publishing Company Limited. 606-728.

Nair M. (2016). Current limiting reactors for power system application. Power Transmission. pp. 1-4. Retrieved 9th August, 2016.

NAPTIN (2010). Basic Power System Protection. Kainji: National Power Training Institute of Nigeria (NAPTIN) P1-2010-1, 38-81.

Nasiri, A. and Barahmandpour, H. (2006). Fault Current Limitation of Ramin Power Plant. Tehran: 21st International Power System Conference (PSC), 1640-1646.

Nasrallah E., Brikci F. and Perron S. (2007). Make/Break contacts in power circuit breaker. Electric energy T&D Magazine. pp. 1-12. Retrieved 9th August, 2016.

NERC (2010). The Grid Code for the Nigeria Electricity Transmission System. Abuja: Nigerian Electricity Regulatory Commission (NERC). 73-77.

Neundorfer (2014). Understanding Current Limiting Reactors. (Online), Available: [http://www.neundorfer.com/.../Neundorfer_Understanding-Current-Limiting-Reactors-\(CLRs\)](http://www.neundorfer.com/.../Neundorfer_Understanding-Current-Limiting-Reactors-(CLRs)). Accessed on 1st August 2014.

- Noe, M., Kudymow, A., Fink, S., Elschner, S., Breuer, F., Bock, J., Walter, H., Kleimaier, M., Weck, K.H., Neumann, C., Merschel, F., Heyder, B., Schwing, U., Frohne, C., Schippl, K. and Stemmler, M. (2008). Conceptual Design of a 110 kV Resistive Superconducting Fault Current Limiter Using MCP-BSCCO 2212 Bulk Material. IEEE Transactions on Applied Superconductivity, 17, (2), 1784-1787.
- Nwl (2014). Current Limiting Reactors (CLR): Technical Overview and Measurement Procedures. (Online) Available: <http://www.nwl.com/files/file/Tech%20Bulletins/222.pdf> Accessed on 1st August, 2014.
- Peelo, D.F., Polovick, G.S., Sawada, J.H., Diamanti, P., Presta, R., Sarshar, A. and Beauchemin, R. (1996). Mitigation of Circuit Breaker Transient Recovery Voltages Associated with Current Limiting Reactors. IEEE Transactions on Power Delivery, 11, (2), 865-871.
- Pflaum, E. and Muller, B. (1974). Suitable Means to Insure the Reliability of High Voltage Circuit-Breaker. Paris: International Conference on Large High Voltage Electric Systems. CIGRE WG 13-05 Report, 1-7.
- Rees, V. and Peters, H. (1995). Simplified Hydraulic Operating Mechanism For Broad Applications. Paris: International Conference on Large High Voltage Electric Systems. Colloquium of CIGRE SC 13, Brazil, 1-9.
- Saadat, H. (2002). Power System Analysis. New Delhi: Tata McGraw-Hill Publishing Company Limited.
- Schaad, W. (1980). The Practical Design of the HGF 100 Range of SF6 Outdoor Circuit Breakers. Sprecher News, 1-8.
- Scholl, R.A. (1994). Advances in Arc Handling in Reactive and Other Difficult Processes

in Society of Vacuum Coaters. 37th Annual Technical Conference Proceedings, 312-316.

Seyedi, H. and Barzan, T. (2012). Appropriate Placement of Fault Current Limiting Reactors in Different HV Substation Arrangements. Tabriz: Scientific Research, Circuits and Systems. 3, 52 – 262.

Stroud K.A. (2005). Advanced Engineering Mathematics. New York: Palgrave Macmillan.

Studyelectrical (2014). Sulphur hexafluoride (SF6) circuit breakers – construction, working and advantages. (Online), Available: <https://www.studyelectrical.com/2014/07/sulphur-hexafluoride-circuit-breakers-construction-working-and-advantages>. Accessed on 9th August, 2016.

TCN (2010). Operational Procedures. Abuja: Transmission Company of Nigeria (TCN), OP4, 1-7.

Theraja, B.L. and Theraja, A.K. (2012). A Textbook of Electrical Technology. New Delhi: S. Chand & Company Ltd.

Trenchgroup (2014). Current Limiting and Power Flow Control Reactors. (Online), Available: <http://www.trenchgroup.com/Current-Limiting-&-Power-Flow-Control-Reactors-Air-Core Reactors>. Accessed on 1st August, 2014.

Uppal, S.L. and Rao, S. (2012). Electrical Power Systems. India: Romesh Chander Khanna.

Vincent-Saporita, P.E. (1999). Don't Be Failed by Higher Fault Currents. Electrical Construction & Maintenance (EC&M) Magazine. pp. 12-17. Retrieved 17th January 2017.

Walter, R., Juan, C.L., Larry, M. and Ashok, S. (2009). Superconducting & Solid-state

Power Equipment. Office of Electricity Delivery and Energy Reliability, America. pp. 1-2. Accessed on 17th January, 2017.

Wikipedia (2014). Circuit Breakers Wikipedia. (Online), Available:
http://www.en.wikipedia.org/wiki/Circuit_breaker. Accessed on 24th July 2014.

Wikipedia (2014). Current Limiting Reactor Wikipedia. (Online), Available:
http://www.en.wikipedia.org/wiki/Current_Limiting_Reactor. Accessed on 1st August 2014.

Wikipedia (2017). The Free Encyclopedia. (Online), Available:
http://www.en.wikipedia.org/wiki/Adapter#cite_note-1. Accessed on 20th September, 2017.

Zensol (2007). Electrical contacts in MV & HV Power Circuit Breakers. (Online), Available: <http://www.zensol.com/Articles/ZensolJan-Fev2007.pdf>. Accessed on 9th August, 2016.

Zhang, J.J., Liu, Q., Rehtan, C. and Rudin, S. (2006). Investigation of Several New Technologies for Mega City Power Grid Issues. Chongqing: International Conference on Power System Technology, pp. 1-6.

APPENDIX A

MATLAB codes for Figure 3.2 and Table 3.4: Effect of CLR reactance on fault current level

V=132;%System voltage in kilo volts

A=1.732;%Square root of 3

Z1=2;

Z2=2.5;

Z3=3;

Z4=3.5;

Z5=4;

Z6=4.5;

Z7=5;

Z8=5.5;

Z9=6;

Z10=7;

Z11=8;

Z12=8.5;

Z13=9;

Z14=9.5;

Z15=10;

$$Z16=10.5;$$

$$Z17=11;$$

$$Z18=12;$$

$$Z19=13;$$

$$Z20=14;$$

$$Z=[$$

Z1,Z2,Z3,Z4,Z5,Z6,Z7,Z8,Z9,Z10,Z11,Z12,Z13,Z14,Z15,Z16,Z17,Z18,Z19,Z20]%CLR

impedance in ohms

$$I1=V/(A*Z1);$$

$$I2= V/(A*Z2);$$

$$I3= V/(A*Z3);$$

$$I4= V/(A*Z4);$$

$$I5= V/(A*Z5);$$

$$I6= V/(A*Z6);$$

$$I7= V/(A*Z7);$$

$$I8= V/(A*Z8);$$

$$I9= V/(A*Z9);$$

$$I10= V/(A*Z10);$$

$$I11= V/(A*Z11);$$

$$I12= V/(A*Z12);$$

$$I13= V/(A*Z13);$$


```
I14= V/(A*Z14);
```

```
I15= V/(A*Z15);
```

```
I16= V/(A*Z16);
```

```
I17= V/(A*Z17);
```

```
I18= V/(A*Z18);
```

```
I19= V/(A*Z19);
```

```
I20= V/(A*Z20);
```

```
I=[ I1,I2,I3,I4,I5,I6,I7,I8,I9,I10,I11,I12,I13,I14,I15,I16,I17,I18,I19,I20]% fault current in  
kA
```

```
plot(Z,I,'+b-')
```

```
axis([1 15 1 40])
```

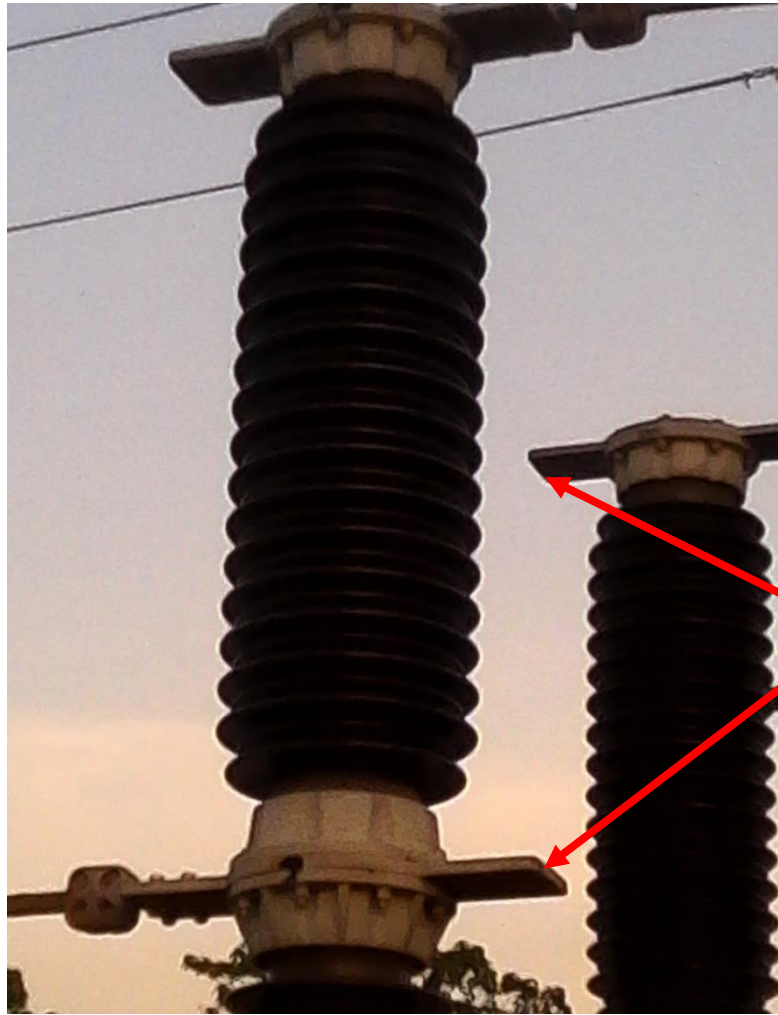
```
xlabel('REACTANCE[ohms]')
```

```
ylabel('FAULT CURRENT [kA]')
```

```
grid
```

APPENDIX B

Terminals of the existing CB for fitting the Adapter shown in Figures 3.13 and 3.14

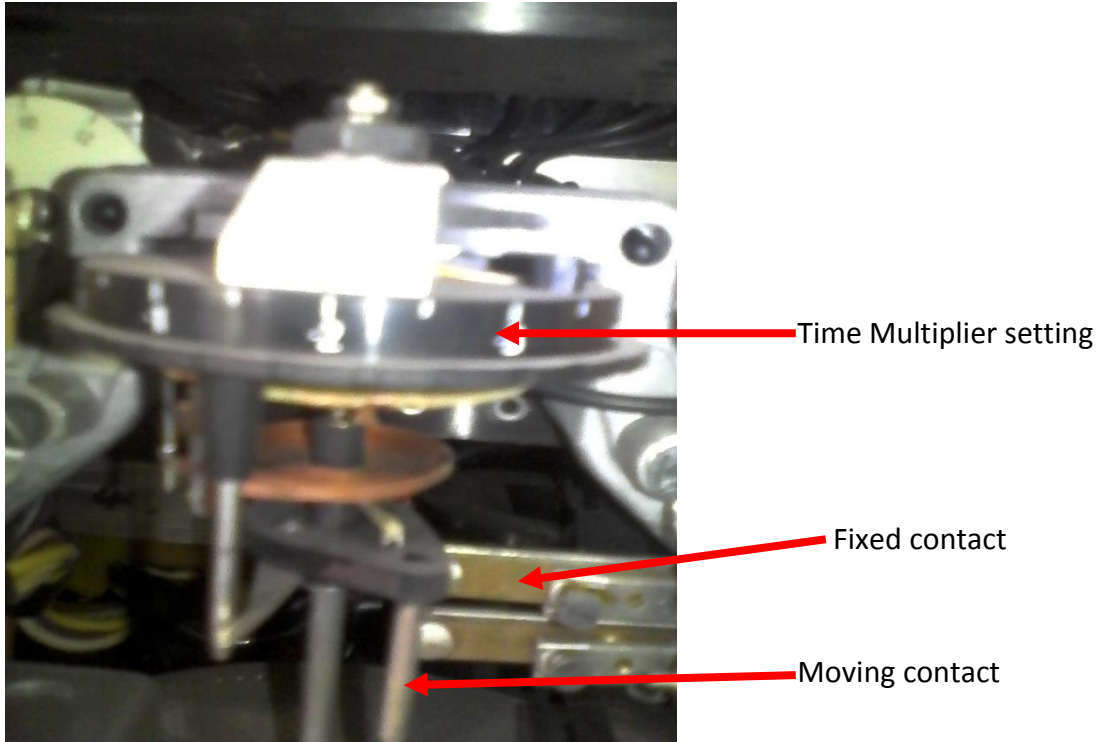


Terminals of the existing CB for fitting the adapter

Source: Transmission Company of Nigeria (TCN)

APPENDIX C

Time Multiplier Setting (TMS), for an Electromechanical Relay



Transmission Company of Nigeria (TCN)

APPENDIX D

Plug Setting Multiples (PSM), for an Electromechanical Relay.

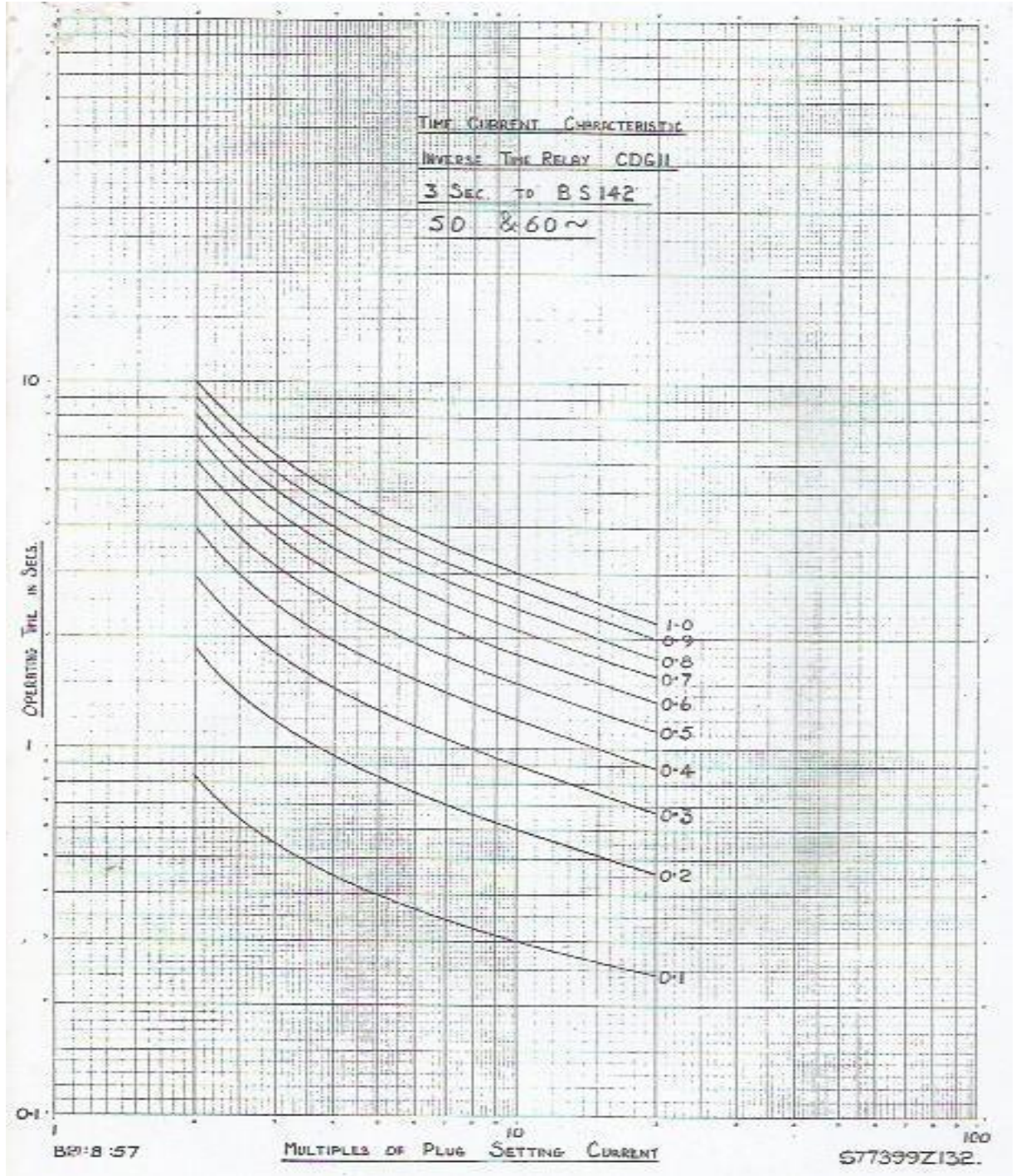


Current plug
setting
multiplier (PSM)

Transmission Company of Nigeria (TCN)

APPENDIX E

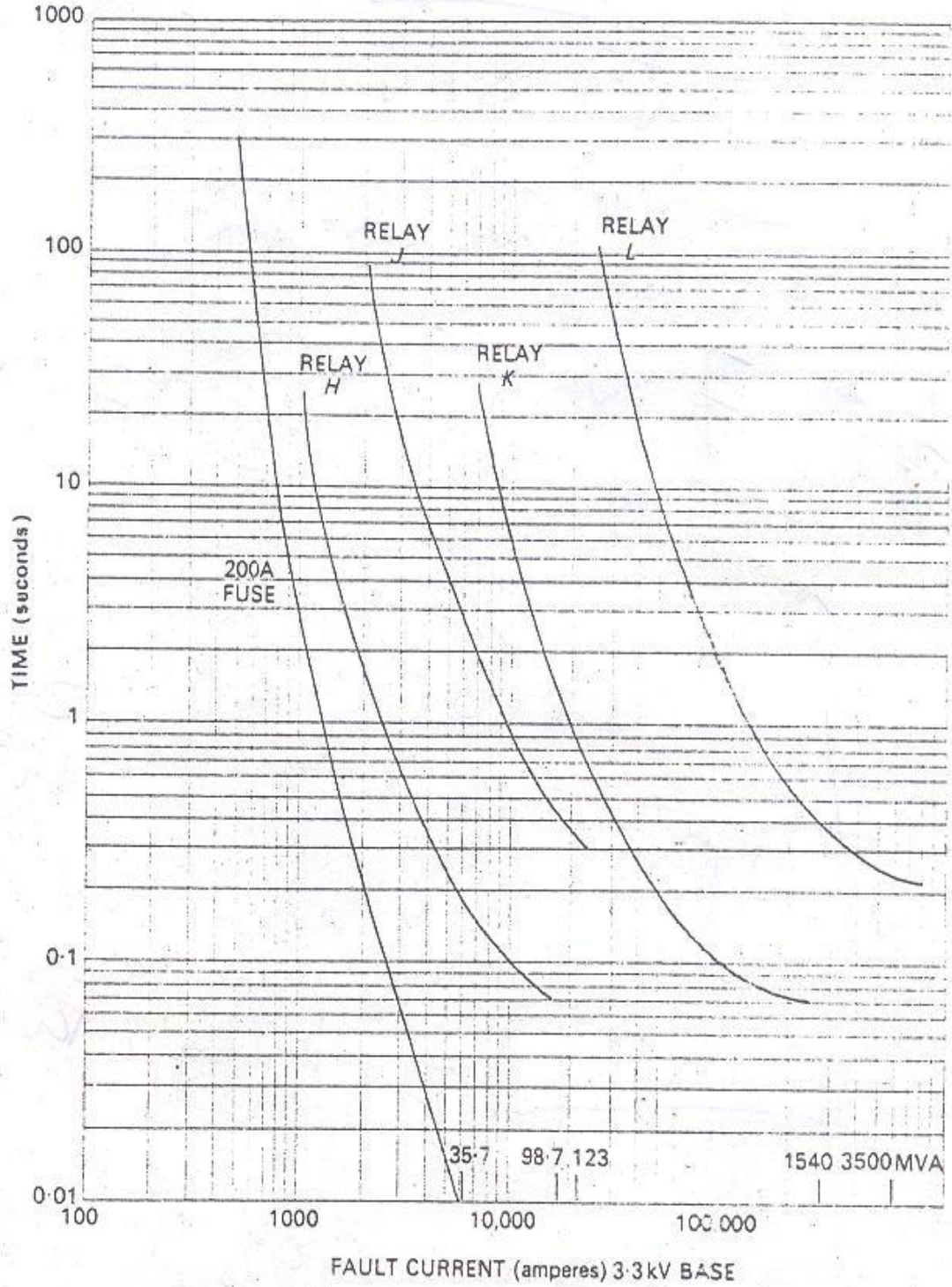
Time - Current Characteristic Curves for a Standard 3.0 seconds Inverse Time Relay CDG11 for 50HZ and 60HZ (BS 142)



National Power Training Institute of Nigeria (NAPTIN)

APPENDIX F

Relay Discrimination Curves



National Power Training Institute of Nigeria (NAPTIN)

APPENDIX G

Input Data for the Simulated Network

S/N	From Bus Number	To Bus Number	Circuit Number	Branch Device Type	R	X
1	1	2	1	Line	0.00839	0.01647
2	2	3	1	Line	0.00001	0.00002
3	2	3	2	Line	0.00552	0.01083
4	3	4	1	Line	0.00839	0.01647

APPENDIX H

Simulation result (Line Records (branch state)) for the power flow on Nkalagu–Abakaliki 132kV Line with the existing CB without CLR (Figures 3.23 and 3.24)

S/N	From Bus Number	To Bus Number	Circuit Number	Status	Branch Device Type	MW From	Mvar From	MVA From	MW Loss	Mvar Loss
1	1	2	1	Open	Line	0	0	0	0	0
2	2	3	1	Closed	Line	82.7	39.4	91.6	0	0
3	3	4	1	Closed	Line	82.7	39.4	91.6	0.7	1.38

APPENDIX I

Simulation result (Bus Records) for the power flow on Nkalagu–Abakaliki 132kV Line with the existing CB without CLR (Figures 3.23 and 3.24)

S/N	Bus Number	Nominal kV	PU Volt	Volt (kV)	Angle (Deg)	Load MW	Load Mvar	Gen MW	Gen Mvar
1	1	132	1	132	0	0	0	0	0
2	2	132	1	132	0	0	0	82.7	39.38
3	3	132	0.999	131.99	0	0	0	0	
4	4	132	0.987	130.23	-0.6	82	38	0	

APPENDIX J

Simulation result (Line Records (branch state)) for the power flow on Nkalagu–Abakaliki 132kV Line with the modified CB and CLR in closed position connected as earlier shown in Figure 3.20 in Figures 3.25 and 3.26

S/N	From Bus	To Bus	Circuit	Status	Branch Device Type	MW From	Mvar From	MVA From	MW Loss	Mvar Loss
1	1	2	1	Open	Line	0	0	0	0	0
2	2	3	1	Closed	Line	82.5	39.3	91.4	0	0
3	2	3	2	Closed	Line	0.2	0.1	0.2	0	0
4	3	4	1	Closed	Line	82.7	39.4	91.6	0.7	1.38

APPENDIX K

Simulation result (Bus Records) for the power flow on Nkalagu–Abakaliki 132kV Line with the modified CB and CLR in closed position connected as earlier shown in Figure 3.20 in Figures 3.25 and 3.26

S/N	Bus Number	Nominal kV	PU Volt	Volt (kV)	Angle (Deg)	Load MW	Load Mvar	Gen MW	Gen Mvar
1	1	132	1	132	0	0	0	0	0
2	2	132	1	132	0	0	0	82.7	39.4
3	3	132	0.999	131.99	0	0	0	0	0
4	4	132	0.987	130.23	-0.6	82	38	0	0

APPENDIX L

Simulation result (Line Records (branch state)) for the Power Flow on Nkalagu – Abakaliki 132kV Line with the modified CB and CLR during opening operation connected as earlier shown in Figure 3.21 in Figures 3.27 and 3.28

S/N	From Bus	To Bus	Circuit	Status	Branch Device Type	MW From	Mvar From	MVA From	MW Loss	Mvar Loss
1	1	2	1	Open	Line	0	0	0	0	0
2	2	3	1	Open	Line	0	0	0	0	0
3	2	3	2	Closed	Line	83.2	40.3	92.5	0.47	0.93
4	3	4	1	Closed	Line	82.7	39.4	91.6	0.72	1.41

APPENDIX L1

**Simulation result (Bus Records) for the Power Flow on Nkalagu – Abakaliki
132kV Line with the modified CB and CLR during opening operation
connected as earlier shown in Figure 3.21 in Figures 3.27 and 3.28**

S/N	Bus	Nominal kV	PU Volt	Volt (kV)	Angle (Deg)	Load MW	Load Mvar	Gen MW	Gen Mvar
1	1	132	1	132	0	0	0	0	0
2	2	132	1	132	0	0	0	83.19	40.33
3	3	132	0.99	130.82	-0.39	0	0	0	0
4	4	132	0.97	129.04	-1.00	82	38	0	0

APPENDIX M

**Simulation result (Line Records (branch state)) for the Power Flow on
Nkalagu – Abakaliki 132kV Line with the existing CB and CLR connected as
earlier shown in Figure 3.3 in Figures 3.29 and 3.30**

S/N	From Bus	To Bus	Circuit	Status	Branch Device Type	MW From	Mvar From	MVA From	MW Loss	Mvar Loss
1	1	2	1	Open	Line	0	0	0	0	0
2	2	3	1	Closed	Line	83.2	40.3	92.5	0	0
3	3	4	1	Closed	Line	83.2	40.3	92.5	0.47	0.93
4	4	5	1	Closed	Line	82.7	39.4	91.6	0.72	1.41

APPENDIX M1

**Simulation result (Bus Records) for the Power Flow on Nkalagu – Abakaliki
132kV Line with the existing CB and CLR connected as earlier shown in
Figure 3.3 in Figures 3.29 and 3.30**

S/N	Bus	Nominal kV	PU Volt	Volt (kV)	Angle (Deg)	Load MW	Load Mvar	Gen MW	Gen Mvar
1	1	132	1	132	0	0	0	0	0
2	2	132	1	132	0	0	0	82.19	40.33
3	3	132	0.99998	131.997	0	0	0	0	0
4	4	132	0.99105	130.818	-0.39	0	0	0	0
5	5	132	0.97755	129.037	-1.00	82	38	0	0

APPENDIX N

MATLAB codes for the Response curve of CB total break time (t_0) against the kinetic energy requirement (W_{KIN}) shown in Figure 4.3

```
f=50; %system frequency in Hz

to1=.05;

to2=.048;

to3=.045;

to4=.042;

to5=.04;

to6=.038;

to7=.035;

to8=.0333;

to9=.03;

to10=.028;

to=[to1,to2,to3,to4,to5,to6,to7,to8,to9,to10];%total break time in seconds

tBR1=to1-(2*f)^-1;

tBR2=to2-(2*f)^-1;

tBR3=to3-(2*f)^-1;

tBR4=to4-(2*f)^-1;

tBR5=to5-(2*f)^-1;
```


$$tBR6=to6-(2*f)^{-1};$$

$$tBR7=to7-(2*f)^{-1};$$

$$tBR8=to8-(2*f)^{-1};$$

$$tBR9=to9-(2*f)^{-1};$$

$$tBR10=to10-(2*f)^{-1};$$

tBR=[tBR1,tBR2,tBR3,tBR4,tBR5,tBR6,tBR7,tBR8,tBR9,tBR10] %breaker ready time in seconds

$$Wkin1=(tBR1)^{-2};$$

$$Wkin2=(tBR2)^{-2};$$

$$Wkin3=(tBR3)^{-2};$$

$$Wkin4=(tBR4)^{-2};$$

$$Wkin5=(tBR5)^{-2};$$

$$Wkin6=(tBR6)^{-2};$$

$$Wkin7=(tBR7)^{-2};$$

$$Wkin8=(tBR8)^{-2};$$

$$Wkin9=(tBR9)^{-2};$$

$$Wkin10=(tBR10)^{-2};$$

W=[Wkin1,Wkin2,Wkin3,Wkin4,Wkin5,Wkin6,Wkin7,Wkin8,Wkin9,Wkin10] %kinetic energy requirement of CB in joules.

plot(to,W,'+b-')

axis([0.025 0.052 600 3200])

```
xlabel('Total break time  $t_0$ [sec]')
```

```
ylabel('KINETIC ENERGY (WKIN)[joules]')
```

```
grid
```

APPENDIX O

MATLAB codes for the Response curve of blast pressure against fault current shown in Figure 4.4

```
k = 2.77; %proportionality constant in kg/ampere-cm^2

x1=18240;

x2=35700;

x3=40000;

x4=54000;

x5=61500;

x6=68000;

x7=74500;

x8=81000;

x9=87000;

x10=93000;

x11=98700;

i=[x1,x2,x3,x4,x5,x6,x7,x8,x9,x10,x11] ;% fault current (A)

I=i.^1.4;

N=2;

n=N^-0.28;

P=k*I*n; %blast pressure necessary for arc quenching
```

```
plot(P,i,'+b-')  
  
axis([1000000 23000000 15000 100000])  
  
xlabel('BLAST PRESSURE [kg/cm^2]')  
  
ylabel('Fault current [amperes]')  
  
grid
```

APPENDIX P

MATLAB codes for the fault current and the corresponding blast pressure shown in Table 4.7

```
k = 2.77; %proportionality constant in kg/ampere-cm^2

x1=20000;

x2=35700;

x3=40000;

x4=54000;

x5=61500;

x6=68000;

x7=74500;

x8=80000;

x9=87000;

x10=93000;

x11=98700;

i=[x1,x2,x3,x4,x5,x6,x7,x8,x9,x10,x11] % fault current (A)

I=i.^1.4;

N=2;

n=N^-0.28;

P=k*I*n %blast pressure necessary for arc quenching
```

APPENDIX Q

MATLAB codes for the response curve of the moving contact area against the fault current shown in Figure 4.5

```
k=0.0000364; % proportionality constant in m2/ampere
```

```
x1=18240;
```

```
x2=35700;
```

```
x3=40000;
```

```
x4=54000;
```

```
x5=61500;
```

```
x6=68000;
```

```
x7=74500;
```

```
x8=81000;
```

```
x9=87000;
```

```
x10=93000;
```

```
x11=98700;
```

```
i=[x1,x2,x3,x4,x5,x6,x7,x8,x9,x10,x11]; % fault (A)
```

```
I=i.0.3;
```

```
N=2; % number of breaks
```

```
n=N0.14;
```

```
A=I*n*k; % cross sectional area of the moving contact rod
```

```
plot(A,i,'+b-')  
  
axis([.0007 .0013 15000 100000])  
  
xlabel('AREA[m^2]')  
  
ylabel('Fault current[amperes]')  
  
grid
```

APPENDIX R

MATLAB codes for the response curve of compression work against fault current shown in Figure 4.6

```
x1=35.7;
x2=42.5;
x3=49;
x4=54;
x5=61.5;
x6=68;
x7=74.5;
x8=81;
x9=87;
x10=93;
x11=98.7;
i=[x1,x2,x3,x4,x5,x6,x7,x8,x9,x10,x11] % fault current (kA)
I=i.^1.7;
N=2; % number of breaks
n=N^0.86;
W=n*I/1000 % CB compression work requirement
plot(W,i,'+b-')
```



```
axis([0.5 4.5 30 100])
```

```
xlabel('COMPRESSION WORK[kilo Newtons]')
```

```
ylabel('Fault current[kA]')
```

```
grid
```

APPENDIX S

MATLAB codes for Figure 4.7

```
d=8960; %density of copper in kg/m^3

h1=1.2; %length of moving contact when not forked in m

k=0.0000364; % proportionality constant in m^2/A

x1=20000;

x2=35700;

x3=40000;

x4=54000;

x5=61500;

x6=68000;

x7=74500;

x8=81000;

x9=87000;

x10=93000;

x11=98700;

i1=[x1,x2,x3,x4,x5,x6,x7,x8,x9,x10,x11]; %fault current (A)

I1=i1.^0.3;

N=2; %number of breaks

n=N^0.14;
```

$A1=I1*n*k$; %cross sectional area of moving contact when not forked (m^2)

$v1=h1.*A1$; %volume of moving contact when not forked (m^3)

$m1=d.*v1$; %mass of moving contact when not forked (kg)

$h2=1.24$; %overall length of forked moving contact (m)

$a1=20000$;

$a2=35700$;

$a3=40000$;

$a4=54000$;

$a5=61500$;

$a6=68000$;

$a7=74500$;

$a8=85300$;

$a9=85400$;

$a10=87000$;

$a11=93000$;

$i2=[a1,a2,a3,a4,a5,a6,a7,a8,a9,a10,a11]$; %fault current (A)

$I2=i2.^{0.3}$;

$A2=I2*n*k$; %total cross sectional area of forked moving contact (m^2)

$v2=h2.*A2$; %volume of forked moving contact (m^3)

$m2=d.*v2$; %mass of forked moving contact (kg)

```
plot(m1,i1,'+b-',m2,i2,'ob-')
```

```
legend('NO CLR used on straight moving contact','CLR used on forked moving contact to  
reduce i from 98.7kA downwards')
```

```
axis([8 14 15000 120000])
```

```
xlabel('MASS[kg]')
```

```
ylabel('Fault current[amperes]')
```

```
grid
```

APPENDIX T

MATLAB codes for Tables 4.9 and 4.10

```
d=8960; %density of copper in kg/m^3

h1=1.2; %length of moving contact when not forked in m

k=0.0000364; % proportionality constant in m^2/A

x1=20000;

x2=35700;

x3=40000;

x4=54000;

x5=61500;

x6=68000;

x7=74500;

x8=81000;

x9=87000;

x10=93000;

x11=98700;

i1=[x1,x2,x3,x4,x5,x6,x7,x8,x9,x10,x11]; %fault current (A)

I1=i1.^0.3;

N=2; %number of breaks

n=N^0.14;
```

$A1=I1*n*k$; %cross sectional area of moving contact when not forked (m^2)

$v1=h1.*A1$; %volume of moving contact when not forked (m^3)

$m1=d.*v1$ %mass of moving contact when not forked (kg)

$h2=1.24$; %overall length of forked moving contact (m)

$a1=20000$;

$a2=35541$;

$a3=35542$;

$a4=35858$;

$a5=40000$;

$a6=54000$;

$a7=61500$;

$a8=68000$;

$a9=74500$;

$a10=87000$;

$a11=93000$;

$i2=[a1,a2,a3,a4,a5,a6,a7,a8,a9,a10,a11]$; %fault current (A)

$I2=i2.^0.3$;

$A2=I2*n*k$; %total cross sectional area of forked moving contact (m^2)

$v2=h2.*A2$; %volume of forked moving contact (m^3)

$m2=d.*v2$ %mass of forked moving contact (kg)

APPENDIX U

MATLAB codes for Table 4.11

```
d=8960; %density of copper in kg/m^3

h1=1.2; %length of moving contact when not forked in m

k=0.0000364; % proportionality constant in m^2/A

i=40000; %fault current (A)

I=i^0.3;

N=2; %number of breaks

n=N^0.14;

A1=I*n*k; %cross sectional area of moving contact when not forked (m^2)

v1=h1.*A1; %volume of moving contact when not forked (m^3)

m1=d.*v1 %mass of moving contact when not forked (kg)

h2=1.24; %overall length of forked moving contact (m)

a1=40000;

a2=35859;

a3=35858;

a4=35542;

a5=35541;

a6=35000;

i2=[a1,a2,a3,a4,a5,a6]; %fault current (A)
```

$$I_2 = i_2.^{0.3};$$

$$A_2 = I_2 * n * k; \text{ \%total cross sectional area of forked moving contact (m}^2\text{)}$$

$$v_2 = h_2 * A_2; \text{ \%volume of forked moving contact (m}^3\text{)}$$

$$m_2 = d * v_2 \text{ \%mass of forked moving contact (kg)}$$

APPENDIX V

MATLAB codes for Table 4.12

```
d=8960; %density of copper in kg/m^3

h1=1.2; %length of moving contact when not forked in m

k=0.0000364; % proportionality constant in m^2/A

i=35000; %fault current (A)

I=i^0.3;

N=2; %number of breaks

n=N^0.14;

A1=I*n*k; %cross sectional area of moving contact when not forked (m^2)

v1=h1.*A1; %volume of moving contact when not forked (m^3)

m1=d.*v1 %mass of moving contact when not forked (kg)

h2=1.24; %overall length of forked moving contact (m)

a1=35000;

a2=34000;

a3=33700;

a4=31376;

a5=31375;

a6=30000;

i2=[a1,a2,a3,a4,a5,a6]; %fault current (A)
```

$$I_2 = i_2.^{0.3};$$

$$A_2 = I_2 * n * k; \text{ \%total cross sectional area of forked moving contact (m}^2\text{)}$$

$$v_2 = h_2 * A_2; \text{ \%volume of forked moving contact (m}^3\text{)}$$

$$m_2 = d * v_2 \text{ \%mass of forked moving contact (kg)}$$

APPENDIX W

MATLAB codes for Table 4.13

```
d=8960; %density of copper in kg/m^3

h1=1.2; %length of moving contact when not forked in m

k=0.0000364; % proportionality constant in m^2/A

i=30000; %fault current (A)

I=i^0.3;

N=2; %number of breaks

n=N^0.14;

A1=I*n*k; %cross sectional area of moving contact when not forked (m^2)

v1=h1.*A1; %volume of moving contact when not forked (m^3)

m1=d.*v1 %mass of moving contact when not forked (kg)

h2=1.24; %overall length of forked moving contact (m)

a1=30000;

a2=29000;

a3=26894;

a4=26893;

a5=26655;

a6=25000;

i2=[a1,a2,a3,a4,a5,a6]; %fault current (A)
```

$$I_2 = i_2 \cdot 0.3;$$

$$A_2 = I_2 \cdot n \cdot k; \text{ \%total cross sectional area of forked moving contact (m}^2\text{)}$$

$$v_2 = h_2 \cdot A_2; \text{ \%volume of forked moving contact (m}^3\text{)}$$

$$m_2 = d \cdot v_2 \text{ \%mass of forked moving contact (kg)}$$

APPENDIX X

MATLAB codes for Table 4.14

```
d=8960; %density of copper in kg/m^3

h1=1.2; %length of moving contact when not forked in m

k=0.0000364; % proportionality constant in m^2/A

i=25000; %fault current (A)

I=i^0.3;

N=2; %number of breaks

n=N^0.14;

A1=I*n*k; %cross sectional area of moving contact when not forked (m^2)

v1=h1.*A1; %volume of moving contact when not forked (m^3)

m1=d.*v1 %mass of moving contact when not forked (kg)

h2=1.24; %overall length of forked moving contact (m)

a1=25000;

a2=24000;

a3=22411.5;

a4=22411;

a5=22213;

a6=20400;

i2=[a1,a2,a3,a4,a5,a6]; %fault current (A)
```

$$I_2 = i_2 \cdot 0.3;$$

$$A_2 = I_2 \cdot n \cdot k; \text{ \%total cross sectional area of forked moving contact (m}^2\text{)}$$

$$v_2 = h_2 \cdot A_2; \text{ \%volume of forked moving contact (m}^3\text{)}$$

$$m_2 = d \cdot v_2 \text{ \%mass of forked moving contact (kg)}$$